DESIGN AND DEVELOPMENT OF DEEP SUBMERGENCE UNDERWATER ACOUSTIC TRANSDUCERS

A THESIS

submitted by

SUBASH CHANDRABOSE M. R.

for the award of the degree

of

DOCTOR OF PHILOSOPHY

NAVAL PHYSICAL AND OCEANOGRAPHIC LABORATORY
(Recognised Research Centre)
COCHIN UNIVERSITY OF SCIENCE AND TECHNOLOGY
KOCHI - 682022

OCTOBER 2017

DESIGN AND DEVELOPMENT OF DEEP SUBMERGENCE UNDERWATER ACOUSTIC TRANSDUCERS

Ph.D. Thesis in the Field of Underwater Transducers

Author

Subash Chandrabose M. R.
Research Scholar, Registration No: 3879,
Naval Physical and Oceanographic Laboratory,
(Recognised Research Centre of CUSAT)
Defence Research and Development Organisation,
Thrikkakara, Kochi-682 021, India.
E-Mail: subashbos@gmail.com

Supervising Guide

Dr. D. D. Ebenezer
Scientist - 'G', Associate Director (T&M),
Naval Physical and Oceanographic Laboratory,
Defence Research and Development Organisation,
Thrikkakara, Kochi-682 021, India.
E-Mail: d.d.ebenezer@gmail.com

October 2017

Dedicated to

My parents, wife, and kids

THESIS CERTIFICATE

This is to certify that this thesis entitled "***DESIGN AND DEVELOPMENT OF DEEP SUBMERGENCE UNDERWATER ACOUSTIC TRANSDUCERS***" submitted by **Mr. Subash Chandrabose M. R.** to the Cochin University of Science and Technology, Kochi for the award of the degree of Doctor of Philosophy under the Faculty of Engineering is a bonafide record of the research work carried out by him under my supervision and guidance at the Naval Physical and Oceanographic Laboratory (Recognised Research Centre of Cochin University of Science and Technology), DRDO, Thrikkakara, Kochi-682021. The contents of this thesis, in full or in parts have not been submitted to any other University or Institute for the award of any degree or diploma.

<div align="right">

Dr. D. D. Ebenezer
Supervising Guide
Scientist - 'G',
Associate Director (T & M),
Naval Physical and Oceanographic Laboratory,
Kochi - 682021.

</div>

Kochi - 682021
26th October 2017

DECLARATION

I hereby declare that the work presented in this thesis entitled '*DESIGN AND DEVELOPMENT OF DEEP SUBMERGENCE UNDERWATER ACOUSTIC TRANSDUCERS'* is based on the original research work carried out by me under the supervision and guidance of **Dr. D. D. Ebenezer**, Scientist - 'G', Associate Director (T&M), NPOL, Kochi, for the award of the degree of Doctor of Philosophy of Cochin University of Science and Technology. I further declare that the contents of this thesis, in full or in parts have not been submitted to any other University or Institute for the award of any degree or diploma.

<div align="right">

SUBASH CHANDRABOSE M. R.
Research Scholar,
Naval Physical and Oceanographic Laboratory,
Kochi- 682 021.

</div>

Kochi - 682021
26th October 2017

CERTIFICATE

This is to certify that this thesis entitled "***DESIGN AND DEVELOPMENT OF DEEP SUBMERGENCE UNDERWATER ACOUSTIC TRANSDUCERS***" submitted by **Mr. Subash Chandrabose M. R.** has been modified to incorporate all the relevant corrections and modifications suggested by the audience during the pre-synopsis seminar and recommended by the Doctoral Committee.

<div align="right">

Dr. D. D. Ebenezer,
Supervising Guide,
Scientist - 'G',
Associate Director (T&M),
Naval Physical and Oceanographic Laboratory,
Kochi - 682021.

</div>

Kochi - 682021
26th October 2017

ACKNOWLEDGEMENTS

ABSTRACT

KEYWORDS: Deep submergence transducer; free-flooded ring transducer; segmented ring transducer; Finite element analysis; ATILA.

Underwater electroacoustic transducers for naval and civilian applications are required to be operated at various depths, from few meters to full ocean depth. Deep submergence transducers are needed for submarine sonars, dunking sonars, acoustic modems, underwater sensor networks, oceanographic studies and underwater acoustic beacons of aircraft where these transducers are operated at great depths and subjected to very high hydrostatic pressure. The high-pressure acting on the transducer can affect the acoustic performance as well as the structural and watertight integrity of the transducer. Fluid-filled, pressure compensated design concepts are sometimes used for deeper operations of the transducer, but this leads to additional complexities in design. In the present work, an alternate design approach, without pressure compensation is explored.

The major objectives of the research are design and development of underwater acoustic transducers that radiate acoustic energy even when subjected to high hydrostatic pressure. Development of Omni and directional transducers operating at frequencies below 10 kHz with a depth capability of 1000 m or more with a minimum source level of 190 dB re 1 μPa at 1 m are aimed. The thesis gives an overview of underwater transducers including transduction methods and transducer characteristics. The requirement of deep submergence transducers and the objectives of the research are specified. A detailed review of published reports is carried out with an emphasis on deep submergence transducers. Design aspects and methodology used for the development of deep submergence transducers are explained in detail. Finite element

analysis has been used for the design of transducers since it can be used to model and solve complex geometries of transducers with elastic, piezoelectric materials interacting with the fluid medium. Commercially available finite element software, ATILA is used for the modelling and parametric studies of transducers. Lead Zirconate Titanate (PZT) ceramics are used as the active material in this study since they are readily available in various shapes and sizes indigenously.

A detailed study on the design and development of Omnidirectional free-flooded ring transducers based on radially polarised cylinders (RPC), all-ceramic segmented ring with wedge shaped ceramics, and segmented ring with metal wedges and stacks of ceramic slabs are presented. Polyurethane over-moulding and rubber housing filled with oil are tried for encapsulation of transducers. Directional transducer design and development based on RPC and metal ceramic segmented ring are also presented. The transducers developed are tested initially in an open acoustic tank at 10 m depth and then in a pressurised vessel for its acoustic performance such as resonance frequency, and transmitting voltage response at different pressures up to 7 MPa. Power handling capability, source level, and directivity were also measured for the transducers. All the transducers were subjected to hydrostatic pressure for its depth withstanding capability in a pressure vessel at 10 MPa, and three of them were also tested in a hyperbaric pressure test facility upto 60 MPa.

The research has led to the development of different types of Omni and directional transducers with resonance frequency less than 10 kHz, source level more than 190 dB re 1 μPa at 1 m and capable of withstanding 6000 m of water. Finally, main findings and further works that can be attempted in future are presented.

TABLE OF CONTENTS

LIST OF TABLES

LIST OF FIGURES

xix

ABBREVIATIONS

AC	-	Alternating Current
ADP	-	Ammonium Dihydrogen Phosphate
BW	-	Beam Width
CW	-	Continuous Wave
dB	-	Decibel
DC	-	Direct Current
DF	-	Directivity Factor
DI	-	Directivity Index
FEM	-	Finite Element Method
FRP	-	Fibre Reinforced Plastic
FT	-	Flextensional Transducer
ID	-	Inner Diameter
IR	-	Insulation Resistance
MAVART	-	Mathematical model for Analysis of the Vibrations and Acoustic Radiation of Transducers
OCV	-	Open Circuit Voltage
OD	-	Outer Diameter
PAFEC		Program for Automatic Finite Element Calculations
PMN-PT	-	Lead Magnesium Niobate - Lead Titanate
PU	-	Polyurethane
PVC	-	Polyvinyl Chloride
PZT	-	Lead Zirconate Titanate.
RPC	-	Radially Polarised Cylinder
RS	-	Receiving Sensitivity
SL	-	Source Level
TCR	-	Transmitting Current Response
TVR	-	Transmitting Voltage Response

CHAPTER 1

INTRODUCTION

Electroacoustic transducers, which are of high relevance in the underwater scenario, had its advancement and widespread use during the World War II for sonar applications due to the military threat of submarines. The quartz crystals and Rochelle salt used for early transducers have been replaced with transduction materials like ammonium dihydrogen phosphate (ADP), lithium sulphate and other crystals in the early 1940's (Massa, 1985). Piezoelectricity was discovered in permanently polarised barium titanate ceramics in 1944 and polarised lead zirconate titanate (PZT) ceramics in 1954. Even today, PZTs are the most widely used active material in underwater transducers. However, materials like lead magnesium niobate (PMN) and single crystals compounds have the potential for improvement over PZTs in some applications.

The useful spectrum of underwater sound extends from about 1 Hz to over 1 MHz with most applications in large bodies of water. Applications over this broad frequency range require many different transducer designs. The transducers can be classified as active, passive and active cum passive. Naval applications like submarine detection use dunking sonars which are deployed in the water by a helicopter and other applications like underwater communication use underwater acoustic modems. Civilian applications include oceanographic studies carried out using moored systems, locating wreckage in the ocean using underwater acoustic beacons etc. All these devices use underwater transducers which need to be operated at a few metres depth to full ocean depth (Sherman and Butler, 2016). Fig 1.1 depicts different types of transducers used for various applications.
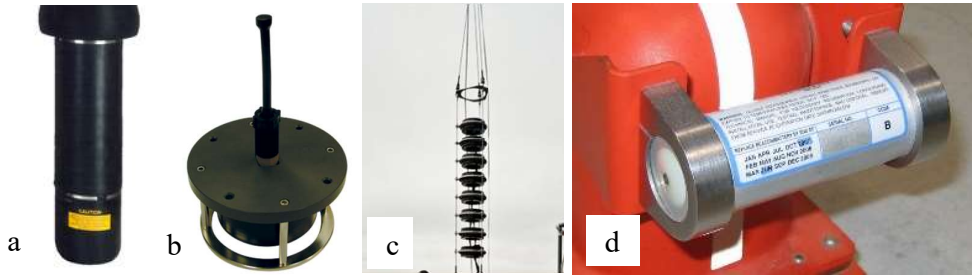
Fig. 1.1 Transducers used for, (a) Dunking sonars (b) Underwater acoustic modems (c) Oceanographic studies and (d) Underwater acoustic beacons.

1.1 ACTIVE TRANSDUCER

An active electroacoustic underwater transducer converts electrical energy to acoustical energy in water. Conceptually it is similar to the loudspeaker of air. It is also called a projector. Generally, it is operated at resonance to get maximum acoustic pressure in the medium.

1.2 PASSIVE TRANSDUCER

The device that converts acoustic energy to electrical voltage is called hydrophone or a passive transducer. Conceptually it is similar to the microphone of air. They are operated away from resonances to have a flat response over a wide band of frequencies.

1.3 ACTIVE CUM PASSIVE TRANSDUCER

There are situations in which the same transducer needs to operate as a transmitter and receiver. Transducers in underwater communication systems and most ship sonar arrays operate in dual modes.

1.4 ELECTROACOUSTIC TRANSDUCTION MECHANISMS

Underwater acoustic signals are transmitted and received using transducers. An acoustic transducer converts the electrical energy applied between the two terminals

into mechanical energy through a transduction mechanism. The mechanical vibrations are coupled to the surrounding medium through fluid-structure interactions, which produce acoustic waves in the medium. The sound waves propagate in the medium with a velocity characteristic of the medium. It is purely a reversible process. Therefore, a sound wave propagating in the medium excites the surface of the transducer and produces an electric field.

There are different physical mechanisms used to achieve electroacoustic energy conversions. However, even when attention is restricted to underwater sonic and ultrasonic applications, the wide frequency range involved from about l Hz to the low megahertz range requires a great variety of techniques and devices. The essential features of main transduction mechanisms are explained in the following sections.

1.4.1 Electrostrictive Transducer

The primary difference between electrostriction and piezoelectricity is that while piezoelectricity has a linear relationship between mechanical strain and electric field, electrostriction has a nonlinear relationship. Electrostriction is a property of all dielectric materials and is caused by the presence of randomly aligned electrical domains. When an electric field is applied to the dielectric material, the opposite sides of the domains become differently charged and attract each other, reducing material thickness in the direction of the applied field. The resulting strain is proportional to the square of the polarisation. Electrostrictive materials are with a low coercive force that must be used with a constant bias for projector applications. PMN and PMN-PT in ceramics or single crystal form promise as new materials for

underwater transducers. The electric field dependence and the temperature dependence of some of the properties probably need further investigation for PMN-PT.

The need to provide a biasing circuit is an added burden that reduces overall efficiency. The Curie temperature of these materials are in the range of 130-160 °C, and it is much lower compared to 328 °C for PZT4 materials (Zhou *et al.,* 2008; Berlincourt, 2010). Non-availability in different shapes and sizes is also a drawback compared to PZTs. However, the promising electromechanical properties of the PMN based materials indicate that their use may be advantageous in spite of the need for bias in some applications.

1.4.2   Magnetostrictive Transducer

Magnetostriction is the change in dimensions that accompanies a change in magnetisation of solid materials. In many respects, it is the magnetic analogy of electrostriction with the largest effects occurring in ferromagnetic materials. Both positive and negative magnetostriction occurs in nature. The mechanical response of magnetostrictive materials to an applied magnetic field is nonlinear and depends on even powers of the field. Thus, for small fields, it is essentially a square law, and a magnetic bias is required to obtain a linear response. Direct current windings can get the bias on the magnetostrictive material or by a permanent magnet forming part of the magnetic circuit. Terfenol-D is the most commonly used magnetostrictive material. Low frequency magnetostrictive transducers operating at 200 Hz are used for 1000 km propagation studies for ocean acoustic tomography (Nakamura *et al.,* 1996). Electrical and magnetic losses in magnetostrictive materials result in much lower efficiency.

1.4.3 Moving Coil Transducer

The moving coil transducer or the electrodynamic transducer is more familiar than any other transducer because it is used as the loudspeaker in most music and speech reproduction systems. Moving coil transducers are used in underwater acoustic calibration where low frequency, broadband sound sources of moderate power are needed. The transducer consists of a coil of wire suspended in a magnetic field. When an alternating electrical current is passed through the coil, mechanical forces are developed between the coil's electromagnetic field and the field in which it is mounted (Massa, 2017). The motion of the coil is transmitted to the diaphragm connected to the housing by mechanical springs. The movement of the diaphragm radiates sound into the external medium. The maximum forces on the moving coil are limited by the strength of the magnetic field generated in the gap and the number of turns used in the coil.

1.4.4 Piezoelectric Transducer

The piezoelectric properties of certain crystals are used by the piezoelectric transducers to transforms one type of energy to another. When a piezoelectric material is subjected to stress or force, it generates an electrical potential or voltage proportional to the magnitude of the force making the piezoelectric transducer an ideal device to convert mechanical energy or force into electric potential. Piezoelectric ceramics have replaced the piezoelectric crystals made from quartz crystals after its development. Piezoceramics became the dominant material for transducers due to their excellent piezoelectric properties and their ease of manufacture into different shapes and sizes. The first piezoceramic barium titanate has been followed by lead zirconate titanate compositions, which are now the most

commonly employed ceramic for making transducers. The lead zirconate titanate compositions fall into two main categories. One category is intended for high power transmitter applications with low dielectric loss maintained upto high fields and low internal mechanical losses like PZT4 ceramic. The other category is intended for use in hydrophones with high permittivity and sensitivity like PZT5 ceramics.

1.5   TRANSDUCER CHARACTERISTICS

1.5.1 Impedance and Admittance

When driven with an alternating electrical current, the current drawn by the transducer varies with frequency. The ratio of voltage to current drawn is called the electrical impedance, and its inverse is the electrical admittance of the piezoelectric transducer. The impedance is a complex quantity given by, $Z = R + jX$, where the real part of impedance is the resistance, R and the imaginary part is the reactance, X. The magnitude and phase of impedance are given by, $|Z| = \sqrt{(R^2+X^2)}$ and $\phi = \tan^{-1}(X/R)$.

1.5.2   Resonance and Antiresonance Frequencies

A piezoelectric transducer excited by an alternating electric field changes dimensions cyclically, at the frequency of the field. The frequency at which the element vibrates with maximum amplitude in response to unit electrical input is called the resonance frequency. At resonance frequency, the transducer has the minimum impedance, and it depends on the composition of the piezoceramic material, shape and volume of the element. Antiresonance frequency is the frequency at which the transducer has the maximum impedance. Transducers are designed to operate at resonance frequency to maximise the displacement for a given voltage. Also, when they are used as receivers, they produce a larger electrical signal for a given sound pressure.

1.5.3 Transmitting Response

Transmitting Voltage Response (TVR) of a projector is the ratio of the acoustic pressure amplitude (P) extrapolated back from the far field to 1 m from the source to the amplitude of driving voltage (V). It is expressed in decibel form referred to a standard pressure of 1 µPa as, TVR = 20 log (P/V) dB re 1 µPa/V at 1 m (Kinsler *et al.*, 2000). Transmitting Current Response (TCR) of a projector is the ratio of the acoustic pressure amplitude (P) extrapolated back from the far field to 1 m from the source to the amplitude of driving current (I). It is expressed in decibel form referred to a standard pressure of 1 µPa as, TCR = 20 log (P/I) dB re 1 µPa/A at 1 m (Kinsler *et al.*, 2000).

1.5.4 Receiving Sensitivity (RS)

Receiving sensitivity of a hydrophone is the ratio of the electrical output voltage (V), with the output open-circuited, to the applied sound pressure (P), usually expressed in decibel form, i.e. RS (dB re 1 V/µPa) = 20 log (V/P). The measurement frequency must be specified. Two forms of sensitivity are used. The more common form is the 'free-field sensitivity', for which the voltage is referred to the acoustic pressure in a plane wave which would have existed at the hydrophone position in the absence of hydrophone. It is sometimes more convenient to relate the output voltage to the actual acoustic pressure which exists on the face of the hydrophone when it is in the field. This is referred to as the pressure sensitivity of the hydrophone (Stansfield, 1990).

1.5.5 Directivity Factor and Directivity Index

Directivity Factor (DF) of a projector is the ratio of the transmitted acoustic intensity along the acoustic axis (I_0) to the intensity, which would have resulted from radiating the same power uniformly in all directions (I_{ref}), both measured at the same distance

from the source. Therefore, $DF = I_0/I_{ref}$. Directivity Index (DI) of a projector is the logarithmic expression of DF, therefore, $DI = 10 \log DF$.

1.5.6 Beam Width

The beam pattern is the relative sensitivity of a transducer as a function of spatial angle. This pattern is determined by factors such as the frequency of operation, size, shape, and acoustic phase characteristics of the vibrating surface. The beam pattern of a transducer is the same whether the transducer is used as a transmitter or receiver. Transducers can be designed to radiate sound in many different types of patterns, from Omnidirectional to narrow directional beams. The beam pattern of a transducer is usually calculated and plotted to show the relative reduction in sensitivity as a function of angle, with the maximum sensitivity of the transducer along the main acoustic axis set to 0 dB. The beam angle of the transducer is equal to the total arc encompassed by the beam between the angles when the pressure is reduced to a level of -3 dB on either side of the main acoustic axis.

1.5.7 Bandwidth

Bandwidth is the frequency range over which the response of the transducer remains constant within 3 dB.

1.5.8 Source Level

Source Level (SL) is the intensity of the radiated wave in a specified direction, in decibels, relative to the intensity of a plane wave of rms pressure 1 μPa, referred to a point 1 m from the acoustic centre of the projector in its maximum response axis. The

source level can be determined from the power (P), DI and efficiency (η) using the relation, SL = 170.9 + 10 log P +10 log η_+ DI dB re 1 µPa at 1 m (Stansfield, 1990).

1.5.9 Efficiency

Efficiency (η) of a transducer is the ratio of the acoustic power generated to the input electrical power. Part of the energy supplied is used to produce acoustic power in the medium, and the rest is dissipated as heat.

1.5.10 Quality Factor

The Quality Factor, Q, of a transducer is a value that indicates the width of the frequency band in the region of resonance over which it can operate with high output. Q is calculated by dividing the resonance frequency by the bandwidth, which is defined as the frequency band over which the response of the transducer lies within 3 dB of the peak response. Therefore, $Q = f_0/\Delta f$, where, f_0 is the centre frequency and Δf is the bandwidth (Massa, 2017).

1.5.11 Coupling Coefficient

Electromechanical coupling coefficient, k, is an indicator of the effectiveness with which a piezoelectric material converts electrical energy into mechanical energy or mechanical energy into electrical energy. It is calculated from the values for minimum impedance frequency and maximum impedance frequency. It depends on the mode of vibration and the shape of the ceramic element. Dielectric losses and mechanical losses also affect the efficiency of energy conversion or the coupling coefficient

1.6   DEEP SUBMERGENCE TRANSDUCER

The operational depth of a transducer varies with the type of application. There are situations in which the transducer needs to operate at full ocean depth. Deep submergence transducers are required for various uses such as submarine sonars, dunking sonars, acoustic modems, underwater sensor networks, tsunami detection devices, remotely operated vehicles (ROV), autonomous underwater vehicles (AUV), oceanographic studies and underwater acoustic beacons for aircraft (Adam, 1985; Benson *et al*., 2010; Eyries, 2004; Galle *et al*., 1999; Kumar *et al*., 2013; Moscaa *et al*., 2013; Roberts *et al*., 2012; Sanchez *et al*., 2011; Singh *et al*., 2009; Wills *et al*., 2006). The depth capability of transducers is limited by the failure of its housing, seals, degradation of the piezoelectric ceramic under hydrostatic pressure, and by the stress limits of the ceramic and the structure (Kuntsal and   Bunke, 1992).

When operating in shallow waters, the design concepts usually involve "hard shell" design techniques. However, the pressure is the most significant environmental factor acting in the deep sea. In the deep sea, the range of pressure is from 2 to over100 MPa. This makes the hard shell design method not very convenient for deep ocean operational requirements. Better would be an approach of not trying to fight the depth pressure, but to design for and live with the pressure (Mehnert, 1972). Transducer design can be accomplished by fluid-filling and pressure compensating deep submergence systems since fluid to seawater pressure differentials is then minimal. Structural housing and seal requirements for such systems are less demanding than for a hard shell approach. The compensating device provides fluid volume compensation for changing physical conditions, both ambient and internal.   Fluid-filled, pressure compensated design concepts used for deeper operations of the transducer leads to additional complexities

10

in design. In the present work, an alternate design approach without pressure compensation is explored.

1.7   OBJECTIVES OF RESEARCH

Detailed reports are not available in the open literature on the design, development and performance of transducers under deep submergence conditions and this has motivated to take up the research in this area. The major objectives of the research are design and development of Omni and directional transducers operating at frequencies below 10 kHz with a depth capability of 1000 m or more with a minimum source level of 190 dB re 1 µPa at 1 m. The design of the transducer was taken up based on a detailed literature review and using a proven commercial finite element software, ATILA, developed for the design of underwater transducers (ATILA user's manual, 1997). Finite element analysis was used for the design of transducers since it can be used to model and solve complex geometries of transducers with elastic, piezoelectric materials interacting with the fluid medium. Parametric studies of transducers were carried out using ATILA to find out the effect of various parameters on Transmitting Voltage Response (TVR). Lead Zirconate Titanate (PZT) ceramics are used as the active material in this study because they are readily available in many shapes and sizes indigenously. The transducers designed based on the modelling were manufactured, and their acoustic performances under high hydrostatic pressure were measured. The depth withstanding capability of the transducers was also tested. Even though the depth capability specified for the transducer is 1000 m, efforts are taken to realise a depth capability of 6000 m so that the transducers can be used in more than 98% of the ocean floor where the depth is less than 6000 m (Mero, 1965).

1.8   ORGANIZATION OF THE THESIS

An introduction to the thesis and an overview of transducers including transduction methods and transducer characteristics are presented in Chapter 1. The requirement of deep submergence transducers and objective of the research are specified. The organisation of the thesis is also presented. In Chapter 2, a detailed review of published reports on different types of transducers are explored with an emphasis on deep submergence type transducers. In Chapter 3, design aspects and methodology planned in the research for the development of deep submergence transducers are discussed.

In Chapter 4, design and development of Omnidirectional free-flooded ring transducers based on radially polarised cylinders (RPC), all-ceramic segmented ring with wedge shaped ceramics, and segmented ring with metal wedges and stacks of ceramic slabs are described in detail. In Chapter, 5 directional transducer design, and development based on RPC and metal ceramic segmented ring are presented. Finally, in Chapter 6, the major conclusions are summarised, and further work that can be attempted in future are presented.

1.9   SUMMARY

This chapter briefly discusses the different types of transducers, transduction mechanisms, as well as transducer characteristics. The objectives and relevance of the research for the design and development of deep submergence transducers are discussed. The organisation of thesis is also presented in this chapter.

CHAPTER 2

REVIEW OF PAST WORK

2.1   INTRODUCTION

The ocean bottom is divided as continental shelf, continental slope, continental rise, deep ocean basin and the trenches as shown in Fig. 2.1. The continental shelf extends underwater from the landmasses, and it is the submerged portion of the continents. The shelf has features similar to those we see on land, including hills, ridges, and canyons. The size of the shelf varies. It may be virtually non-existent in some areas; elsewhere it may extend from shore for several hundred kilometres. The shelf's average distance is about 64 km. It is beyond the continental shelf that the "deep sea" begins at a depth of about 200 m (Marine diversity wiki, 2017). The depth of water is less than 6000 m in more than 98% of the ocean floor, but it can be as deep as 10850 m in Mariana trench (Mero, 1965). There are many applications where transducers need to operate at full ocean depths. The design of transducers to operate at great depths requires associated components like PZTs, cables, seals, and connectors capable of withstanding these pressures and harsh environment.

2.2   DEEP SUBMERGENCE TRANSDUCERS

Deep submergence transducers are required for scientific research and military purpose. When transducers are needed to operate at considerable depth, they are subjected to a large static force resulting from the hydrostatic pressure acting on its radiating surface. The common approach in the past to accommodate the hydrostatic force has been to use pressure release materials, which can withstand the force and yet offer low mechanical impedance to the resonator so that it remains decoupled from the housing.

Depending on the depth, different materials like celltite rubber, corprene or stacks of paper are used as pressure release material, which enables transducers to operate to depths of the order of 300 m before it becomes too stiff to provide appreciable sound isolation (Woollett, 1963). The best available pressure release material is a compressed gas, if we should omit the pressure release pad. If the housing were filled with a compressed gas maintained at the same pressure as the surrounding water, we would get good performance at all depths. However, the reliability and impedance variation of gas with depth is its major disadvantage. Therefore, its use is limited to fixed depth operation (Woollett, 1980).
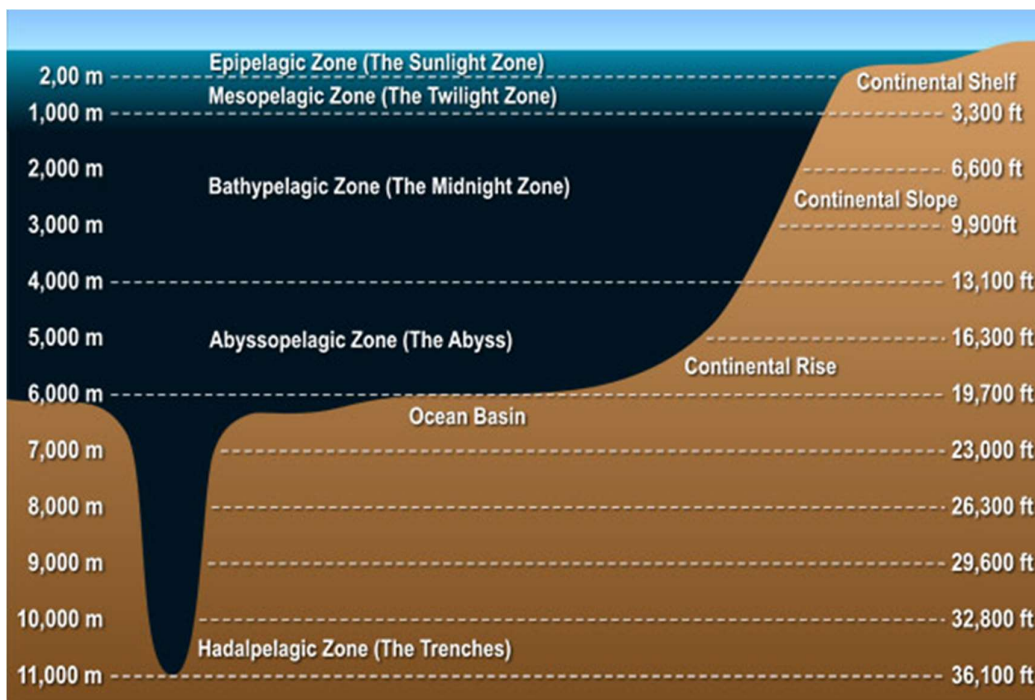
Fig. 2.1   Different zones of ocean

At very high depths, the solid pressure release materials are ineffective, and the gas systems are considered impractical, so liquid filled transducer design is to be adopted. The most compressible liquids available are about twice as compressible as water; arid

Silicone fluid is the most commonly used. The enclosed liquid in housing adds stiffness to the vibratory system, thereby raising the resonant frequency and lowering the electromechanical coupling factor of the transducer. By proper design, these effects may be made tolerable. On the rear of the housing, an oil reservoir and pressure equalising system are provided which compensates for the hydrostatic compression of the oil inside the housing. The effective compressibility of the liquid inside the housing can be increased if compliant tubes are immersed in it. Operating depth of the transducers varies by orders of magnitude based on their application. Different design approaches need to be adopted for various operating depths. The design approaches for different depths are reported by Woollett (1980) as shown in Fig. 2.2.
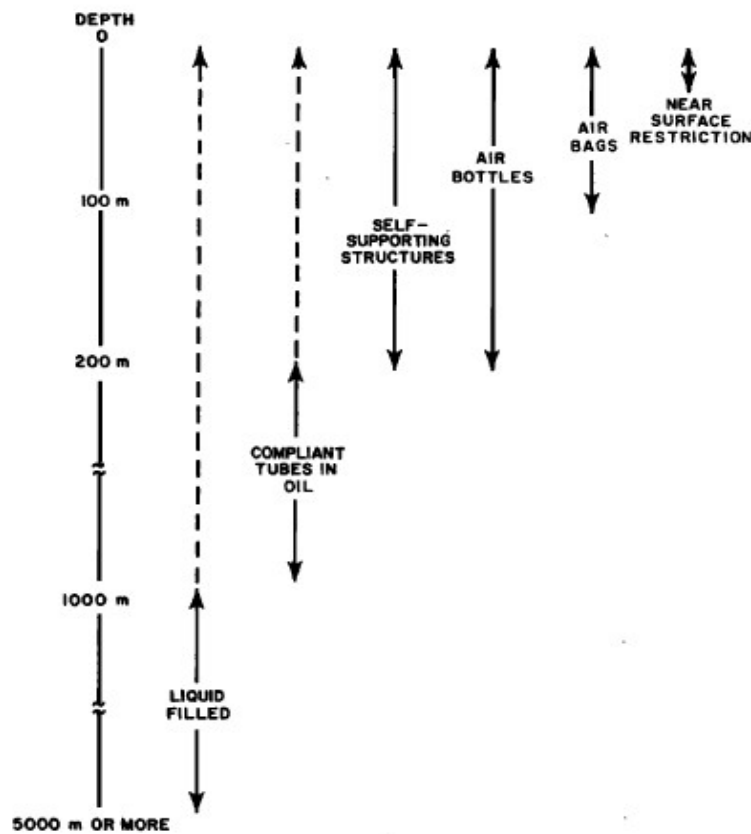
Fig. 2.2   Different techniques used for achieving depth capability.

15

Deep submergence transducer designs are of two categories. The first one is the free-flooded water backed type. This design is simple, efficient and does not require any complicated mechanisms and has nearly unlimited depth capability. The second category is the fluid-filled, pressure compensated transducers that require complex and bulky equipment for pressure balancing.

2.2.1 Free-Flooded Ring Transducer

The operating depth affects the performance of a projector since acoustic isolation materials lose their compressibility under high hydrostatic pressure. Acoustic isolation is often needed to reduce radiation from surfaces that may be out of phase or to prevent vibration from communicating with the transducer housing. The properties of piezoelectric ceramic can also change under high hydrostatic pressure since the permanent bias can change under the pressure cycling that occurs in submarines. One solution to the deep submergence problem is the free-flooded ring, where the hydrostatic pressure is the same on the inside and the outside.

A free-flooded cylindrical transducer is usually made up of a radially polarised piezoceramic ring and is encapsulated with rubber or polyurethane. There are two fundamental vibration modes associated with these transducers, the radial resonance of the shell and cavity resonance of the enclosed water column. McMahon (1964) has carried out detailed theoretical and experimental studies on cavity resonance of open, radially polarised ceramic rings. The frequency of cavity resonance decreases with the increase of h/a ratio where 'h' is the height, and 'a' is the radius of the ring. Junger (1969) also reported the effect of diameter and height on resonance frequency. Since the radial resonance frequency of the ring is dependent on diameter, its size becomes

large as frequency comes down so it can be typically used for frequencies above 4000 Hz (Hughes, 1998). The free-flooded transducer performance can be enhanced by using segmented cylinders, with associated complications in fabrication. Problems related to the manufacture of a solid ceramic ring of large diameter for low frequencies can be solved by the segmented ring cylinders (Harris, 1964; Green, 1965). Metal straps over the boot (Clearwaters, 1962), metallic wedges (Edourd, 2000, 2002; Roux, 2005) or fibreglass winding over the cylinder can be used to pre-stress the segmented cylinders (Parker, 1966). Bolts are also used for pre-stressing segmented transducer made of rectangular piezoceramic blocks. Stacks of ceramics are initially formed, and then they are joined together to form the transducer (Falcus, 1998).

Renna (1972) in his US patent has reported oil filled, fibreglass wound segmented ring transducer that enhances the bandwidth by close coupling the cavity and hoop mode resonances. He also provides the nominal size of the transducer and suggests that the cavity resonance should be below the operating band and a minimum ratio of radial to cavity resonance 'f_r/f_c', and minimum impedance variation to keep the mechanical 'Q' low. Low ratios of element thickness to diameter 't/d' and element height to radius 'h/a' will give a low mechanical 'Q'. A transducer with an outer diameter of 11 inch and height 4.3 inch, designed for f_r/f_c ratio of 1.48 with 'h/a' less than 1.0, and 't/d' approximately equal to 0.04, produced a cavity resonance of 2.1 kHz with efficiency of 60% and ring resonance of 2.8 kHz with 75 % efficiency. Behrendt (1971) proposed a piezoceramic ring transducer in a hollow annulus, filled with high dielectric oil like transformer oil, so that hydrostatic pressure regardless of magnitude is perfectly equalised inside and outside the annulus to obviate all pressure gradients.

The resonance frequency of the free-flooded ring transducer can be reduced by replacing alternate piezoceramic segments by more compliant metallic or non-metallic segments like Lucite. Butler (1976) studied the segmented ring transducer with inactive segments and derived an equation of motion and equivalent circuit. The wedge shaped non-piezoceramic spacing strips helps to make the transducer with pre-fabricated stacks from the regular rectangular cross-section, instead of the wedge-shaped ceramics. This concept reduces much of the problem associated with making the segmented transducer by gluing a number of wedge shaped ceramic strips. Bandwidth of more than two octaves is achieved by alternate lead, ceramic stave construction by utilising the cavity, radial and bending resonance with discrete dimensioning (Holloway, 1974). The composite ring transducer resonates at a lower frequency with higher bandwidth, however, at the cost of reduced power. A multiport design, in that two coaxial resonant chambers are created to bring down the resonance frequency of the free-flooded ring transducer. There are two co-axial tubes in this design where the inner tube has a piezoelectric ring in the centre (Butler *et al*., 2002; George *et al.*, 2013).

A free-flooded ring transducer is a useful directional source even with a size smaller than the acoustic wavelength. Its horizontal directivity is Omnidirectional, and the vertical directivity is toroidal. The transducer can be made more directional by stacking more rings along the axis and forming an array. When a number of cylinders are to be stacked one over the other for large depth operation, decoupling members between the cylinders can be used to isolate them to improve its transmitting power (Sernit *et al.*, 1998). Kuntsal (2003) studied the gap between the cylinders in a vertical array of three free-flooded rings of 5.2 inches OD 0.35-inch thick and 2-inch height. As the gap between the rings is increased to one inch with water in between them, the acoustic

interaction reduced and the rings behaved closer to their individual performance. He reported that apart from the ring dimensions the encapsulation material also affects the cavity resonance. He has reported improvement in acoustic performance of a free-flooded ring with the addition of inactive end tubes. He has made a vertical array of five rings and observed that the efficiency of individual rings and array are not equal.

Brown (2004) has reported in his US patent the use of an acoustic baffle to make a free-flooded ring and an array of rings directional. The baffle he proposed can be made of materials like syntactic foam; closed cell air filled foam, laminate structures of composite materials, a thin air or air bubble layer. Good directionality is reported in the 25-40 kHz frequency band.

Sreejith and Ebenezer (2009) modelled and measured characteristics of free-flooded radially polarised broadband transducers. TVR and directivity are computed using the FEM software ATILA. The effect of average diameter, length, and wall thickness of the piezoceramic shell and wall thickness of the encapsulant on the TVR is studied by varying one parameter at a time. The effect of dimensions on TVR obtained using model are validated by experiments, and the results are in good agreement. Xin-ran (2012) reported perforated wedges to improve the bandwidth and lower the resonance frequency of free-flooded ring transducer. Jiwu (2016) reported a broadband free-flooded segmented ring transducer for underwater communication.

Butler *et al.* (2000, 2001, 2003, 2004) developed a directional multi-mode transducer using RPCs. The transducer is in the form of a coaxial array of piezoelectric rings which provide vertical directionality through the array length and horizontal directionality through multi-modal excitation of the cylinders. A combination of Omnidirectional,

19

dipole and quadrupole modes of vibration is used to attain a horizontal directional and electrical steerable beam. The modes are excited through selective electrical summing of the signals on the silver stripping of the cylinder. With this method, identical beam patterns may be obtained over a range of frequencies. It has been shown that highly directive beams may be obtained from the cylindrical radiator. Analytical and finite element modelling was performed to verify expectations before the design was implemented to achieve cardioid and super-cardioid horizontal directional patterns. Measured results are presented and are shown to agree reasonably well with calculated and finite element results.

Broadband multimode baffled piezoelectric cylindrical shell transducers with directional beams in the horizontal plane are developed by stripping the electrode vertically inside and outside of the cylinder and exciting them in different modes (Oishi *et al*., 2007; Aronov *et al*., 2001). The bandwidth of fluid-filled piezoceramic transducers can be increased by utilising an acoustically rigid internal structure to control the impedance presented to the vibrator at the shell structure interface (Martin, 1964). Semenov *et al*. (1994) studied the magnetostrictive ring transducers for ocean exploration purposes. Magnetostrictive ring transducers can be used in tomography systems due to their reliability, robustness, deep water operation potential and low electrical impedance. However, in the frequency range below 1 kHz resonance, transducers dimensions become too large. This problem may be solved by the use of thin-walled cores (not more than 10 mm thickness for the diameter of the order of 1 m). He has reported relation of frequency to geometrical dimensions of radiator and parameters of magnetostrictive material. This formula is proven to be correct in the limits 15-20 percent, and it is confirmed by experiments with a series of ring transducers

20

made of nickel-cobalt alloy with radius 100 - 1000 mm, different height and thickness. A transducer, with diameter 1 m, height 250 mm, thickness 7.5 mm was tested to have resonance frequency 470 Hz and acoustical power 1.0 kW. Transducer with diameter 1.5 m, height 500 mm, thickness 6 mm was tested to have resonance frequency 220 Hz and acoustical power 200 W. Gallaher (1997) used PAFEC to model an array of free-flooded ring transducer to get directionality in the horizontal plane. Narrow beam width is obtained from a diamond array of four ring transducers when quarter wavelength separated the sources and driven them with a phase difference. Free-flooded transducer with segmented or radially polarised ceramic ring may be an ideal solution for deep submergence applications. If the ceramic driver is placed in an oil filled annular cavity of a rubber boot, it may help to couple the transducer to the exterior fluid environment in a better way. This can also avoid the complexities associated with moulding directly over the ceramic ring.

2.2.2 Tonpilz Transducer

Tonpilz type transducers were invented in 1959 in their currently used state by Miller (1989). A picture of that invention in a disassembled state for better visibility of its constituents is shown in Fig. 2.3. Tonpilz is the most commonly used sonar transducer where there is a requirement of directivity and beamforming (Morris, 1984). The Tonpilz transducer consists of a piezoceramic stack held between a head mass, exposed to water, and a tail mass of high impedance to maximise the vibrations of head mass. The stack is usually pre-stressed to prevent the ceramic operating in tensile mode (Miller, 1963). The outer diameter of the PZT stack is pre-stressed with fibreglass wound around it for added strength under shock. Typically, the head mass is Aluminium, the tail mass is steel, the stress rod is high-strength steel or Beryllium

copper, and the piezoceramic rings are Navy Type I or III. The housing is usually steel, and the watertight boot is neoprene or butyl rubber and occasionally polyurethane for short-term immersion. The rubber boot is vulcanised to the head to ensure proper bonding with no air pockets (Sherman and Butler, 2016).
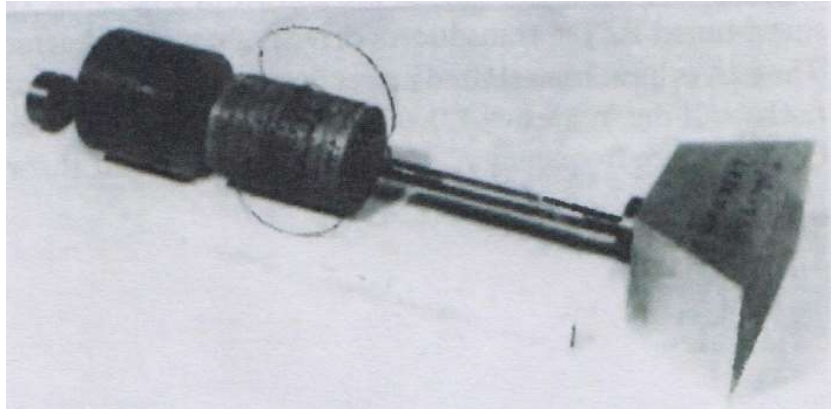
Fig. 2.3   Tonpilz Transducer (Miller, 1989).

Tonpilz transducers are normally air-backed and affected by the higher depth of operation. The static stress acting on the head mass of Tonpilz transducers gets amplified by the ratio of cross sections of head mass and the piezoceramic rings. This problem can be countered by compensating for the differential pressure by equalising the air pressure inside the transducer housing to the exterior water pressure. Pressure compensation is achieved by injecting air from compressed air bottles, which increases the total weight of the system (Woollett, 1980). An alternative method is to use compliant bellows to counter the pressure difference (Behrendt *et al.*, 1970). The head mass must be effectively decoupled from the housing by providing a compliant mechanism at the interface to achieve high acoustic performance. Bellows used in the transducer assembly takes additional load acting on the head mass due to the hydrostatic pressure. These techniques have been successfully employed for depths up to 1000 m.

A more effective method is to introduce a compliant structure between the head mass and the housing. The purpose of the compliant ring is to decouple the head mass and counter the static pressure. Anisotropic materials such as FRP which has high compliance along the axial direction and high stiffness along the lateral direction are widely used as filters. Ehrlich (1992) proposed a version of tonpilz transducer capable of operating at great depths without subjecting the ceramics to the hydrostatic pressure. Widener (1986) reported an air-backed tonpilz transducer with a nodal clamp and a special toroidal Beryllium copper seal between head mass and tail mass capable of operating upto 1300 m at 12.95 kHz. The resonance frequency of the transducer reduced to 11 kHz when the pressure was raised to an equivalent depth of 1000m. Butler *et al.* (2011) reported an array of tonpilz transducer with common tail mass called modal projector in which weighted summation of acoustic monopole, dipole and quadrupole modes are used to generate directional beams. Thompson *et al*. (1992) reported a doubly resonant wideband transducer. Butler (2002) reported a triply resonant broadband transducer with the addition of inactive materials in the stack of a tonpilz transducer. Debus *et al.* (1996) reported a low frequency polygonal ring transducer made of segmented head masses and piezoceramic ring stacks capable of withstanding 2000 m of depth.

2.2.3   Fluid-Filled Tonpilz

Widener (1986) tested a 27 kHz oil filled transducer and observed a reduction in source level of 9 dB compared to an air-backed design. An array of tonpilz transducers in a Silicone fluid-filled housing without any pressure compensation was developed and tested upto 700 m of water by Kendig and Clarke (1965, 1967). The transmitting voltage response was insensitive to pressure, and the variation was only within ±1 dB which is

approximately the accuracy of underwater acoustic measurement. However, the resonant frequency of the liquid filed transducer was increased by 11%. The impedance of the fluid-filled array is different from an air-backed array. The Silicone fluid provided additional insulation and conducted away the heat produced. Tocquet (1979) reported a tonpilz transducer with a viscoelastic material filled inside the housing between the stack and casing for great depth application. Since the fluid-filled design of tonpilz transducer reduces the source level considerably and increases the resonance frequency, it is not widely used for deep submergence application.

2.2.4 Flextensional Transducer

Flextensional transducers (FT) radiate acoustic energy through the flexing of a shell caused by the longitudinal extension and contraction of the driver, usually, a piezoceramic stack, fixed inside the shell under compression. Hayes invented the flextensional transducer concept in 1929 and patented in 1936 (Hayes, 1936). He used the transducer as a foghorn. However, the credit for improving the flextensional transducer for underwater application goes to Toulis (1966a, 1966b) through his 1966 patents. The detailed construction of the convex elliptic shaped transducer, currently known as class IV FT, and an array of transducers are given in his first patent. In the second patent, how the transducer and the array can be modified to withstand deeper depths is given. Fluid-filling with rubber bag attachment and compliant tube are proposed in this patent. The concave form of the class I flextensional transducer, was patented by Merchant (1966). Flextensional transducers with concave shells such as the Class I Barrel Stave are more efficient acoustic radiators. When excited, the volume velocity of concave shells is more than that of convex shaped shells and the acoustic pressure in the surrounding water is therefore higher. Flextensional transducers are

24

classified into different classes based on the shape of the shells (Royster, 1970). Some

of the seven classes have a convex shell and the others having concave shells were

invented later. The seven classes are shown in Fig. 2.4 (Jones, 1996; Jones *et al*. 1993,

1999) reported class I barrel stave transducers depth related performance   and

development of a broadband class III FT.

There has been an increasing interest in flextensional transducers, and this is reflected

by the growing number of research and review publications (Brigham and Glass, 1980;

Decarpigny, 1991; Jones, 1995; Rolt, 1990; Royster, 1970). Several theoretical

approaches have been used to model flextensional transducers. Brigham (1974) used a

longitudinal wave theory to model the stack, differential equations based on wave

mechanics to model the shell and elliptic radiation, and an infinite cylinder model for

the radiated pressure field. Finite element analysis has significantly reduced the effort

and time taken to develop flextensional transducers to meet stringent specifications

(Hamonic *et al.*, 1989).

Class IV transducer is the most extensively used FT. This is probably because of the

ease of design, manufacture, and assembly. Proprietary software based on a mechanical

model was employed by Oswin and Turner (1984) to prepare design curves. However,

all the details of the projector are not given, so it is not possible to verify the design

curves experimentally or by using other computational methods. Bose and Ebenezer

(2001a) reported design curves for class IV FTs with detailed dimensions of the

transducer for the frequency band of 1-4 kHz. The effect of major to minor axis ratio,

length of shell on the resonance frequency and TVR, were also reported.
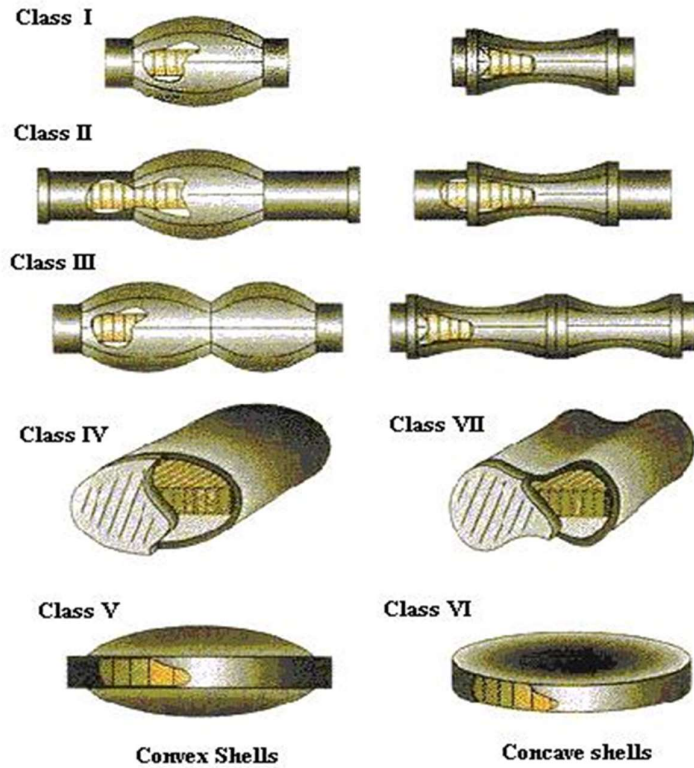
Fig. 2.4   Classes of Flextensional Transducers (Jones, 1996).

The shell is manufactured with different materials like aluminium, titanium and GRP. Aluminium is the most preferred shell material, but titanium (Oswin and Turner, 1984; Oswin, 1995), GRP (Brind, 1988) and carbon graphite composites (Bromfield, 1990) are also reported in the literature. Titanium has the advantage of the best depth and power handling capability and no need for any corrosion protective boot but its cost is very high, and the weight is more compared to Aluminium and GRP. Comparative merits and demerits of different shell materials are reported by Oswin and Turner (1995).

Hydrostatic pressure due to high depth of operations causes grave consequences to the structural integrity of flextensional transducers. In extreme cases, the shell may buckle.

The static stress compresses the elliptical shell along the minor axis and elongates along the major axis, resulting in the release of compressive bias applied on the piezoceramic stack. This significantly limits the operating power and depth of flextensional transducers. At stress levels more than the biasing stress, the driver stack gets released from the shell causing catastrophic failure of the transducer (Hardie, 1990). Even with the addition of stress bolt running through the piezoceramic stack, the maximum depth capability of flextensional transducers is limited to about 300 m (Boucher, 1996).

There are different techniques for pre-stressing the FT. In Class IV FT, the piezoceramic stack can be pre-stressed by applying a force along the minor axis of the shell, to elongate the shell along the major axis and then inserting the stack. The force is then removed to form an interference fit. The maximum stress induced in the shell is usually much greater than the applied stress and must not exceed the elastic limit for the shell.   Pre-stress can also be provided to the stack by driving a central wedge in the ceramic stack. In this technique, we have to reduce the number of ceramics to provide space for the wedge (Ponchaud, 1988). In both these methods, the shell is also required to undergo pre-stress. To avoid pre-stressing the shell, especially when it is made of glass reinforced polymer, the stack can be wrapped in fibre (Arnold and Bromfield, 1996) or pre-stressed using tie rods and a shell formed in the required shape is electron beam welded to the side plates (Dahlstrom, 1988). In this method, the stack is not accessible for any repair. The stack can also be pre-stressed with a central bolt (Boucher, 1996) but from maintenance and leakage point of view, this is not a good option. Bose and Ebenezer (2001b) estimated the pre-stress requirement and the interference required between the shell and stack for a class IV FT considering the operating depth and drive voltage. In this paper, various techniques used to pre-stress

the driver are discussed. A method to calculate the maximum voltage that can be applied to an FT, as a function of depth, for a particular pre-stress level is then presented. Numerical results obtained using ATILA are also presented to illustrate the method. Falcus (1994) reported the details of shell loading for ceramic stack insertion in a class IV FT by the uniform application of pressure on the shell surface.

Butler *et al.* (1997) developed a directional class IV FT and a six element line array by exciting the shell simultaneously in Omni and dipole mode by operating the stack into extensional and bending modes. A front to back ratio of more than 30 dB is achieved. The single element Omni mode produced an SL of 211dB and in directional mode SL of 215 dB when driven at 394 V/mm. The six element array produced an SL of 225 dB.

Moosad (2011) studied the class IV FT with a parabolic reflector for directional application and reported a front to back ratio of 21 dB. Anifrani (1990) developed a new type of class V FT using ATILA. The transducer consists of segmented rings to which octagonal rings are attached in the form of an inscribed polygon. Concave shells are connected to the segmented ring. McMahon *et al*. (1985) and McMahon (1990) reported class V ring shell projector with pressure compensation using a rubber bladder inside the projector.

Letiche and Scala (1990) reported a class V FT using a novel design incorporating a dynamic filter into the stack; it isolates the effect due to static load and the dynamic load generated by the piezoceramic stack. This filter has a unique property that its low stiffness at static conditions accommodates the shell deformation and retains the pre-stress. The stiffness of the filter increases under dynamic conditions provides necessary coupling between the stack and the shell. Flextensional transducers assembled with

dynamic filter have been tested as stable up to a depth of 500 m of water. Dufourcq *et al*. (1991) reported a similar concept of dynamic filter for a class IV FT.

2.2.5   Fluid-Filled FT

Moosad (2003) studied class IV FT filled with water and Silicone oil and reported fluid-filling increases the resonance frequency of class IV FT, but it helps to improve the bandwidth of the transducer at the expense of TVR. Ahmad *et al.* (1995, 1996) modelled free-flooded, and fluid-filled class I barrel stave FTs with convex shells. They have used 3D models using the FEM package PHOEBE. The free-flooded transducer results showed that the transducer produced a low power, high Q, and the device was an inefficient radiator. The first flextensional mode, caused by the piston mode of the stack, was absent because this mode needs a huge volume change. The compliant material inside the fluid-filled FT helped to improve the results. They used both water and Flourinert FC-72 as fill fluids and a closed cell polymer D300 as compliant material. Introducing the fluid and compliant material leads to the increase of resonance frequency, reduction in power output and increases the Q factor. Oswin and Steel (1990) reported a free-flooded Flextensional transducer with unlimited depth capability by introducing an additional shell cavity to the free-flooded FT using Helmholtz resonance. Armstrong and McMahon (1984) developed a pressure compensated class V FT of 349 Hz resonance and a source level of 205 dB. They reported that the resonance frequency of the gas compensated ring shell projector increases with increasing depth due to the decreasing compliance of the internal gas. Use of FTs beyond 500 m need complex pressure compensation devices, and fluid-filled FTs are much inferior to air backed FTs. Bonin and Hutton (1996) reported a barrel stave transducer filled with compressed air to increase the depth capability, but the resonance

frequency of the transducer increased 0.4 to 0.6 Hz/m. Yao *et al*. (1996) also reported a fluid-filled barrel stave transducer capable of withstanding upto 500 m depth.

2.2.6   Helmholtz Transducer

Helmholtz resonance is the phenomenon of air resonance in a cavity, such as when one blows across the top of an empty bottle. The name comes from a device created in the 1850's by Hermann von Helmholtz, the "Helmholtz resonator". Compact low-frequency underwater sound sources using piezoceramic drivers are feasible if the driver is incorporated into a Helmholtz resonator. The ceramic driver can be in the form of a spherical shell, a stack of rings, or a flexural-mode disk, but the disk is usually the most advantageous. A liquid-filled Helmholtz transducer is capable of operation at unlimited depths. When the depth requirement is only moderate, however, it is advantageous to replace part of the liquid in the compliance chamber by compliant tubes; this substantially reduces the size of the resonator (Woollett, 1975).

Acoustical oceanography and particularly acoustic tomography (measurement of the dynamic behaviour of the ocean) has needs for low frequency, high efficiency, broadband and great depth transducers. A Janus Helmholtz transducer consists of a piezoelectric ceramic stack inserted between two similar head masses (Scarpitta *et al*., 1996). This structure called a Janus driver is mounted inside a vented rigid cylindrical housing, providing a Helmholtz cavity. The coupling of mechanical resonance and fluid resonance permits a broad frequency bandwidth greater than two octaves. Galle *et al*. (1993a, 1993b, 1994, 1999) describe the frequency and depth capability optimisation of Janus Helmholtz transducers. Free-flooded projectors with the first resonance below 300 Hz are modelled, developed and measured. With compliant tubes in the cavity, Gall

et al. (1993a) demonstrated a depth capability of 1200m. The use of compliant tubes gives Helmholtz transducers a size and weight advantage over other piezoelectric transducers of similar power output (Henriquez *et al.*, 1980). A low frequency magnetostrictive JANUS transducer modelled using FEM is reported by Dubus *et al.* (1996).

2.2.7   Flexural Disc Transducer

Woollet (1976) developed flexural disk transducers for very low frequencies (<400 Hz). Performance calculations have been carried out for underwater transducers using tri-laminar disks of 1 m in diameter. The disks have various thicknesses, and they are employed in different configurations. The tri-laminar disks contain two layers of PZT4 ceramic, arranged so that flexural vibrations are excited piezoelectrically. The designs were intended for applications in the depth range of 200 to 300 m. The depth capability is achieved by use of liquid filled interiors containing compliant metal tubes. Another type of pressure compensated transducer uses a flexural disc attached to one end of a cylindrical cavity which is filled with oil, and the other end is closed with a membrane. This ensures an equal amount of hydrostatic pressure acting on both sides of the flexural disc. However, the cavity modifies the resonance pattern of the transducer. The required pattern can be achieved by properly adjusting the volume and compliance of the cavity. Fife *et al.* (1979) developed flexural disk transducer below 100 Hz to demonstrate potential very low frequency applications and limitations, and another at 250 Hz for evaluation of the power capabilities of large diameter (33 inches) mosaic disks. Tianfang *et al.* (2016) reported a deep water low frequency free-flooded bender disk transducer.

2.2.8 Other Type of Deep Submergence Transducers

A long life, deep submergence, wide frequency range hydrophone was developed by Grover (1971). The hydrophone has been divided into the sensor, preamplifier, and cable assembly. All joints have double 'O' ring seals. The piezoelectric element is double booted with butyl rubber as the water barrier. Each boot is filled with degassed, low water vapour castor oil. All the exterior metal parts are covered with an elastomer to minimise corrosion and to reduce the possibility of electrical crosstalk.

2.3 ACOUSTIC PERFORMANCE UNDER HYDROSTATIC PRESSURE

Acoustic performance of barrel stave transducer is affected by hydrostatic pressure. Jones and Moffett (1993) studied the effect of depth on a low-frequency barrel stave flextensional projector. The transmitting voltage response (TVR), mechanical quality factor 'Q_m', electrical admittance, and electroacoustic efficiency 'H_{ea}' were measured for driving voltages up to 5.0 kV$_{rms}$ at four depths: 30, 61, 91, and 123 m. At 5.0 kV$_{rms}$, the resonance frequency (fo) increased from 780 Hz to 840 Hz, 'Q_m' decreased from 4.4 to 3.3, and 'H_{ea}' decreased from 87% to 71%, as the depth was increased from 30 m to 123 m. Semenov et al. (1994) noticed weak dependence of resonance frequency and emitted power on depth in experiments at depth from 50-300 m on free-flooded ring transducers.

2.4 FLUID COMPENSATION

In the simplest form, the compensating fluid which fills an enclosure is balanced or equalised to all variations of ambient seawater pressure, thus reducing the differential pressure to approximately zero. A flexible moving interface, such as a bladder or diaphragm, is used to communicate external pressure into the compensating fluid and

allows system fluid to expand or contract. A further design consideration is to maintain a slight positive bias or above ambient pressure on the compensating fluid for applications where dynamic seals are employed. Should leakage occur, the rationale is to encourage outward leakage and minimise inward leakage (Mehnert, 1972).

2.4.1 Fluid Compensating Devices

There are different fluid compensating devices for deep submergence applications. A self-contained pressure compensating system has been developed for use with the USRD type Jll moving coil transducer at ocean depths to 600 ft. This system conserves compensating gas for uninterrupted use over a period of 8 hours or more. It responds to changes in depth by holding the pressure differential on the diaphragm of the transducer to less than 0.7 psi with negligible effect on the acoustic response. Nitrogen was used as the compensating fluid (Hugus, 1969). Mehnert (1972) explains the details of fluid compensating devices in the handbook of fluid-filled depth/pressure compensated systems for deep ocean applications, and Fig. 2.5 shows some of the devices.

2.4.2 Compensating Fluid

A fluid pressure compensating system must compensate for changing physical conditions, both ambient and internal. The design scheme used in sizing a compensator is to estimate the most severe volume changes which can occur for any foreseeable condition. The physical characteristics like compressibility over the working pressure range and the coefficient of thermal expansion must be known for a given compensating fluid. A compensating fluid should not suffer excessive volume "shrinkage" as a function of increasing pressure. The term "bulk modulus" is the reciprocal of

compressibility. Thus, a high bulk modulus is desirable. Fluid specific gravity or weight may add appreciably to system weight.

FLAT DIAPHRAGM

CONVOLUTED DIAPHRAGM

(a)

(b)

& VENT PLUG

SCREENED
SEAWATER
INLET

FLUID SUPPLY TO
RESERVOIR

(c)

(d)
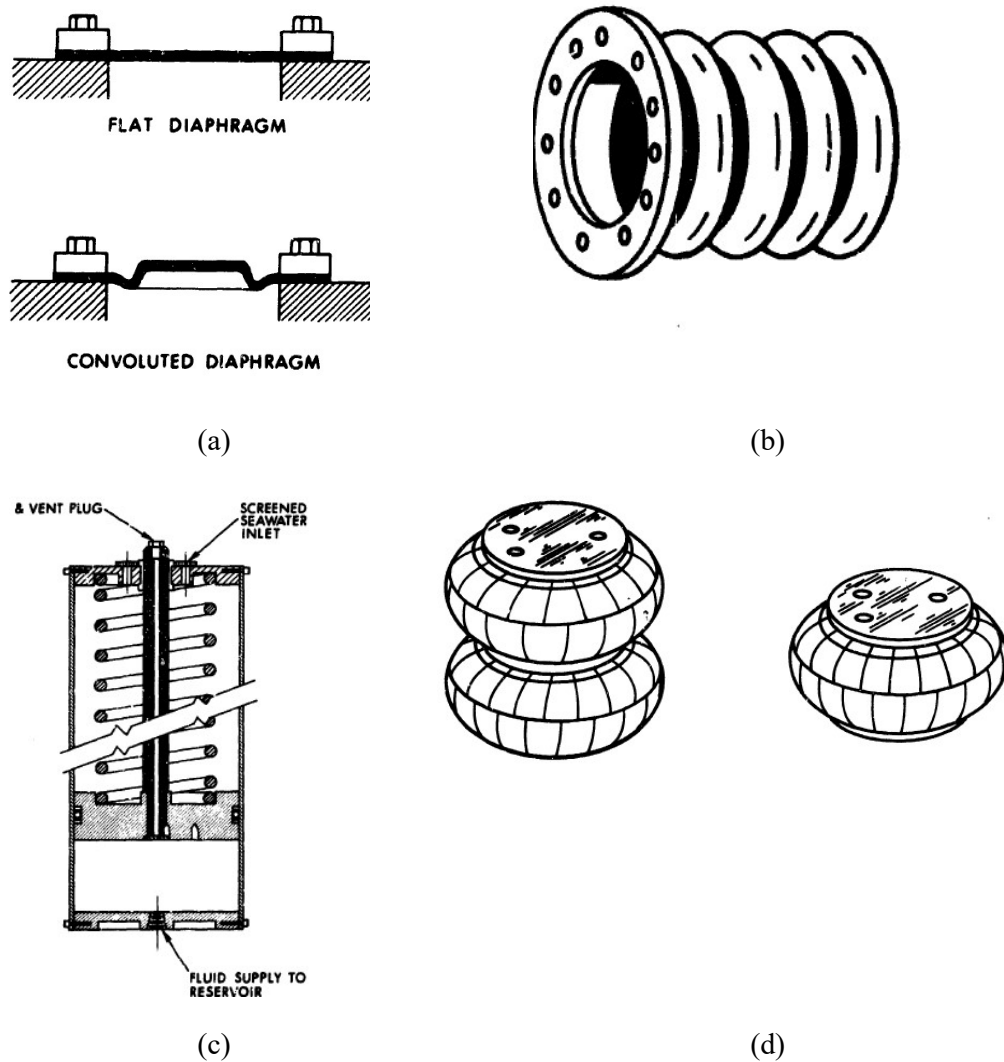
Fig. 2.5   Fluid compensating devices (a) Diaphrams (b) Bellows (c) Spring loaded piston (d) Pneumatic actuators (Mehnert, 1972).

2.4.3   Transducer Fill Fluid

Transducer fill fluids need to meet varied requirements like acoustic, electric compatibility with transducer materials, long-term stability, handling requirements, toxicity and cost (Capps *et al.,* 1981; Mehnert, 1972). In a high-frequency transducer, a

close acoustic impedance match with seawater may be of paramount importance. High volume resistivity is essential to avoid current leakage. This property may become relatively unimportant for low electrical impedance designs. Low vapour pressure is necessary to allow vacuum degassing of the fluid.

A relatively low viscosity is desirable to avoid air entrapment on filling the transducer. For moderately viscous substances, the air entrapment problem may be lessened if the viscosity decreases upon mild heating. Good compatibility with the materials in the transducer environment is necessary to assure long life. An acoustic impedance match with seawater may be important if the fluid is in the acoustic path and operation at higher frequencies is expected. Low acoustic attenuation is necessary but usually, comes into play only at high frequency. A low water solubility limit is required to resist water permeation. Stability to hydrolysis and oxidation, high surface tension to prevent oil creeping and wetting other surfaces, excellent handling properties are also desirable properties. Long-term compatibility can only roughly be estimated from short-term testing (Capps *et al.,* 1981).

The different approaches used for fluid-filling are gravity, forced or pressurised and vacuum filling. Although elaborate and time-consuming, vacuum filling is the more conservative filling method. Vacuum degassing and filtering of the compensating fluid is desirable for any approach. Fill procedures have several objectives. First and most important, is to remove all air and fill all voids in the unit. Most compensating systems are sized to make up the volume lost by compression of the fluid at high pressures, usually allowing for a small amount of trapped and dissolved air. Since the compressibility of air is many times that of liquid, any significant amount of air left in

the unit could cause the compensator to deplete prematurely thus collapsing the case. The second important reason for removing all air is heat transfer and helping the transducer to operate at higher power. It is important to keep in mind that the filling procedure must be carefully planned.

2.4.4 Fill Fluid Properties

The general fluid properties to be considered while selecting the fill fluid for optimum system performance are specific gravity, favourable viscosity characteristics over the range of environmental temperature and pressure, satisfactory lubricating ability, low compressibility, compatible with system materials, corrosion protection, high thermal conductivity, excellent heat transfer properties, good electrical properties, fire resistance, low volatility and high flash point. It should be compatible with conditions of use like low toxicity, easily handled, chemically and thermally stable, low vapour pressure, low gas solubility characteristics, low thermal coefficient of expansion, low foaming tendencies and commercial availability. Commonly used fill fluids and their advantages and disadvantages are given in Table 2.1 (Capps *et al.,* 1991; Mehnert, 1972). Apart from the above, Transformer oil, Motor oil, Flourinert and Flourolube are also used as fill fluids. Ultra Electronics (2014, 2017) in their free-flooded ring transducer models, uses either a polymerised Dimethyl Silicone oil or Castor oil as the fill fluid. Both oil types are inert; provide high dielectric strength and efficient acoustical coupling. Serviceability at high and low temperatures is excellent. This kind of oil has a long life and are in devices still in service even after 20 years.

Table 2.1   Commonly used fill fluids and their advantages and disadvantages.

Sl No	Type of fluid	Advantages	Disadvantages
1.	Castor oil	Good compatibility and acoustic properties	High viscosity
2.	Lubricin Castor oil	Low viscosity	Not compatible with many transducer materials
3.	Tricresyl phosphate	Fairly good impedance match, compatible with Low viscosity	Compatible with limited number of elastomers
4.	Poly alkaline glycol	Low thermal expansion	High water solubility, Not compatible with many transducer materials
5.	Dow Corning Silicone	Compatibility, low viscosity	Very expensive, poor acoustic match
6.	Isopar L /Isopar M / Norpar M	Buoyant	Incompatibility
7.	Polyalphaolefin	Low water solubility	Incompatibility with rubber
8.	Silicone Oil	Good compatibility	Expensive

2.5   SUMMARY

The literature survey is carried out to study different types of transducers and to identify the type of transducer that can be used for deep submergence applications. The studies reveal the relevance of free flooded or fluid-filled transducers over hard shell designed transducers like tonpilz and flextensional. Free-flooded ring transducers with direct over moulding and oil filled versions are reported for deep submergence applications. Fluid pressure compensating systems and different types of fill fluids are also studied. There are no published papers on the detailed design, manufacturing processes, assembly procedures, and acoustic performance of free flooded transducer variants under hydrostatic pressure. It is proposed to study these aspects of free flooded ring transducer variants in the present research.

CHAPTER 3

TRANSDUCER DESIGN METHODOLOGY

3.1   DESIGN CONSIDERATIONS

The transducer design process usually begins with the specification, which sets the resonance frequency, bandwidth, beam width, power, source level, operating depth as well as the approximate size and weight. To obtain high acoustic output over a frequency band, it is usually necessary to make the resonance occur near the centre of the band. A particular design might achieve the targeted resonance frequency, but it may not meet other requirements. Since a single transducer may not be capable of producing sufficient source level to meet the specifications, an array of transducers is used. At array level also there are a number of performance characteristics like source level, beam width, sidelobe levels in beam pattern, and impedance that are to be met (Waite, 2002; Heuter, 1971). The size and separation of elements in the array are decided based on the beam steering requirements together with other practical aspects such as size, weight and cost of the array. Various limiting factors like electrical power, cavitation, thermal and mechanical stresses are considered during the design stage. Other aspects like corrosion, sealing and cabling are also given due consideration. An iterative design approach is required to satisfy all the design goals. Interfacing the transducer with power amplifier needs due consideration for matching the impedance for maximum power handling and source level. Availability of test facilities to measure the acoustic performance and pressure withstanding capability are also important in the development of deep submergence transducers.

The operating frequency band for a particular application has a strong impact on the type of transducer required. If the transducer is to operate at low frequencies, designs

that have low resonance frequencies and manageable sizes like flextensional transducers are most suitable. At the other extreme of high-frequency operation, the transducers must be small and are usually the piezoelectric ceramic metal sandwich type or piezocomposite based (Howarth *et al.,* 1997, Ramesh *et al.,* 2006). The most common transducer for mid-frequency bands is the tonpilz composed of a stack of piezoelectric ceramic rings with a larger piston radiating head mass and a heavy metallic tail mass. These transducers are most often used to produce intense directional beams for submarine and ship transducer arrays. High output power and efficiency are of paramount importance for any projector of sound, which is hard to achieve if the wideband operation is also required. This leads to designs that have multiple resonances in the mass controlled region above resonance. Deep submergence requires transducers like free-flooded rings. The need for higher output has led to the development of the magnetostrictive material Terfenol-D, the electrostrictive material PMN, and the single crystal electrostrictive material PMN-PT. PMN-PT single crystals have displayed extremely high material coupling coefficient and transducer response compared with PZT ceramics (Zhengyao and Yuan-Ling, 2011; Tressler, 2006).

3.2 POWER HANDLING CAPABILITY

The factors which limit the acoustic power handling capability of a transducer and which are functions of the piezoelectric ceramics are reported by Berlincourt (1964). The factors according to him are the dynamic strength of the ceramic, reduction in efficiency due to internal dielectric losses, and mechanical losses, depolarisation of the ceramic due to an electric field, and temperature rise. Analytical procedures for predicting the power limits of piezoelectric and magnetostrictive transducers are reported by Woollet (1968). According to him the factors for the power limitations are

mechanical, thermal, electrical and cavitation. When the mechanical quality factor 'Q' of a transducer is less than the optimum value, the maximum power output of the transducer at resonance is electric field limited. When 'Q' is greater than this optimum value, the transducer power is stress limited (Moffet, 1993).

3.2.1 Cavitation

When the alternating acoustic pressure produced at the surface of a transducer is increased, the acoustic intensity increases and the peak pressure may reach a value equal to the ambient pressure. If the intensity is increased still further, the acoustic pressure peaks will exceed the ambient pressure and absolute pressure will be negative for part of the cycle. At this point, the medium begins to cavitate. It is found that on the negative half of the acoustic pressure cycle, bubbles form on the surface and just in front of the transducer. These bubbles tend to collapse when positive absolute pressure is re-established. The phenomenon of cavitation gives rise to various undesirable effects (Urick, 1983). The presence of a large number of bubbles near the transducer drastically reduces the radiation through it. The acoustic power is also lost by the creation of bubbles leading to a reduction of electroacoustic efficiency. If the high input power to the transducer is maintained for some time, the transducer may overheat and permanently damaged. Also, the violent action of bubbles collapsing at the surface of the transducer may cause surface erosion.

The theoretical cavitation threshold, at which cavitation may start, can be found by calculating the intensity, 'I', for which the peak acoustic pressure, p, reduces the absolute pressure to zero. Thus, the cavitation threshold is defined as $I = p^2/(2\rho c)$ where 'ρ' is the density and c is the sound speed of the medium. At sea level, the absolute

pressure is reduced to zero if the peak acoustic pressure is equal to $10^5\,\text{N/m}^2$. This gives a cavitation threshold intensity of $0.3\,\text{W/cm}^2$. For very pure water free of nuclei, the cavitation threshold can be much higher than the theoretical limit.

The cavitation threshold of a transducer may be raised by increasing the frequency, decreasing the pulse length, or increasing the depth. The process of bubble formation during the cavitation process requires a finite time. As the frequency is increased the period of negative pressure become shorter and the cavitation threshold rises. The frequency dependence is small below 10 kHz, but after that, the cavitation threshold increases rapidly as frequency increases. The cavitation threshold can be increased by reducing the pulse length below about five milliseconds (Urick, 1983).

The effect of an increased depth of operation is to increase the ambient pressure. The cavitation threshold at depth 'h' becomes, $I_c = 0.3(1.8 + h/10)^2$ W/cm^2. From this, the maximum acoustic power, P, that a transducer can radiate at the onset of cavitation may be estimated by using the relationship $P = I_c A$, where 'A' is the radiating surface area (Stansfield, 1990).

3.2.2 Mechanical Limitation

Driving a transducer with high power input levels leads to large dynamic stresses. Beyond a certain power, one may exceed the maximum rated dynamic stress of material and at this point, the material is liable to fail. Depending on the transducer design, the failure will most likely occur within a ceramic element or at the glue joint between two materials, which is a point of tensile weakness. The mechanical limitations of transducers operating in the low and medium frequency range can usually be

counteracted by using mechanical bias (Miller, 1960, 1963, 1989). The application of mechanical bias depends on the transducer design. However, a conventional method is to run a centre bolt through the middle of the transducer and apply the desired torque. The maximum mechanical bias tolerated is dependent upon the ceramic composition and the orientation of the stress. The maximum compressive stress and the dynamic stress allowed for the Morgan ceramics PZT4 and PZT8 ceramics are 520 MPa (Berlincourt *et al.*, 2010). Woollett (1962) suggests a dynamic stress limit of 40 MPa for PZT. Pre-compression to the tune of 240 MPa is applied to offset the loss of compression due to hydrostatic pressure as in the case of flextensional transducers (Butler and Rolt, 1994). Maximum stress is decided by taking into consideration the fatigue. The dynamic strength of piezoelectric ceramics is dependent upon configuration and perfection of fabrication.

"The mechanical, electrical, thermal or acoustical phenomena which limit the available power need to be controlled. To determine the mechanical limitations of a transducer, knowledge of both the mechanical limit of the materials and the stress field in the structure is essential. Although there are many experimental data available to designers, the classical transducer models are restricted to simple geometries" (Dubus *et al.*, 1991). They have used the finite element code ATILA to compute the stress field, so that a comparison with the mechanical limit of the material can be carried out. The method was then applied for the analysis of the mechanical behaviour of a length expander transducer. The problem of interest is the application of pre-stressing, as well as the dynamic behaviour at high drive levels. In both cases, excellent agreement was found when the computed results were compared to strain gauge measurements.

3.2.3 Electric Field

The maximum electric field that can be applied to a transducer is ultimately limited by the composition of the ceramic employed. The electric field strength required to depole PZT4 and PZT8 ceramics at room temperature is 1000 $kV_{r.m.s.}m^{-1}$. However, an electric field sufficient to cause depolarisation produces extremely high dielectric losses and therefore low efficiencies. Thus, such fields are appreciably larger than normally applied in practice. For most piezoelectric transducers, the critical limiting factor is the electrical breakdown of the ceramic. The potential that can be safely applied to a dielectric material is finite. When the threshold value is exceeded, sparking and dielectric breakdown occurs. However, electrical failure is usually more likely to be caused by flashover between the electrodes. Flashover takes place through the air, or more probably, across the surface of the ceramic, where the dielectric strength would have been degraded with the presence of grease, dirt, or moisture.

DeAngelis *et al*. (2016) has reported that PZT4 might be best suited for continuous drive ultrasonic power applications, where maximum drive amplitude is less important but less heating, and lower impedance is more desirable. The limiting electric field which can safely be applied to a transducer depends on the material properties of the ceramic and the method of construction. Woollett (1968), Moffet and Clay (1991) recommends a limiting field of 400 $kV_{r.m.s.}m^{-1}$ for lead zirconate titanate ceramics. Stansfield (1990) suggests a more conservative figure of 200 $kV_{r.m.s.}m^{-1}$. The safe voltage limit recommended for CW (continuous wave) application of PZT4 is 120 $kV_{r.m.s.}m^{-1}$ and 300 $kV_{r.m.s.}m^{-1}$ for PZT8. For a long-term application with a 20% duty cycle, 350 $kV_{r.m.s.}m^{-1}$ is also reported (Butler and Rolt, 1994).

3.2.4 Thermal Limitation

While mechanical and dielectric losses adversely affect efficiency, usually of greater concern is the temperature rise, they cause in high duty cycle or CW operation of the transducer (Woollett, 1962). Under such conditions, the transducer is likely to be thermally limited. That is, the dielectric and mechanical losses result in the generation of heat within the ceramic material. If the temperature reaches the Curie point of the material, it will spontaneously lose its piezoelectric properties. In practice, the temperature of the ceramic material must be kept well below this critical point to avoid degradation of the piezoelectric properties. Thus, the temperature limitation may require a lower driving field to be employed than that for low duty cycle operation. The Curie point and maximum operating temperature for PZT4 and PZT8 ceramics are 328 and 300 °C (Berlincourt, 2010). In practice, non-reversible damage may occur in the electrically passive materials before the ceramic is affected. For example, epoxy resin glue, often used in transducer construction, can denature if exposed to temperatures greater than 80 °C for any significant length of time. The danger of overheating can be minimised by choosing a ceramic with low internal losses. The mechanical and dielectric loss factors for PZT4 ceramics are 0.002 and 0.004 and that for PZT8 ceramic are 0.001 and 0.004. The low losses of the Navy Type III composition, much lower than Navy Type I ceramics at high drive levels, make it particularly well suited to CW operation in high power transducers.

The power limits imposed by the water medium can be dropped in this study as we are considering the depth of water around 1000 m. We are left with an electrical limit, a mechanical limit, and a thermal limit. By assuming low duty cycle operation, we can ignore the thermal limit and concentrate on the electrical and mechanical limits.

3.3   ENCAPSULATION AND WATERTIGHT INTEGRITY

Water and water vapour are responsible for most failures in underwater transducers. Designers have sought materials that have low water vapour permeability and metals that do not corrode. The water barriers and acoustic windows of earliest sonar transducers and hydrophones were natural rubber. Failure rates of transducers were high as a result of high water vapour permeability of natural rubber and the water solubility of Rochelle salt and Ammonium Di-Hydrogen Phosphate. Even a minute amount of water vapour caused surface electrical leakage and low electrical resistance while larger quantities of water dissolved the crystals (Groves, 1971).

Neoprene replaced natural rubber in many transducer applications because of its advantage of superior resistance to oil and weather, but it provided only slight reduction in water permeability. Butyl rubber is now widely used because of its much better water permeability compared to natural rubber, neoprene or polyurethane. Butyl rubber is not difficult to mould or to bond to metal parts when the mould is properly designed, and the correct primer is used on the metal. The disadvantage of using butyl rubber for encapsulation is its change in sound speed with lower temperature. It changes from 1630 m/sec at 25 °C to 1985 m/sec at 5 °C. For the same temperature range, it changes from 1518 m/sec to 1578 m/sec in natural rubber. The sound speed in seawater changes in the opposite direction as temperature decreases, going from 1570 to 1510 m/sec. The acoustic impedance mismatch is not as severe as these figures might imply, because at audio and low ultrasonic frequencies, the elastomer thickness is small in comparison with a wavelength, and with a wall thickness of 6.35 mm do not affect the response seriously, as long as the acoustic window is of uniform cross-section, and the upper frequency is not higher than 40 kHz. A thinner wall can permit operation to higher

frequencies (200 kHz), but usually with some change in response characteristics as a function of temperature (Groves, 1971).

Polyurethane (PU) is also widely used as an encapsulant since it can be moulded at room temperature and does not need any heavy moulds as in the case of rubber. Many polyurethane compounds are readily available in the market for the encapsulation process. Adhesion with different materials like PZT, metals, FRP, and neoprene is a challenge, and at times this can be a problem as well. However, there are adhesion-promoting compounds, which can solve these issues. In applications like free-flooded ring transducers PU is an ideal option, but when there are multiple joints for the transducers like tonpilz, it is better to go for rubber moulding. Williams *et al.* (2013) reported various aspects of urethane-based potting of acoustic transducers. The oil filled rubber boot is another option for the housings of deep submergence transducers. For deep sea applications oil filled rubber boot gives some advantage over direct moulding of PU, like higher source level and better maintainability.

3.4 CABLES

Neoprene is the outer jacket on many cables because it is tough, flexible, and abrasion resistant. Polyethylene, also, has many superior qualities as an insulating material and as jacketing on underwater cables. It stands up well in the sea environment. The electrical resistance is high, and the water permeability is low. Usually, polyethylene jackets are colour pigmented to protect them from ultraviolet radiation. Butyl rubber is an excellent insulating material with low water vapour permeability. Butyl has excellent weathering properties and heat resistance, but it does not perform well when exposed to mineral oil or some silicone fluids. Compatibility of cable outer sheath with

transducer encapsulant for moulding to be checked before deciding the type of cable if it is to be integrated with the transducer housing as a pigtail. Otherwise, compatibility with the connector needs consideration.

3.5   CONNECTORS

In an application like sonar system, there can be hundreds or thousands of transducers. Each of them needs a connector for electrical input. Connectors, junction boxes and connector chains are another area, which needs some major consideration. One can use a simple built-in rubber moulded connector on the casing or a metallic connector. Rubber connectors and connector chains are cost efficient and have a long life if made properly. Metal connectors can be used as an off the shelf item with less complicated housing for the transducer. Figs. 3.1 and 3.2 show rubber connector, connector chains and metallic connector.

3.6   CORROSION RESISTANCE

Corrosion is another aspect the designers need to consider seriously during the design and selection of materials that are exposed to seawater. Detailed information is available in the literature about the selection and performance of materials in the marine environment. Titanium can be considered for housing material because of its excellent corrosion resistance.   Some Aluminium alloys also have excellent corrosion resistance in seawater.

3.7   TRANSDUCER MODELS

Design of transducer to meet the performance parameters such as resonance frequency, transmitting and receiving sensitivities, bandwidth and power handling capability

depend on many factors. Historically, designs for such transducers were carried out with one-dimensional (1-D) equivalent circuit models. These 1-D tools provide only approximations of transducer behaviour based on simplified, lumped circuit representations of transducers using inductors, capacitors, and resistors. The resulting models do not accurately represent the actual characteristics and multiple degrees of freedom of complex transducers. This leads to the manufacture and testing of many prototypes until we get the desired specifications (Clayton, 2009). Finite element modelling is the best alternate option for the design and development of transducers with a minimum number of prototypes to finalise the design.
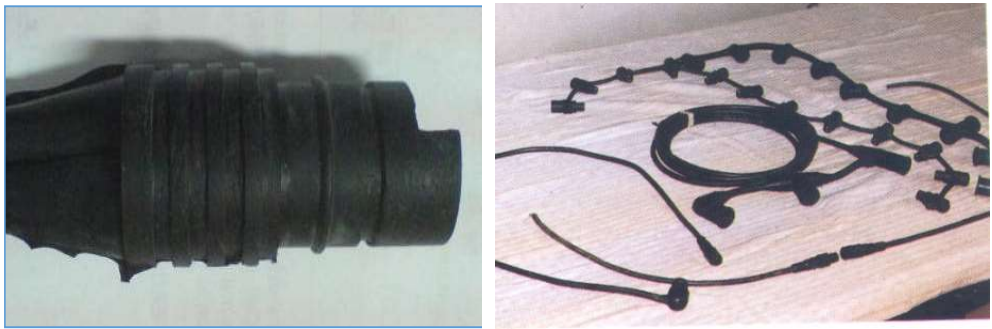
Fig. 3.1   Rubber connector and connector chains.

Fig. 3.2   Metallic connectors.

3.7.1 Finite Element Modelling

The finite element method (FEM) is widely used to solve complex engineering problems. The method was first developed in 1956 for the analysis of aircraft structures. Within a decade it was recognised that the finite element technique could be applied to the solution of many other classes of problems. The development of a numerical treatment for piezoelectric elements has allowed the finite element method to be applied to the field of electroacoustic transducer design. Transducer designers are currently using this method extensively to model different types of transducers. Easily accessible high-speed computers with large memory and user-oriented finite element computer programs that include piezoelectric, magnetostrictive, moving coil, and acoustic radiation elements have revolutionised the design of transducers. It is possible to develop and design complicated transducers and predict results to agree very well with measured results if accurate material properties are known (Sherman and Butler, 2016).

There are specific numerical analysis packages currently available that are dedicated to the design of electroacoustic transducers. The structure of a finite element or boundary element package involves three distinct modules.

- Pre-processor module
- Solver and
- Post-processor module

The pre-processor module deals with all the information necessary for the analysis of the problem. The module must accomplish three functions (1) description of the geometry of the object (2) mesh generation and (3) definition of the regions and the boundaries. The postprocessor module outputs the relevant information. The module

must perform two tasks (1) extraction of significant information and (2) graphical presentation of numerical data.

3.7.2 FEM Based Piezoelectric Transducer Design

The FEM based piezoelectric transducer design, in the beginning, focused on the vibration analysis. As the FEM technique and the computation technique improved, much more analysis can be done. The finite element acoustic medium uses fluid elements that describe the pressure field with pressure values at the nodes of the elements, in contrast to the mechanical elements with displacement values at the nodes. Consequently, a fluid surface interface, FSI, element is needed to join the mechanical and fluid elements at the surface of the transducer and its housing. At the outer side of the fluid field, the acoustic impedance matched absorbers are often used to satisfy the radiation condition of no reflection from the far field. Three-dimensional acoustic fluid elements are available that can satisfy all three conditions of the interface, fluid element, and absorber. There are also special spherical elements that apply infinite acoustic continuation of the wave in addition to absorbing the wave. These spherical wave elements require a spherical fluid field with a specific coordinate centre (Bossut, 1989). FEM can be used to predict resonance frequencies, vibration modes, stress distribution, the amplitude at all nodes, the impedance, the transmitting voltage response and receiving sensitivity and directivity patterns.

3.7.3 ATILA

ATILA is a finite element software package specifically developed for the analysis of sonar transducers. It permits the static, modal, harmonic and transient analysis of piezoelectric transducers. It can perform analysis of axisymmetric, two or three-

dimensional structures. Depending on the problem, it provides the displacement field, stress field, near-field and far-field pressures, transmitting voltage response, directivity patterns and electrical impedance. Pre-processor, PREATI or GiD can be used for the description of the geometry, creation of the mesh and data file preparation. Graphic display of the distorted structure, voltage response or directivity pattern can be obtained from the post-processing tools. The post-processing tool can also be used for animated views of the vibrating structure and plotting contours of constant values like displacement, pressure, potential, and stresses. ATILA has an integrated materials database which contains a set of materials that are available in the market. Materials can also be added to this database by entering values for the characteristics of the materials (ATILA users manual, 1997).

3.7.4   MAVART

MAVART is an acronym representing mathematical model for analysis of the vibrations and acoustic radiation of transducers. MAVART can model the steady-state response of a piezoelectric driven body immersed in an acoustic fluid of infinite extent. The variables, for example, displacement, are assumed to vary sinusoidally at a specified frequency. MAVART assumes that the geometry has infinite fold axial symmetry, but it can accurately model transducers having moderate deviations from this symmetry, such as the ring shell projector if appropriate material modifications are made. The complex solution returned by MAVART comprises displacements at solid nodes, pressures at fluid nodes and voltages at nodes having an electrical degree of freedom. This solution is post-processed to give the far field transmitting response, directivity pattern, electrical impedance, stresses and strains at solid nodes, near-field pressures and pressure gradient in the fluid (McMahon and Skiba, 1991).

Armstrong and McMahon (1984) reported the finite element modelling and performance of ring shell projectors, a class V type of flextensional projector using MAVART. A ring shell projector can be used near its resonance frequency as a high power source, or as a moderate power broadband source. The ring shell projector designed has a resonance frequency of 349 Hz, a mechanical Q factor of 10.6 and a source level of 205 dB. Finite element predictions of the transmitting response and admittance show good agreement with the measured values.

3.7.5   PHOEBE

PHOEBE is a three-dimensional transducer analysis package. This software, which runs on an IBM compatible personal computer in the MS-DOS environment, was developed by Francis *et al*. (1996) at the University of Birmingham. PHOEBE uses a combined finite element and boundary element method that permits in air and in water modelling. Twenty node quadratic isoparametric brick elements are implemented for the finite element mesh and the exposed faces of these elements, which represent the radiating face of the structure, are the boundary elements. (Meglio and Francis, 1996).

3.7.6   ANSYS

Using the direct coupled field analysis capabilities of ANSYS Multiphysics software, based on finite element analysis can be used to quickly and effectively arrive at optimal transducer designs without the delays, guesswork, and inaccuracies of other methods. ANSYS simulations include the effect of water loading for acoustic performance predictions. ANSYS utilises a full 3-D simulation of the transducer with piezoelectric, mechanical and acoustic formulations to characterise dynamic responses of the transducer. Fluid-structure interaction (FSI) and acoustic elements model water loaded

behaviour in determining attributes such as frequency dependent beam patterns, directivity, transmit power and receive sensitivity (Clayton, 2009).

3.7.7 PAFEC

The program, PAFEC (Program for Automatic Finite Element Calculations), was developed, at the mechanical engineering department at Nottingham University in 1976 (Macey, 2001). Originally the capability was for stress, vibration, and thermal analysis and extended for underwater shock analysis and steady-state harmonic analysis. Further functionality was added, extending the application areas, and user base, to sonar, audio, automotive and other sectors. In PAFEC Vibro Acoustics the fluid medium is modelled with acoustic finite elements, wave envelope elements, and boundary elements. It is often important to include the interaction with a structure, which may be the source, receiver, or may be an important boundary condition for the acoustic region. This can be modelled with a wide range of structural finite elements. The structural and acoustic models can be uncoupled or fully coupled.

Brind (1988) has analysed a low-frequency flextensional transducer made of GRP using PAFEC. He has used 3D modelling for the in-air and in water analysis. Prediction of in-air fundamental frequency was in reasonable agreement. The prediction for the in-water fundamental frequency was made using the PAFEC fluid loading elements and was in excellent agreement with measured values. Effect of hydrostatic pressure on depth capability of the transducer was also analysed and matched with that observed in the prototype transducer. He also studied stress distribution in the transducer due to interference fitting of the stack and ambient pressure. Gallahar (1995) studied an array of free-flooded rings using PAFEC to predict the performance.

3.7.8   PZFlex

PZFlex is a time domain finite element program for solving piezoelectric, ultrasonic and wave propagation problems developed by M/s Weildinger Associates Inc, USA. It can be used to model sonar systems and imaging systems using piezoelectric transducers. It can also be used for modelling 1-3 and 2-2 piezocomposite transducers, noise and vibration control studies and wave propagation studies. Models can be made in 2D plane strain, axisymmetric or 3D. Isotropic elastic, anisotropic elastic, piezoelectric or nonlinear, viscoelastic damping materials can be modelled. PZFlex works in the time domain, broadband response of a device can be computed with a single computation instead frequency by frequency. It can handle a large number of elements depending on the capability of the computer used (PZFlex, 2017).

Commercially available FE packages are widely used for the analysis of sonar transducers. Table 3.1 shows a list of FEM related papers that modelled different type of transducers. The table indicates the type of transducer, parameters determined by FEM, analysis type, number of degrees of freedom, geometry solved and software package used. It can be seen that the most widely reported software is ATILA. Problems reported in the papers include modal and harmonic analysis for the in air and in water analysis using 2D and 3D geometries.

Table 3.1   FEM based papers on analysis of transducers.

No.	Application/ Device	Parameters determined by FEM	Geometry solved	Analysis Type	Degrees of freedom	FEM Package
1.	Piezoceramic ring (Li *et al.,* 2001)	Resonance frequency, Mode shapes, Impedance.	2 D axisymmetric	Modal and Harmonic	Ux, Uy, and Φ (2 translations, electrical potential).	ANSYS
2.	Piezoceramic ring (Ramesh and Ebenezer, 2005)	Resonance frequency. Admittance	2 D axisymmetric	Modal and Harmonic	Ux, Uy, and Φ (2 translations, electrical potential).	ATILA
3.	Cymbal transducer (Haijun *et al.,* 2010)	Admittance, Transmitting Voltage Response(TVR), Receiving Sensitivity (RS)	2 D axisymmetric	Harmonic	Elastic elements-Ux, Uy PZT- Ux, Uy, and Φ Fluid- Pressure FSI- Pr on Fluid side Ux, Uy on structure side	ANSYS
4.	Free-flooded ring (Gallahar, 1997)	TVR Directivity	3D	Harmonic	Elastic elements-Ux, Uy, Uz PZT- Ux, Uy, Uz and Φ Fluid- Pressure FSI- Pr on Fluid side Ux, Uy, Uz on structure side	PAFEC
5.	Langevin Transducer (Iula *et al.,* 2002)	Resonance frequency Axial and radial displacements	2 D axisymmetric/ 3D	Harmonic	Elastic elements-Ux, UY for 2D Ux, Uy, Uz- 3D PZT-UX, Uy/ Ux, Uy,,Uz and Φ	ANSYS
6.	Flextensional Transducer (Hamonic *et al*., 1989)	Resonance frequency, Displacement and pressure TVR, Directivity	2 D axisymmetric	Modal and Harmonic	Elastic elements-Ux, Uy, Uz PZT- Ux, Uy, Uz and Φ Fluid- Pressure FSI- Pr on Fluid side Ux, Uy, Uz on structure side	ATILA
7.	Tonpilz Transducer (Kai *et al*., 2011)	TVR Conductance	2 D axisymmetric	Modal and Harmonic	Elastic elements-Ux, Uy, Uz PZT- Ux, Uy, Uz and Φ Fluid- Pressure	ANSYS

					FSI- Pr on Fluid side Ux, Uy, Uz on structure side	
8.	Stepped Horn Transducer (Xu *et al.,* 2007)	Resonance frequency Impedance Displacements	2 D axisymmetric	Harmonic	Ux, Uy, and Φ (2 translations, electrical potential).	ANSYS
9.	Wideband multimode tonpilz transducer (Chhith and Roh, 2009)	Transmitting Voltage sensitivity (TVR)	2 D axisymmetric	Harmonic	Ux, Uy, and Φ (2 translations, electrical potential). Fluid- Pressure FSI- Pr on Fluid side Ux, Uy, Uz on structure side	ANSYS
10.	Class V flextensional transducer (Blottman, 1990)	Resonance frequency, mode shapes Admittance, TVR, directivity	2 D axisymmetric	Modal and Harmonic	Ux, Uy, and Φ (2 translations, electrical potential). Fluid- Pressure FSI- Pr on Fluid side Ux, Uy, Uz on structure side	ATILA
11.	Fluid-filled flextensional transducer (Ahmad *et al.*, 1995)	Resonance frequency, mode shapes	3D	Modal	Ux, Uy, and Φ (2 translations, electrical potential).	PHOEBE
12.	Cymbal Transducer (Zhang *et al.*, 1999)	Resonance frequency, displacements	2 D axisymmetric	Modal	Ux, Uy, and Φ (2 translations, electrical potential).	ATILA
13.	Transducer Array (Butler *et al.*, 1997)	Transmitting Voltage sensitivity (TVR) and Directivity	2D	Harmonic	Ux, Uy, and Φ (2 translations, electrical potential). Fluid- Pressure FSI- Pr on Fluid side Ux, Uy, on structure side	ATILA
14.	Barrel Stave Transducer (Jarng, 2003)	TVR displacement and Directivity	3D	Harmonic	Ux, Uy, and Φ (2 translations, electrical potential) Fluid- Pressure FSI- Pr on Fluid side Ux, Uy, Uz on structure side	ATILA

15.	Cymbal Transducer (Erman, 2003)	Displacements, Resonance frequency, Admittance	2 D axisymmetric	Harmonic	Ux, Uy, and Φ	ANSYS
16.	1-3 composite transducer (Ramesh *et al.*, 2006)	Resonance frequency Mode shapes, RS Impedance	3D	Modal and Harmonic, Hydrostatic	Ux, Uy, Uz and Φ	ATILA
17.	Flextensional transducer (Anifrani, 1990)	Transmitting Voltage Response	2D	Harmonic,	Ux, Uy, and Φ (2 translations, electrical potential)	ANSYS
18.	Tonpilz Transducer (Desilets *et al.*, 1999)	Resonance frequency Mode shapes Impedance	2D axisymmetric and 3D	Modal	Ux, Uy, and Φ for 2D Ux, Uy, Uz and Φ for 3D	PZ Flex
19.	Low frequency Projector (Cymbal Transducer) (Naidu *et al.*, 2010)	Receiving Sensitivity, TVR, Resonance frequency	2 D axisymmetric	Harmonic	Ux, Uy, and Φ (2 translations, electrical potential).	ATILA
20.	High Power Ultrasonic Transducer (Pak *et al.*, 2008)	Resonance frequency, Mode Shapes	2D axisymmetric and, 1/4th 3D and full 3D	Modal Harmonic,	Ux, Uy, Φ, and Thermal for 2D Ux, Uy, Uz, Thermal and Φ for 3D	ANSYS
21.	Class IV Flextensional transducer (Moosad, 2003)	TVR Directivity, Resonance frequency, mode shape	2 D	Harmonic	Ux, Uy, and Φ Fluid- Pressure FSI- Pr on Fluid side Ux, Uy, on structure side	ATILA
22.	Free-flooded ring (Kuntsal, 2003)	Resonance frequency, Admittance, TVR Directivity	3D	Harmonic	Elastic elements-Ux, Uy, Uz PZT- Ux, Uy, Uz and Φ Fluid- Pressure FSI- Pr on Fluid side Ux, Uy, Uz on structure side	ATILA
23.	Janus-Helmholtz Transducer (Gall *et al.*, 1993)	Resonance frequency, Conductance, TVR	3D	Harmonic	Elastic elements-Ux, Uy, Uz PZT- Ux, Uy, Uz and Φ Fluid- Pressure FSI- Pr on Fluid side Ux, Uy, Uz on structure side	ATILA

24.	Hydrophone (Zhang, 1995)	Receiving Sensitivity, Directivity	2D axisymmetric		Elastic elements-Ux, Uy, PZT- Ux, Uy, and Φ Fluid- Pressure FSI- Pr on Fluid side Ux, Uy, on structure side	ANSYS
25.	Tonpilz Transducer (Boucher, 1990)	Resonance frequency Mode shapes TVR,	2D axisymmetric	Modal Harmonic	Elastic elements-Ux, Uy, PZT- Ux, Uy, and Φ Fluid- Pressure FSI- Pr on Fluid side Ux, Uy, on structure side	ATILA
26.	Cymbal Transducer (Dogan, 2006)	Receiving Sensitivity, TVR, mode shape, Resonance frequency	2 D axisymmetric	Harmonic	Elastic elements-Ux, Uy, PZT- Ux, Uy, and Φ Fluid- Pressure FSI- Pr on Fluid side Ux, Uy, on structure side	ATILA
27.	Flextensional Transducer (Bose and Ebenezer, 2001a)	Resonance frequency Transmitting Voltage Response (TVR)	3D	Modal Harmonic	Elastic elements-Ux, Uy, PZT- Ux, Uy, and Φ Fluid- Pressure FSI- Pr on Fluid side Ux, Uy, on structure side	ATILA

3.8 ACOUSTIC MEASUREMENTS

Reliability and long life of transducers can be achieved only by proper design, selection of components, manufacturing process, inspection and testing at various stages of manufacture and assembly. All the transducers assembled in the current study are subjected to a series of tests during component selection, ceramic stacking, sub-assembly and final assembly before it is cleared for in water acoustic measurements. Ceramics and stacks are inspected for dimensional accuracy and specifications like capacitance, resonance frequency, conductance and insulation resistance. Stacks are pre-stressed before wiring and encapsulation. The major parameters measured in water are resonance frequency, impedance, Receiving Sensitivity (RS), Transmitting Voltage Response (TVR), Source Level (SL), Power handling, and Directivity. Measurement procedure as per IEC 60565 (2006) is followed for acoustic measurements. LCR meter can be used for capacitance measurement, Megger for insulation resistance and impedance analyser to measure the resonance frequency and impedance.

3.8.1 Receiving Sensitivity

Receiving Sensitivity (RS) is the ratio of the open circuit voltage of the hydrophone to the sound pressure in the undisturbed free field in the position of the reference centre of the hydrophone if the hydrophone were removed. It is calculated by measuring the sound pressure at a point in the sound field, generated by the auxiliary projector, with a calibrated standard hydrophone and then the calibrated hydrophone is replaced by the unknown hydrophone. The ratio of the open circuit voltages of the two hydrophones is equal to the ratio of their free field sensitivities. The measurement setup for the RS measurement is shown Fig. 3.3.

59
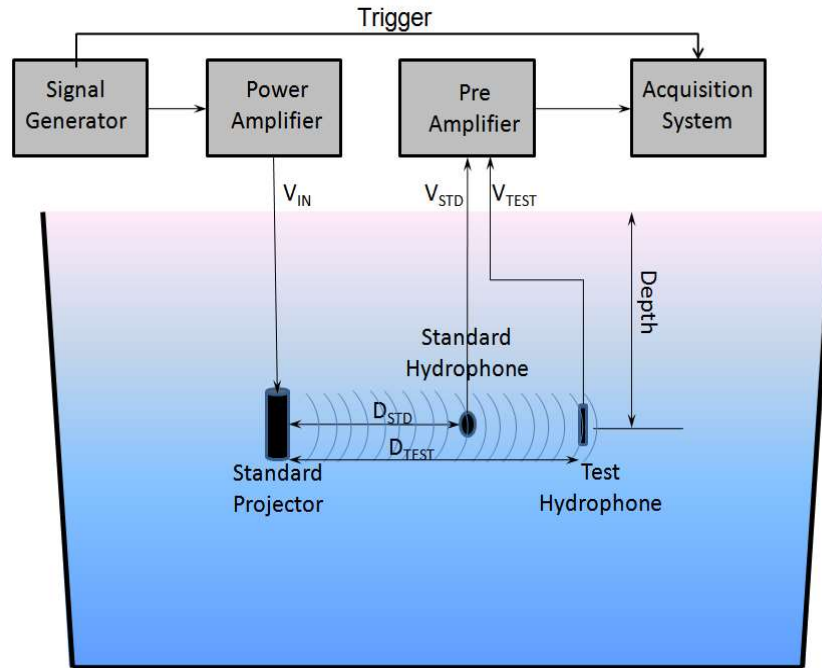
Fig. 3.3   Setup for Receiving Sensitivity measurement.

The projector, test hydrophone, and standard hydrophone shall be lowered in the tank to the same depth and preferably at the centre of the tank. Transducers shall be lowered such that the main response axis of the transducers should be aligned and face to each other always. The separation between the transducer should be determined based on the far-field criteria. The signal used for the testing shall be either a pulsed sine wave or a half sine pulse. A sufficient number of frequencies shall be chosen to ensure that the hydrophone performance is well characterised over the desired frequency range. Measuring the open circuit voltage of the test hydrophone and standard hydrophone, RS can be calculated using the following equation.

$$Receiving\ Sensitivity\ = \frac{OCV_{TH}}{OCV_{SH}}\frac{d_t}{d_s}M_0 \tag{3.1}$$

where, OCV_{TH} is the open circuit voltage of the test hydrophone, OCV_{SH} is the open circuit voltage of the standard hydrophone, d_t is the distance between the projector and test hydrophone, d_s is the distance between the projector and standard hydrophone and M_o is the sensitivity of standard hydrophone.

3.8.2 Transmitting Voltage Response

Transmitting Voltage Response (TVR) is the ratio of the sound pressure apparent at a reference distance in a specified direction from the acoustic centre of the transducer to the voltage applied across the electric input terminals. It is calculated by measuring the sound pressure generated by the projector at a point in the sound field with a standard hydrophone and taking the ratio of the voltage applied to the projector. The projector under test and a calibrated hydrophone shall be lowered to the tank at the same depth. Transducers shall be lowered such that main response axis of both the transducers shall be aligned and face to each other always. The depth of operation should be determined according to the actual operating conditions of the projector and separation between the transducer shall be determined based on the far-field criteria. A sufficient number of frequencies shall be chosen to ensure that the transducer performance is well characterised over the desired frequency range. Test setup for the TVR measurement is shown in Fig. 3.4.

TVR can be calculated using the following equation,

$$\text{Transmitting Voltage Response} = \frac{OCV_{SH}}{V_T}\frac{d}{M_0} \tag{3.2}$$

where, OCV_{SH} is the open circuit voltage of the standard hydrophone V_T is the voltage applied to the test projector, d is the distance between projector and standard hydrophone and M_o is the sensitivity of standard hydrophone.

3.8.3 Source Level

Source Level of a transducer is its output sound pressure level at one-meter distance in decibels referenced to 1 µPa. Source level and power handling capacity are to be measured at the specified frequencies using the setup for TVR measurement. Source level can be calculated using the equation

$$Source\ Level = (20 \times \log_{10}(V_h\ d)) - M_0 \qquad (3.3)$$

Where V_h is the rms voltage of hydrophone signal, d is the distance between the projector and standard hydrophone in meter, M_o is the sensitivity of standard hydrophone.
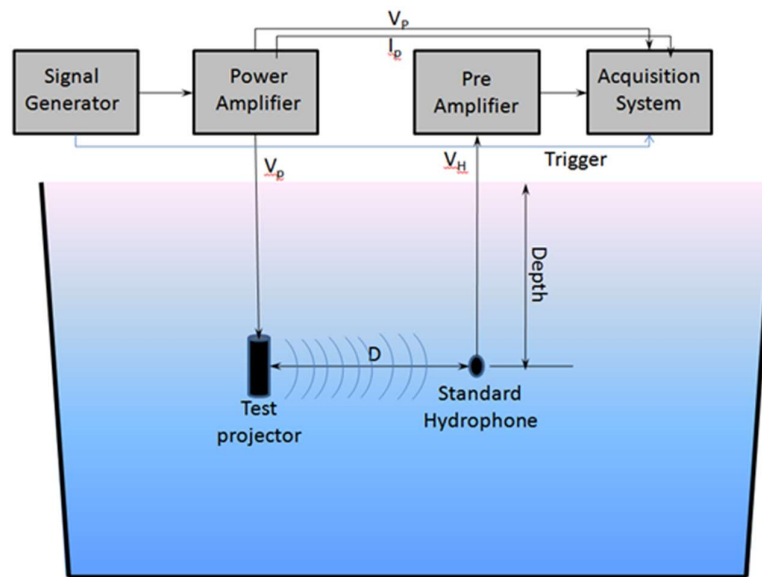
Fig. 3.4   Setup for Transmitting Voltage Response measurement

3.9   TRANSDUCER FAILURES

Even when utmost care is taken in the design of transducers, there are still failures during the operations. The reasons can be attributed to bad manufacturing processes,

poor components, mishandling, improper operation, and storage. Major failures are reduction in insulation resistance due to water ingress through the joints, encapsulant or connectors, cut in the cables or junction boxes, arcing due to high voltage or low insulation, failure in soldered joints, loss of pre-stress due to loosening of nuts, and delamination of the encapsulant (Sandwith *et al.,* 1987). Various failure modes and its effects on the transducer and the system during design stage itself to be ascertained. Sonar systems are tolerant to failures and work satisfactorily even if certain percentages of transducers are failed during its lifecycle. All transducers developed for naval applications are subjected to environmental testing (ET) based on the JSS55555 standard. Transducers are also subjected to environmental stress screening (ESS) which include a test for pressure withstanding capability, pressure cycling, shock, and vibrations.

3.9.1 Design for Buckling Prevention

Transducer housings are subjected to high external pressure when deployed for the deep-water application. One of the common failure modes of thin cylindrical shells subjected external pressure is buckling. Linear buckling analysis can be undertaken to find a structure's potential to buckle under a particular loading. Linear buckling analysis can estimate the maximum load that can be supported before structural instability or collapse. Imperfections and nonlinearities tend to prevent most 'real' structures from achieving their theoretical elastic or "Euler" buckling strength, so the eigenvalue buckling load factors are therefore somewhat overestimated.

For a detailed structural buckling assessment, geometrically nonlinear analyses should be carried out. With this, material and boundary nonlinearity can also be investigated if

required. With a geometrically nonlinear analysis, the stiffness matrix of the structure is automatically updated between loading increments to incorporate deformations which affect the structural behaviour. Nonlinear buckling can be performed on the original structure without imperfection, or by automatically adding, an imperfection based on a scaled deformed shape which could be from a linear buckling model. Special care during the design stage has to be taken to prevent the buckling of transducer housings. The shape of the transducer housing is cylindrical, conical or combination of the two. Cones are essential structural components primarily used in the marine and offshore industries. They can buckle in the elastic-plastic range. A typical application of thick cones includes transition elements between two cylindrical shells of different diameter. When used as transducer housing components, they are mostly subjected to external pressure.

Ifayefunmi and Blachut (2012) investigated the elastic-plastic buckling of short and relatively thick unstiffened truncated conical shells subjected to axial compression and external pressure, using numerical and experimental approach. Experimental results compare well with numerical predictions except for pure axial compression. The results of external air pressure buckling tests of thin-walled, truncated conical steel shells are presented by Barkey *et al*. (2008). Optimised stiffening ring locations were determined by using the finite element method, and were then tested, indicating an experimental improvement in initial buckling pressure of more than 300% over the unstiffened cone. An analytical method for determining buckling pressures of stiffened conical shells is also presented. The results of the analytical method agreed very closely to the finite element method for the stiffened cones, but are 20 to 40% higher than the experimental results.

One of the common failure modes of thin cylindrical shell subjected external pressure is buckling. The buckling pressure of these shell structures is dominantly affected by the geometrical imperfections present in the cylindrical shell which is very difficult to alleviate during the manufacturing process (Prabu *et al*., 2009). Buckle arrestors are used to prevent the local damage to progress over further distances in cylindrical shells and pipelines (Langner, 1999). The pressure required to propel a propagating collapse is much smaller than the pressure needed in initiating collapse. In such cases, it is feasible to install buckle arrestors, such as thick wall rings, at intervals. A series of such arrestors, each sufficiently strong to stop a propagating collapse failure, can limit the extent of damaged pipe in the event of a mishap. In general, the distance between buckle arrestors is selected to enable repair of the flattened section of pipeline between two adjacent arrestors, at a reasonable cost.

In the present study, air backed design with metallic shells are not planned hence no buckling analysis is required. However, stress due to hydrostatic pressure is evaluated, and individual transducers are subjected to pressure testing to find the depth capability.

3.10 METHODOLOGY

Literature survey reveals the relevance of free-flooded ring transducers over hard shell designed transducers for deep submergence applications. Free-flooded ring transducers are preferred for high bandwidth, deep submergence applications that require both transmission and reception of acoustic signals. Three variants of the free-flooded ring transducers with Radially Polarised Cylinders (RPC), all-ceramic segmented ceramic ring using ceramic wedges, and metal ceramic segmented ring using metal wedges and stacks of ceramic slabs are taken up for study. Encapsulation can be carried out using

polyurethane (PU) or using an acoustically transparent rubber boot filled with oil. The oil used to fill the boot couples the transducer to the fluid in which it is immersed. This method reduces the complexities associated with the direct moulding over ceramics and maintenance of transducer. The cavity at the centre of the transducer is free-flooded. Broad bandwidth can be obtained by combining the cavity mode and hoop mode of the transducer. In the fluid-filled category, fill fluids like Silicone oil, Castor oil, Isopar-L and transformer oil are considered.

Omnidirectional beam can be obtained by exciting all the ceramic stacks in the segmented ring simultaneously. The directional beam can be obtained by exciting multiple modes of the cylinder by applying different sectors with different voltages. RPC can also be made directional in a similar way. The internal electrode can be divided into equal sectors by removing it lengthwise at various locations and exciting the sectors with different voltages.

The aim is to design and develop deep submergence, Omni and directional transducers operating below 10 kHz with a minimum source level of 190 dB re 1 µPa at 1 m and depth capability of minimum 1000 m. The transducer development with piezoceramic drivers only is considered because of its easy availability in various shapes and sizes. The transducers developed are tested for its acoustic performance in NPOL's open tank at 10 m depth and in NPOL's Materials and Transducers Simulated (MATS) test facility upto 700 m of water. Pressure withstanding capability of transducers is tested upto 10 MPa in NPOL and subsequently at NIOT, Chennai upto 60 MPa.

ATILA - a software package for the analysis of sonar transducers - is used to study the effect of various parameters on the transmission and reception characteristics of the

transducers. Based on the study, transducer variants are manufactured and tested. For the RPC based transducer, the effect of length, diameter, thickness of RPC, type of PZT, type of encapsulation and fill fluid on TVR and bandwidth are studied. Modelled transducers are encapsulated with PU moulding and assembling in an oil filled rubber boot. Directional transducers using RPC is developed with PU encapsulation only.

All-ceramic segmented ring transducers made of ceramic wedges are modelled to study the effect of various parameters like diameter, wall thickness, height and type of PZT on TVR. Since the development of all-ceramic transducer needs ceramic wedges specially made for each diameter, it is not very popular as the other two versions. However, in applications where weight is a critical parameter like helicopter based dunking sonar, these type of transducer may be an ideal choice. Omnidirectional all-ceramic segmented ring transducers are developed with PU moulding and oil filled encapsulation.

Metal ceramic segmented ring transducers are modelled to study the effect of various parameters like PZT material, wedge material, type of encapsulation, fill fluid, diameter and height on TVR. Both Omni and directional transducers are developed using metal ceramic ring because of the easiness in manufacture. Directional transducers are made with non-metallic wedges and FRP sheets to isolate the sectors.

The research outcome is the technology for the design and development of transducers of given acoustic performance capable of operating in deep sea. The research also aims to generate data on transducer performance under different depths. Currently, depth related performance of free-flooded ring transducers is not available in open literature. It is also intended to make prototype transducers with Omni and directional beam

pattern for various deep submergence applications. It is also intended to study the acoustic performance of the transducer with PU moulding in comparison to liquid-filled transducers. Once the core technology is developed, it can be extended to further depths for future applications for low-frequency applications.

3.11 SUMMARY

The methodology to be adopted for the design and development of transducers is presented in this chapter. Three types of free-flooded ring transducers are to be modelled using the FEM software ATILA. Modelled transducers are to be manufactured and tested for its acoustic performance in an open tank and in a pressurised vessel upto 7 MPa. Transducers are also to be tested for pressure withstanding capability.

CHAPTER 4

OMNIDIRECTIONAL TRANSDUCERS

4.1 INTRODUCTION

The unlimited depth capability, broadband response, as well as the ease of manufacture, make free-flooded ring transducers preferable for deep-sea applications. The transducer can be made from Radially Polarised Ceramic cylinders (RPC), segmented ceramic wedges or stack of ceramic slabs and metal wedge combination as shown Figs. 4.1, 4.2 and 4.3. There are two fundamental vibration modes associated with these transducers, the radial resonance of the shell and cavity resonance of the enclosed water column. The radial resonance frequency of the ring is dependent on the diameter, and it becomes significant as frequency comes down so RPCs can be typically used for frequencies above 4000 Hz (Hughes, 1998). Problems related to the manufacture of a solid ceramic ring of large diameter for low frequencies can overcome by the use of a number of ceramic wedges to form a segmented ring (Green, 1965). However, when we need transducers of different frequencies, we have to make cylinders of different diameters using different size of wedges. The wedge shaped non-piezoceramic spacing strips helps to make the transducer with pre-fabricated stacks from regular slabs of rectangular cross-section, instead of the wedge shaped ceramics.

The horizontal directivity of free-flooded ring transducer is Omnidirectional, and the vertical directivity is toroidal. Transducer encapsulation can be carried out using direct polyurethane or rubber over-moulding or assembling the transducer in a rubber housing filled with oil. Fibreglass winding over the segmented ring can be used to pre-stress the transducer (Busher, 2008). All three versions of free-flooded ring transducers are studied in detail using ATILA and explained in the following sections.
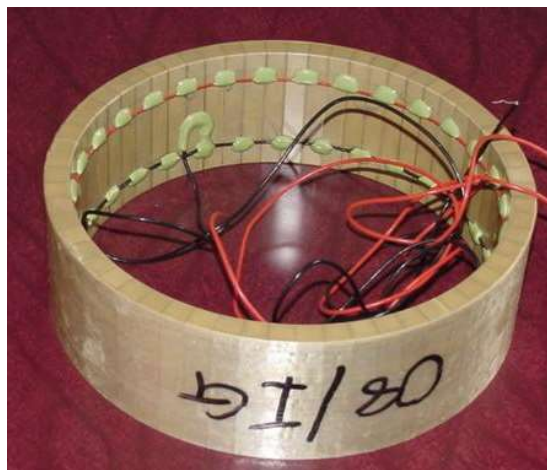
Fig. 4.1　　Radially polarised ceramic ring.

Fig. 4.2　　Segmented ring with ceramic wedges and fibre winding.
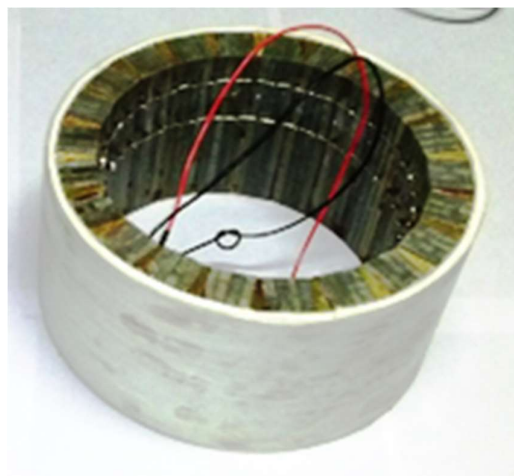
Fig. 4.3　　Segmented ring with metal wedges and ceramic slabs.

4.2   RPC BASED FREE-FLOODED RING TRANSDUCERS

RPC based transducer is the simplest to manufacture among all the three types of free-flooded ring transducers discussed in the previous section. RPC can be connected to a two core cable by soldering to the inner and outer electrodes and encapsulated using a polyurethane compound to make it water worthy. However, manufacture of RPCs of higher diameter is difficult and expensive. The manufacturers, for regular supply restrict the maximum outer diameter of RPCs to about 150 mm. This restriction on size fixes the lower frequency to about 4 kHz. Therefore, the studies related RPCs are restricted to the maximum outer diameter of 150 mm.

4.2.1   RPC Transducer Models

The dimensions of the base model of RPC based transducer considered are outer diameter (OD) of 150 mm, inner diameter (ID) 140 mm (i.e. 5 mm wall thickness) and height of 50 mm. The transducer ceramic material considered is PZT4, and encapsulation material is rubber. A parametric study is carried out by varying one dimension at a time by keeping all other dimensions same. The height of the RPC is varied from 50 to 150 mm to find the effect of height 'h' on TVR.   Effect of outer diameter on TVR is studied by, varying OD to 75, 100, 125 and 150 mm. Effect of wall thickness on TVR is investigated for the 150 mm OD, 50 mm height ring by varying the wall thickness from 5 to 20 mm in steps of 5 mm. Effect of PZT material on TVR is studied using PZT4 and PZT8 materials. Effect of encapsulation is investigated by comparing the PZT ring moulded with rubber, PU and, assembled in a rubber boot filled with oil. Different types of fill fluids like Castor oil, Silicone oil, Transformer oil and Isopar-L are used to study the effect of fill fluid on TVR. Transducers are modelled using the FEM package, ATILA. Material properties of various components used for

71

the modelling of transducers obtained from literature and manufacturers catalogue (Berlincourt et al., 2010) are given in Table 4.1. Since the transducer is symmetric with X and Y axis, one-fourth of the transducer only needs to be modelled as shown in the Fig. 4.4. Axisymmetric modelling is carried out with Y axis as the axis of rotation. Eight noded quadrilateral elements are used to model the piezoelectric, elastic, fill fluid and water surrounding the transducer.

Table 4.1   Material properties of the components of transducers modelled.

Material	Properties		
PZT8	$\rho = 7600$ kg/m^3	$s_{11}^E = 11.1$e-12 m^2/N	$s_{12}^E = -3.7$e-12 m^2/N
	$s_{13}^E = -4.8$e-12 m^2/N	$s_{33}^E = -13.9$e-12 m^2/N	$s_{44}^E = 35.0$e-12 m^2/N
	$s_{66}^E = 29.6$e-12 m^2/N	$d_{31} = -37$e-12 m/V	$d_{33} = 218$e-12 m/V
	$d_{15} = 400$e-12 m/V	$\dfrac{\varepsilon_{11}^S}{\varepsilon_0} = 900$	$\dfrac{\varepsilon_{33}^S}{\varepsilon_0} = 600$
PZT4	$\rho = 7500$ kg/m^3	$s_{11}^E = 12.3$e-12 m^2/N	$s_{12}^E = -4.05$e-12 m^2/N
	$s_{13}^E = -5.31$e-12 m^2/N	$s_{33}^E = -15.5$e-12 m^2/N	$s = 39$e-12 m^2/N
	$s_{66}^E = 32.7$e-12 m^2/N	$d_{31} = -123$e-12 m/V	$d_{33} = 289$e -12 m/V
	$d_{15} = 496$e-12 m/V	$\dfrac{\varepsilon_{11}^S}{\varepsilon_0} = 730$	$\dfrac{\varepsilon_{33}^S}{\varepsilon_0} = 630$
Aluminium	E = 7.14e10 N/m^2	$\sigma = 0.344$	$\rho = 2780$ kg/m^3
Brass	E = 9.5e10 N/m^2	$\sigma = 0.33$	$\rho = 8500$ kg/m^3
Titanium	E = 11.7e10 N/m^2	$\sigma = 0.36$	$\rho = 4510$ kg/m^3
Steel	E = 21.5e10 N/m^2	$\sigma = 0.33$	$\rho = 7\,900$ kg/m^3
FRP	E = 4.1e9 N/m^2	$\sigma = 0.4$	$\rho = 1\,400$ kg/m^3
Rubber	E = 5.93e10 N/m^2	$\sigma = 0.45$	$\rho = 1000$ kg/m^3
PU	E = 4.1e9 N/m^2	$\sigma = 0.47$	$\rho = 1200$ kg/ m^3
Water	B = 2.22e11 N/m^2		$\rho = 1000$ kg/m^3
Silicone Oil	B = 0.1385e10 N/m^2		$\rho = 760$ kg/m^3
Transformer oil	B = 0.1719e10 N/m^2		$\rho = 890$ kg/ m^3
Castor Oil	B = 0.2094e10 N/m^2		$\rho = 956$ kg/ m^3
Isopar-L	B = 0.1738e10 N/m^2		$\rho = 780$ kg/ m^3
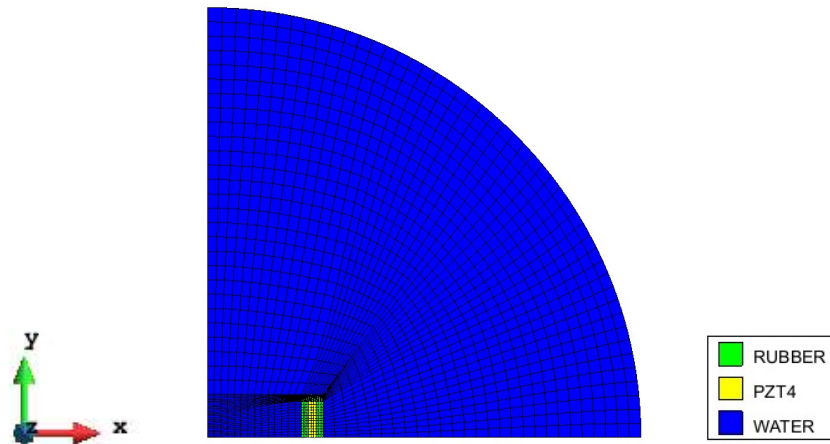
Fig. 4.4   2-D Axisymmetric model of RPC transducer.

The effect of height 'h' on TVR is studied by modelling h=50, 75, 100 and 150 mm and the results are plotted in Fig. 4.5. With the increase in height from 50 to 150 mm, the resonance frequency has come down from 5 kHz to 2.7 kHz because the cavity mode has become more predominant with the increase in volume of entrapped fluid and its acoustic interaction with the surrounding medium. TVR at resonance is also increased. Even though for h=50, the resonance is at a higher frequency, the transducer has a broad bandwidth from 4.5 to 10 kHz.
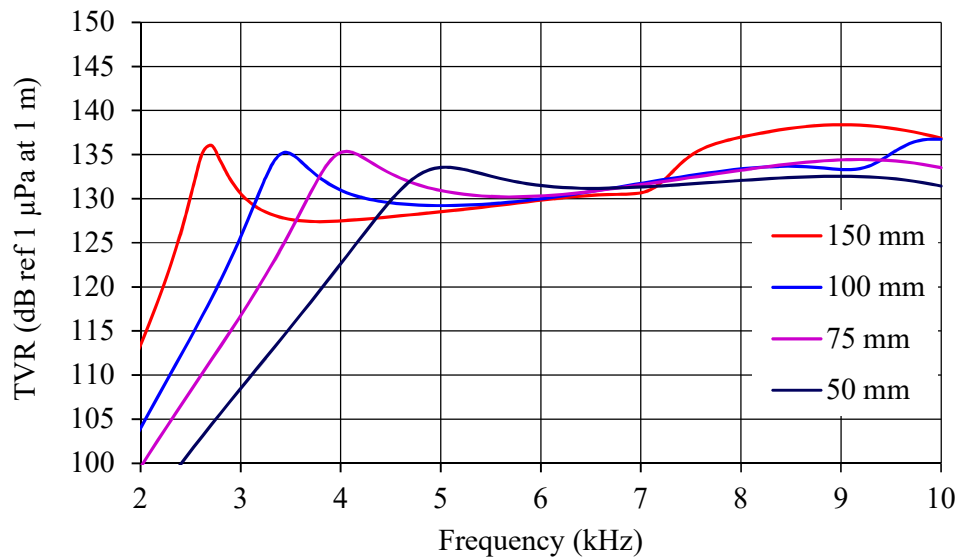
Fig. 4.5   Effect of height on TVR (Model).

73

Effect of outside diameter on TVR is studied by varying the outside diameter to 75, 100, 125 and 150 mm and the results are shown in Fig. 4.6. It indicates that as the outside diameter increases, resonance frequency comes down, TVR and bandwidth increases. When the diameter is increased, the inner water column also is increased, resulting in a stronger cavity mode and lower resonance.
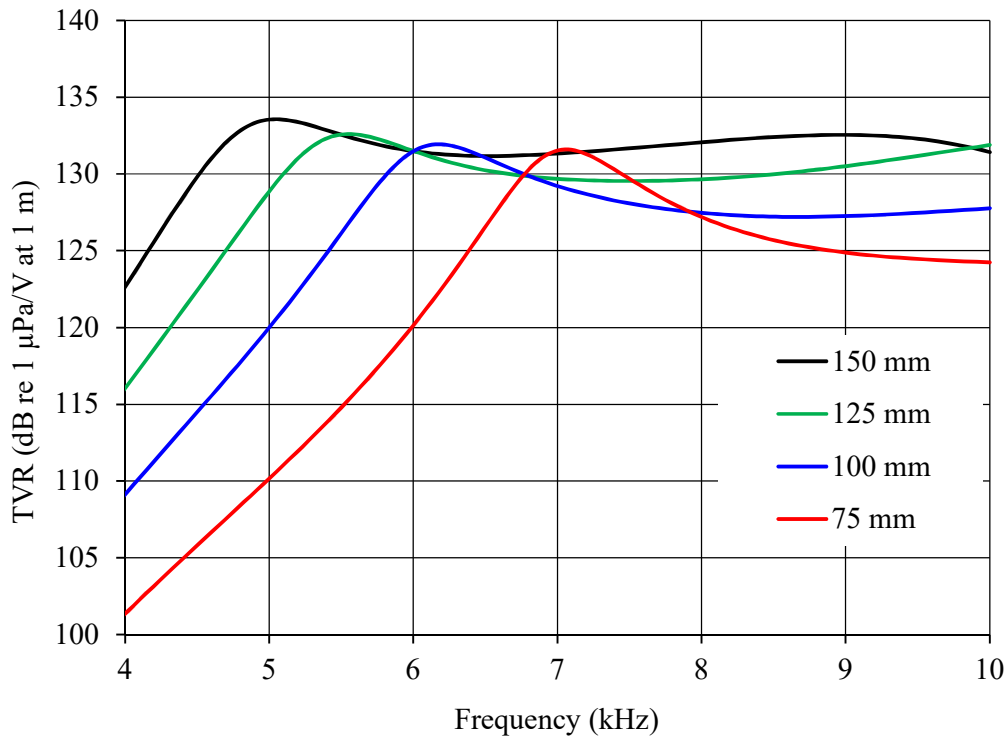
Fig. 4.6   Effect of ceramic OD on TVR (Model).

Effect of the wall thickness of the ceramic ring on TVR is studied by varying the thickness to 5, 7.5, 10 and 15 mm, and the results are shown in Fig. 4.7. The results indicate that TVR increases with reduction in wall thickness because of the higher field, i.e. Voltage to thickness ratio increases. However, with the decrease in wall thickness, the ceramic volume also comes down resulting the reduction of power handling capability.
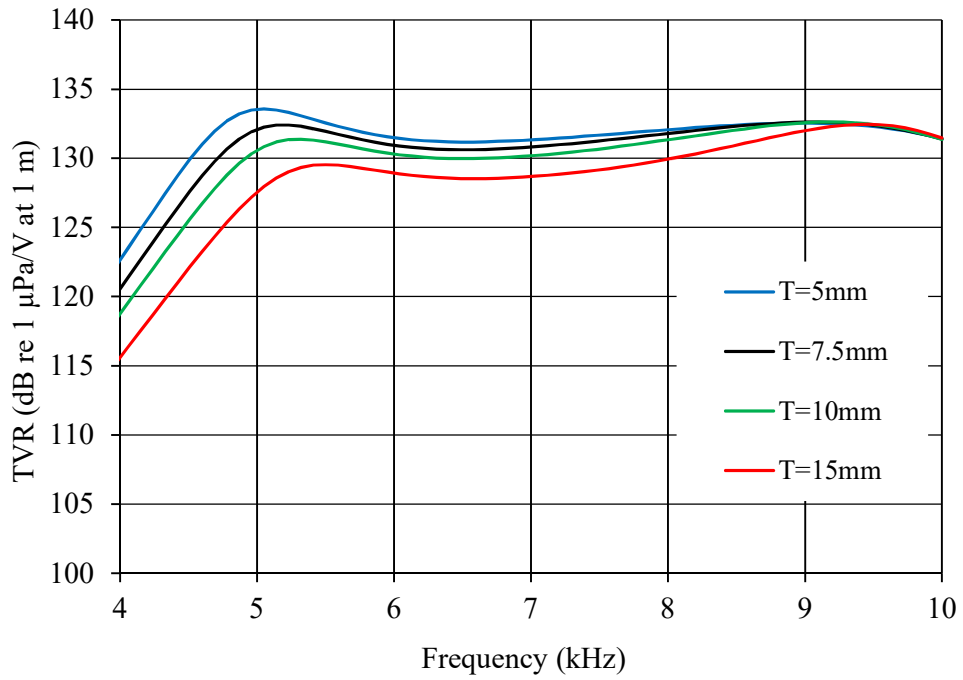
Fig. 4.7   Effect of ceramic wall thickness on TVR (Model).
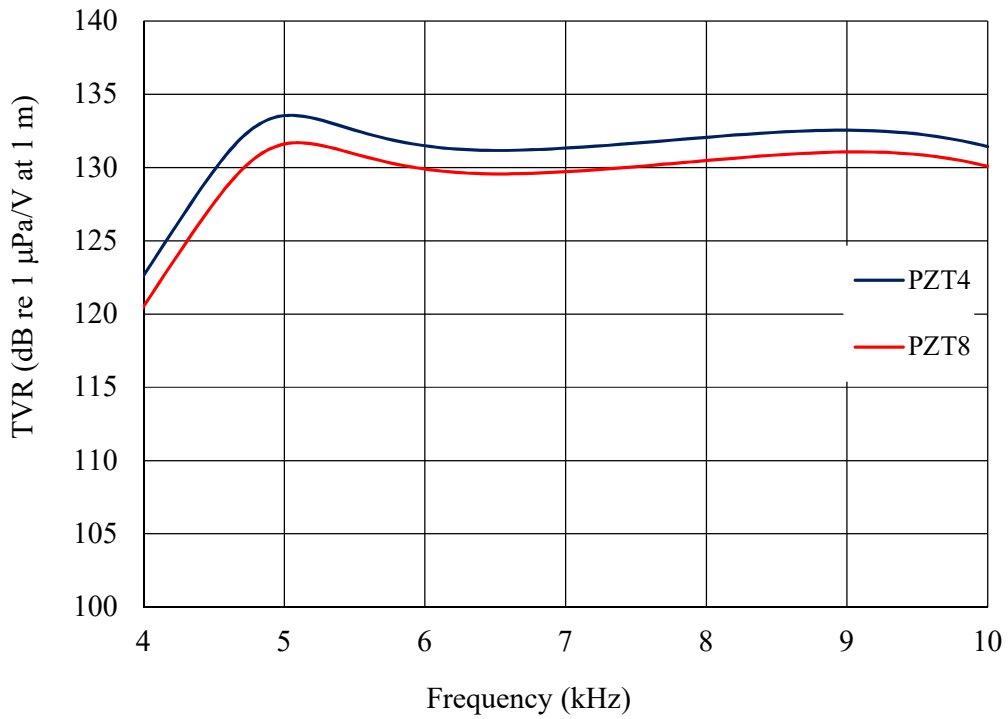
Fig. 4.8   Effect of PZT type on TVR (Model).

75

4.2.2 Oil Filled RPC Transducer

An alternate option to direct over-moulding of free-flooded ring transducer is to use a rubber boot filled with oil. Renna (1972) in his US patent has reported oil filled ring transducer that enhances the bandwidth and efficiency by close coupling the cavity and hoop mode resonances. ATILA is used to study the effect of different types of fill-fluid on the transmission characteristics of the transducer. The construction details of the transducer studied are shown in Fig. 4.9. It consists of a radially polarised PZT4 ring supported on rubber bushes inside a rubber boot and filled with oil. This type of construction helps in overcoming the problems related to direct rubber moulding over the ceramic ring. The transducer is axisymmetric, and it is, therefore, necessary to model only one-fourth of the ring. The 2-D axisymmetric model of the transducer is shown in Fig. 4.10. Effect of oil filled rubber boot encapsulation on TVR in comparison to direct over-moulding like rubber and PU is shown in Fig. 4.11. It is seen that oil filled rubber boot and rubber moulded transducers have almost same resonance frequency and response, but PU moulded one has slightly lower resonance and higher TVR.
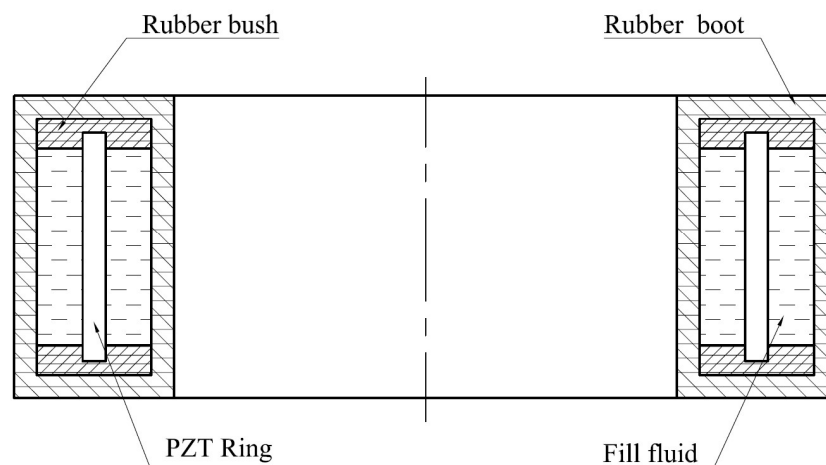
Fig. 4.9   Cross section of oil-filled transducer modelled.
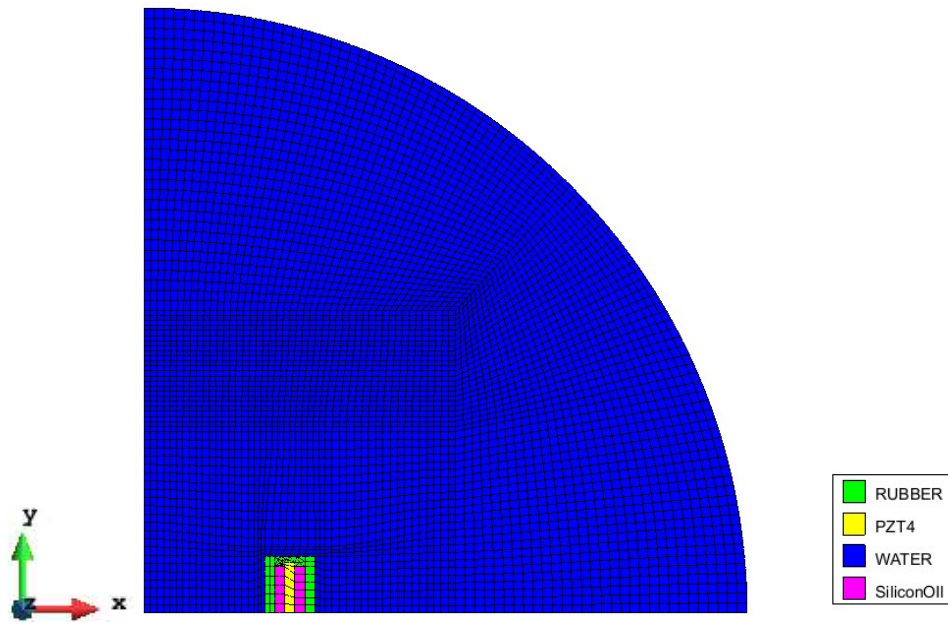
Fig. 4.10   Axisymmetric model of the transducer with oil filled rubber boot.
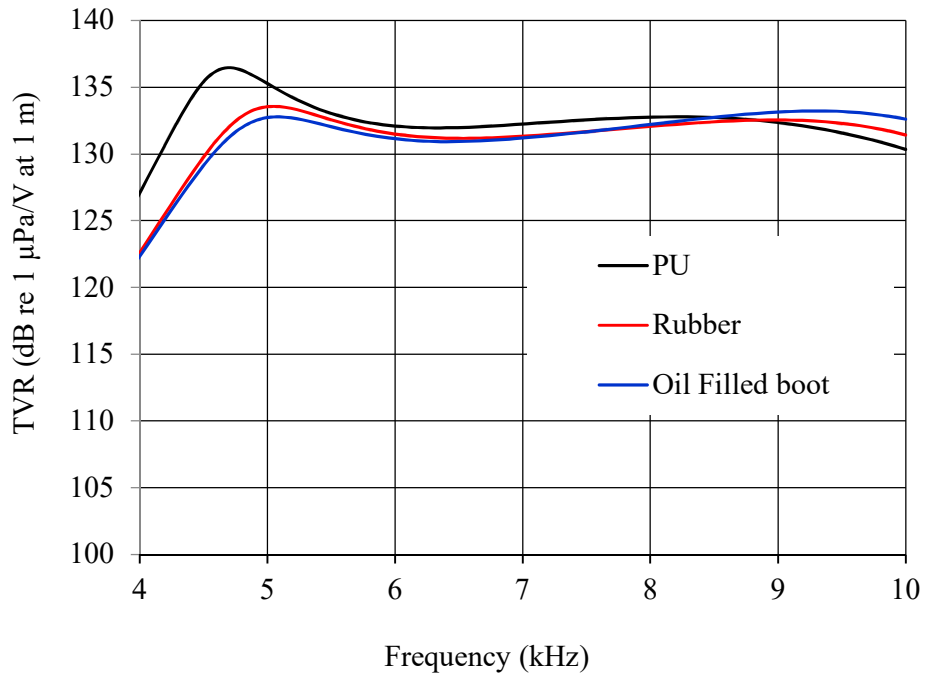
Fig. 4.11   Effect of encapsulation on TVR (Model).

Effect of fill fluids on Transmitting Voltage Response is shown in Fig. 4.12. The results indicate that fill fluids have no significant effect on TVR.
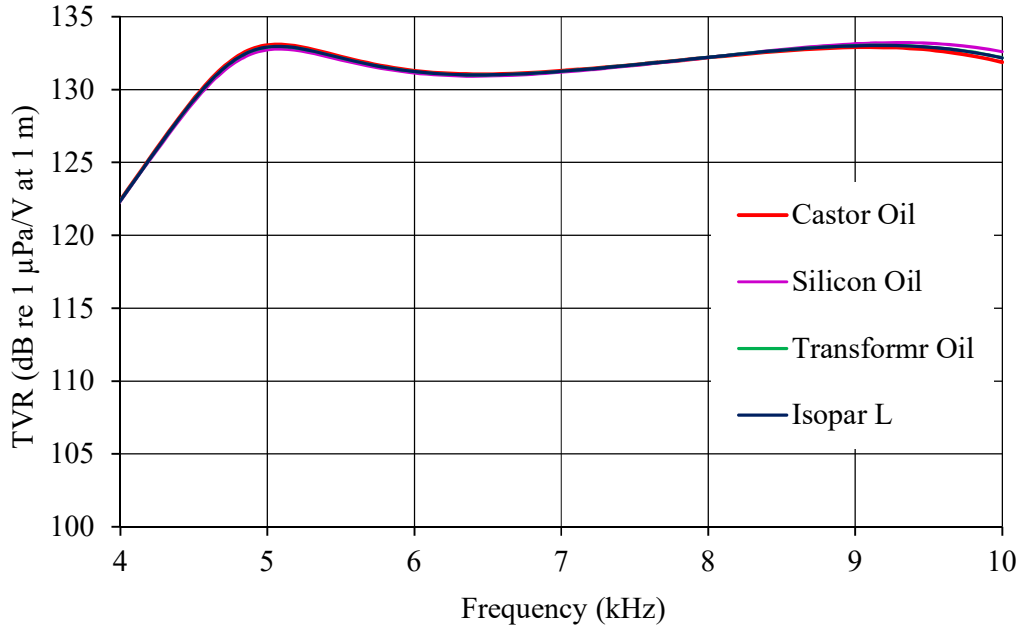
Fig. 4.12   Effect of fill fluid on TVR (Model).
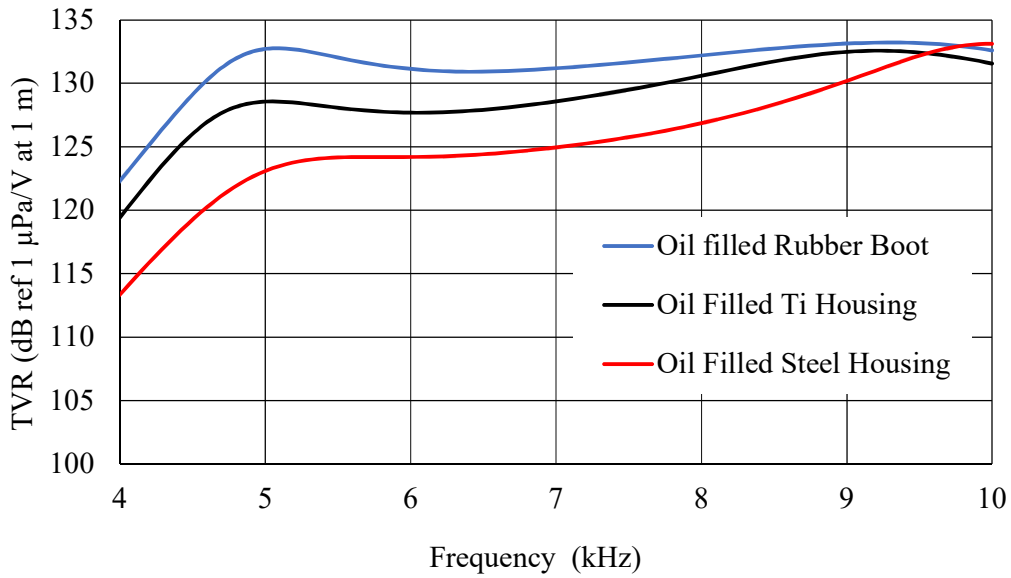
Fig. 4.13   Effect of housing material of oil filled transducer (Model).

Effect of housing material of oil-filled transducer is studied by modelling different housing materials like rubber boot and metals like Titanium and steel. Compared to metallic housings, rubber housing has higher TVR as shown in Fig. 4.13. It can be attributed to the good impedance matching of rubber with sea water compared to metals. A full metallic housing may not withstand the high hydrostatic pressure, and it is not recommended for actual end use.

4.2.3 Stress Analysis

The stresses acting on a transducer are due to pre-stress, hydrostatic operating conditions, and applied voltage. The static stress induced in the piezoceramic stack due to pre-stress can be calculated from the charge measured during pre-stress or from the stress-strain relations based on the pre-stress requirements. The stress due to hydrostatic pressure and dynamic stress due to electrical excitation can be estimated by modelling the transducer using the finite element package ATILA. Then, the calculated static and dynamic stresses can be compared with data from manufacturer's catalogue. In the present study, RPC based transducers are not pre-stressed, so the only static stress is due to hydrostatic pressure. Effect of hydrostatic pressure on the transducer is studied by modelling the transducer with a thin layer of water around it. Stress on the transducer is found by applying 1 Pa pressure around the transducer. The maximum von-Mises stress in the ceramic ring is calculated using the equation (Schmid *et al.*, 2013),

$$\sigma_{v=}\sqrt{0.5[(Sx-Sy)^2+(Sy-Sz)^2+(Sz-Sx)^2]}+\sqrt{3(Sxy^2+Syz^2+Szx^2)} \quad (4.1)$$

where Sx, Sy, Sz are the normal stresses and Sxy, Syz, Szx are the shear stresses. For axisymmetric case, Syz and Szx are zero. The maximum von-Mises stress on the

transducer with 1 Pa pressure is 2.70 Pa. Assuming linear behaviour, the stress at 60 MPa pressure corresponding to 6000 m of water depth is found to be 162 MPa that is much below the maximum compressive strength of 520 MPa for the PZT4 ceramics (Berlincourt *et al.*, 2010). The transducer model and the stress on the ceramics are shown in Figs. 4.14 and 4.15.

The dynamic stress at 5 kHz is shown in Fig. 4.16 when one V_{pp} (peak-to-peak voltage) is applied. The maximum stress in the stack is about 854.14 Pa at 5 kHz. The maximum voltage that can be applied to the RPC of 5 mm wall thickness during actual operation is 200 x 5 = 1000 V. Therefore, the maximum von-Mises stress is 0.854 MPa at 5 kHz. The maximum rated dynamic stress for PZT4 piezoceramics varies from 12,000 psi (83 MPa) at 25 °C to 6,000 psi (41 MPa) at 100^0 C (Vernitron, 1976). The actual stress of 0.854 MPa is much less than the maximum rated stress. Therefore, the operation at 60 MPa pressure with 1000 V is safe with a good safety margin. Table 4.2 shows the maximum stresses due to hydrostatic pressure and one V_{pp} excitation.
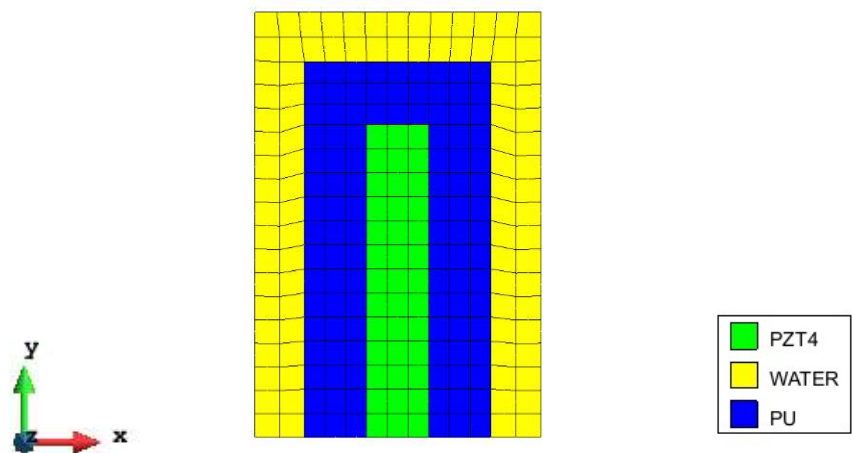
Fig. 4.14   Model for the study of hydrostatic pressure effect.
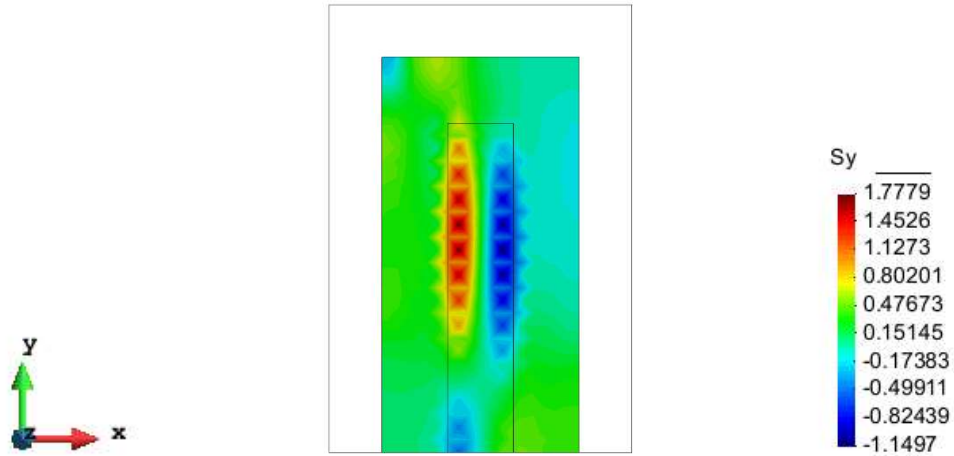
Fig. 4.15   Stress due to 1 Pa hydrostatic pressure.
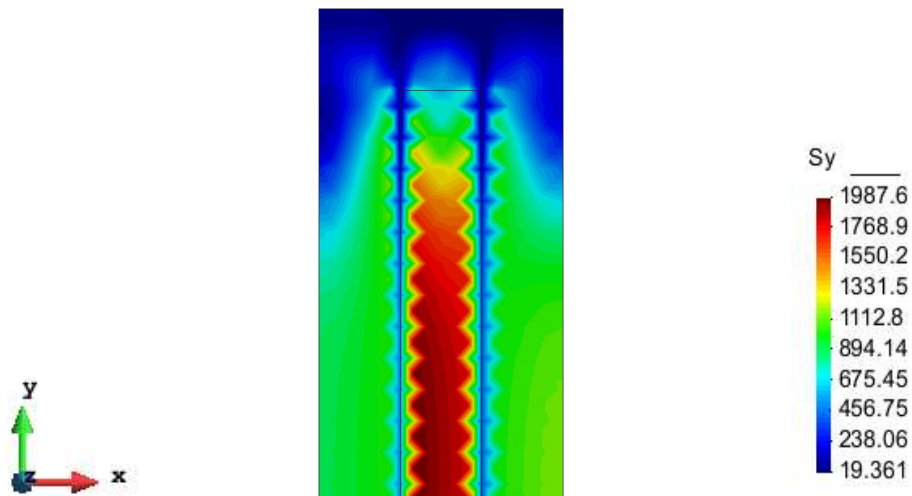
Fig. 4.16.   Dynamic stress due to 1 V_{pp} at 5 kHz.

Table 4.2   Stress due to 1 Pa pressure and 1 V_{pp} excitation.

	Sx (Pa)	Sy (Pa)	Sz (Pa)	Sxy (Pa)	Syz (Pa)	Szx (Pa)	σ_v (Pa)
1 Pa Pressure	0.678	1.77	3.412	0.186	0	0	2.70
1 V_{pp}	1601	1987.6	2181.4	197.65	0	0	854.14

81

4.2.4   Power, Source Level and Cavitation

Electric power handling capability of the RPC transducer with the PZT4 ring can be estimated using the following relation (Stansfeild, 1990).

$$P_e = 2 \, \pi \, f \, Q_m \, k^2 \, \varepsilon_0 \, \varepsilon_r \, E^2 \, V_c \qquad\qquad (4.2)$$

where f-operating frequency in Hz

Q_m- is the mechanical Quality factor

k- coupling coefficient

ε_0- is the dielectric permittivity of free space in F/m

ε_r - is the relative dielectric permittivity of the ceramic

E - Electric field applied in V/m

V_c - Cerami Volume in m^3

Using the above equation, and considering a safe field of 200 kV/m (Stansfield, 1990), it is estimated that the transducer can handle 1.2 kW power at 5 kHz.

The cavitation threshold of the transducer can be estimated from the surface area of the transducer and acoustic power that can be transmitted at a given depth, 'h' using the following relation. Stansfield (1990) gives the relation for cavitation threshold as $0.3(1.8+(h/10))^2$ W/cm² where h is in meters. The surface area of the transducer is 301.6 cm^2. Assuming an electro-acoustic efficiency (η) of 50%,   the depth of water 'h' to apply 1200 W of electric power to the transducer is calculated as 7.8 m. Since the transducer is intended for deep sea application cavitation is not an issue.

Using the relation given by Stansfield (1990), the Source Level (*SL*) of a transducer can be calculated from the input electrical power (P_e), electro-acoustic efficiency η and Directivity Index (DI) as

$$SL = 170.9 + 10 \log P_e + DI + 10 \log \eta \qquad (4.3)$$

DI = 0 for Omnidirectional transducer and assuming 50% efficiency, transducer SL can be calculated as 198.6 dB re 1 µPa at 1 m. Source level of the transducer can also be estimated from the predicted TVR and the voltage (V) applied using the equation,

$$SL = TVR + 20 \log (V) \qquad (4.4)$$

So SL at 5 kHz = 135 + 20 log (1000) = 195 dB re 1 µPa at 1 m for the PU moulded transducer. Since losses are not included in the model from which the TVR is obtained, a conservative figure of about 3 dB reduction in SL is expected.

4.2.5   Manufacture and Assembly of RPC Transducers

Based on the modelling studies and manufacturing feasibility of ceramics, dimensions of the ceramic ring are finalised for the transducer as 150 mm OD, 140 mm ID and 50 mm height. Two types of transducers are manufactured using PZT4 cylinders. In the first case, the transducer has PU moulding over the ceramic ring with an encapsulation thickness of 5 mm all around. In the second case, the RPC is positioned in a rubber boot with locating bush, and the cavity around the ceramic is filled with silicone oil. The schematic of the transducer assemblies with dimensions are shown in Figs. 4.17 and 4.18. Even though transducer with rubber moulding is modelled, it is not taken up for

manufacture because of the high pressure and temperature involved in the moulding process that can cause damage to the PZT and the electrical connections.
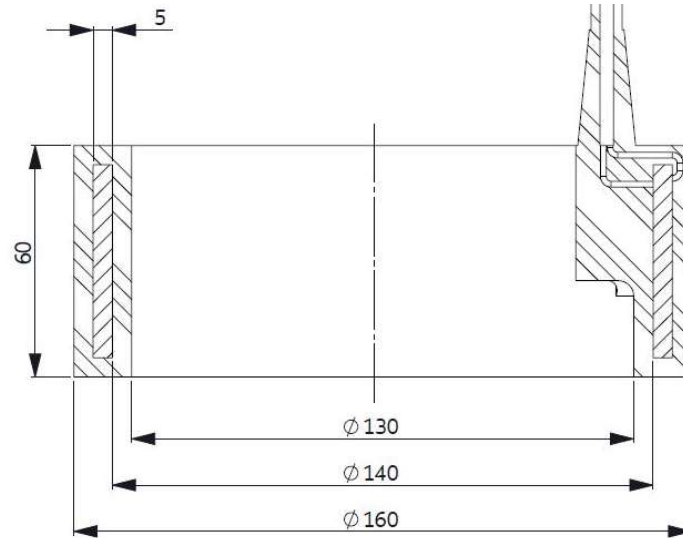
Fig. 4.17   Schematic of the RPC transducer moulded in PU.
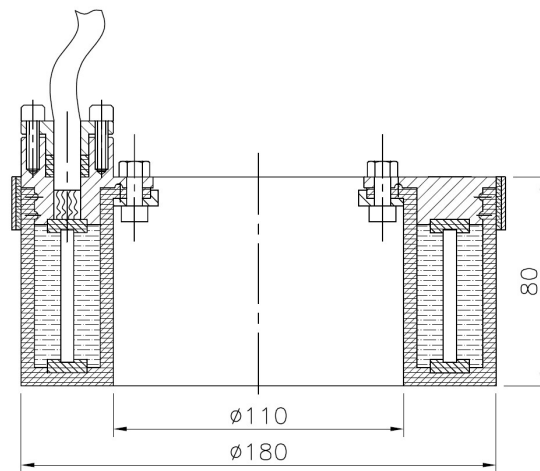
Fig. 4.18   Schematic of the transducer with an oil filled rubber boot.

Manufacture of the modelled transducers requires mould for PU and rubber boot moulding. The PU moulding was carried out using a commercially available PU resin, a two-part rigid urethane casting compound. The fully cured PU has a Shore D hardness of 65 and is white. Two-stage moulding is required for the PU moulding. In the first

stage moulding, a base with a groove for the RPC was moulded, and then the RPC was positioned in the groove. Then the second stage moulding was carried out. Even though the curing time specified is less than an hour, the transducer is deployed in water only after 3 to 4 days. The PU mould and the moulded transducer are as shown in Figs. 4.19 and 4.20. The oil filled transducer in rubber boot and steel housing are shown in Figs. 4.21 and 4.22.
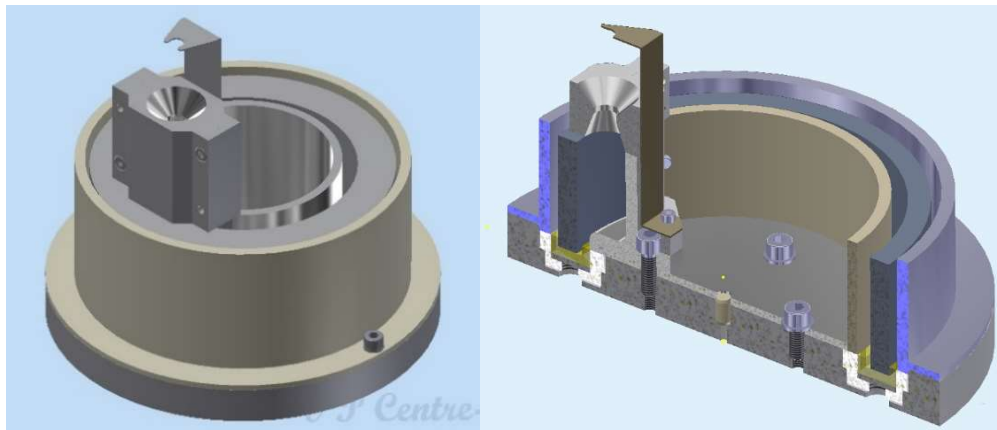
Fig. 4.19   PU mould and its cross section.

Fig. 4.20   PU moulded transducer.

Fig. 4.21   RPC transducer with an oil filled rubber boot.

Fig. 4.22   Oil filled free-flooded transducer with steel housing.

For the oil filled transducer, rubber boot is moulded using a specially made nitrile rubber composition which can withstand oil and seawater environment for a long duration. RPC is positioned inside the moulded rubber boot using a rubber bush with seating groove as shown in Fig. 4.18. Top of the ring is also located using a similar rubber bush. A top cover made of 316 L steel material is used to close the transducer. The outer diameter of the boot is clamped to the top cover using a metallic belly band. The inner diameter of the boot has a flange, and it is bolted between a metallic plate and the top cover. A bottom plate, bolted to the top cover plate, prevent the loading of

the rubber boot due to the ceramic and fill fluid weight. There are two holes on the cover plate for oil filling and air release during oil filling. Silicone oil is used as the fill fluid. Two core shielded cable is used for electrical connection. The cable used is rated for the use of 6000 m of water. Water ingress through the outer diameter of the cable is prevented using cable glands with metal and rubber washers. The two threaded holes provided on the top plate can be used to mount the transducer to the test fixture for measurement in the tank and pressure chamber. The transducer assembled is as shown in Fig. 4.21. Transducer with steel housing also was assembled and tested to find the effect of steel housing on TVR. Since the TVR values are much lower for the transducer with steel housing compared to rubber housing at cavity mode resonance due to high stiffness of the steel housing, only tank level testing was carried out for this particular transducer (Fig. 4.23). For the detailed study of oil filled transducers, rubber housing only is used.

4.2.6 Experimental Studies

The transducers manufactured were tested in an open acoustic tank of 50 m length, 20 m width and 18 m depth. The test facility has an overhead crane, positioning platforms, and necessary instruments for all acoustic measurements as shown in Fig. 4.24. The transducer was positioned at a depth of 10 m and parameters like resonance frequency, transmitting voltage response, and receiving sensitivity, were measured. The measurements were then repeated in the pressurised test chamber shown in Fig. 4.25 (NPOL, 2017). The pressure chamber has a length of 8 m and an inner diameter of 3 m. The pressure inside the chamber can be fixed as per requirement, and the tests were carried out in steps of 1 MPa from 1 to 7 MPa. To check the pressure withstanding

capability, transducers were then tested in a hyperbaric test facility as shown in Fig. 4.26 at NIOT, Chennai (NIOT, 2017).
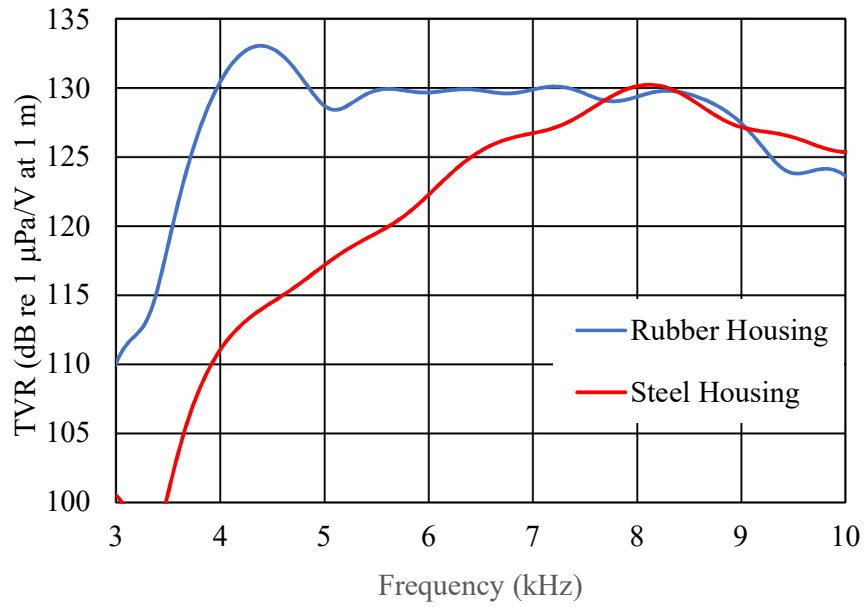
Fig. 4.23   Measured TVR of oil filled transducers.

Fig. 4.24   Open acoustic tank.at NPOL.

Fig. 4.25   Pressurised acoustic test chamber at NPOL.

Fig. 4.26   Hyperbaric test facility.

4.2.7   Results and Discussions

The effect of encapsulation is studied for polyurethane moulded and oil filled RPC transducers. Results of TVR for the model and experiment conducted in an open tank at 10 m depth are shown in Fig. 4.27. Modelled results show a similar trend of TVR

for both the transducers except near resonances. Measured results from the open tank tests show that except near the resonance of oil filled transducer, PU moulded transducer has a higher TVR of 1 to 3 dB in the frequency band of 4 to 8.5 kHz. The measured TVR of the PU moulded transducer is about 4 dB less compared to the model at resonance. However, the resonance frequency and TVR away from resonance are in good agreement between model and experiment. Away from resonance, oil filled transducer also has good agreement between model and experiment. The reason for the difference at resonance and near resonance (4.0 to 5.5 kHz) can be attributed to non-inclusion of material losses in the model and non-availability of correct material properties. The measured receiving sensitivity of the PU moulded, and oil filled RPC transducers are shown in Fig. 4.28. Receiving sensitivity of both the transducers is above -190 dB in the band of 3-8 kHz.
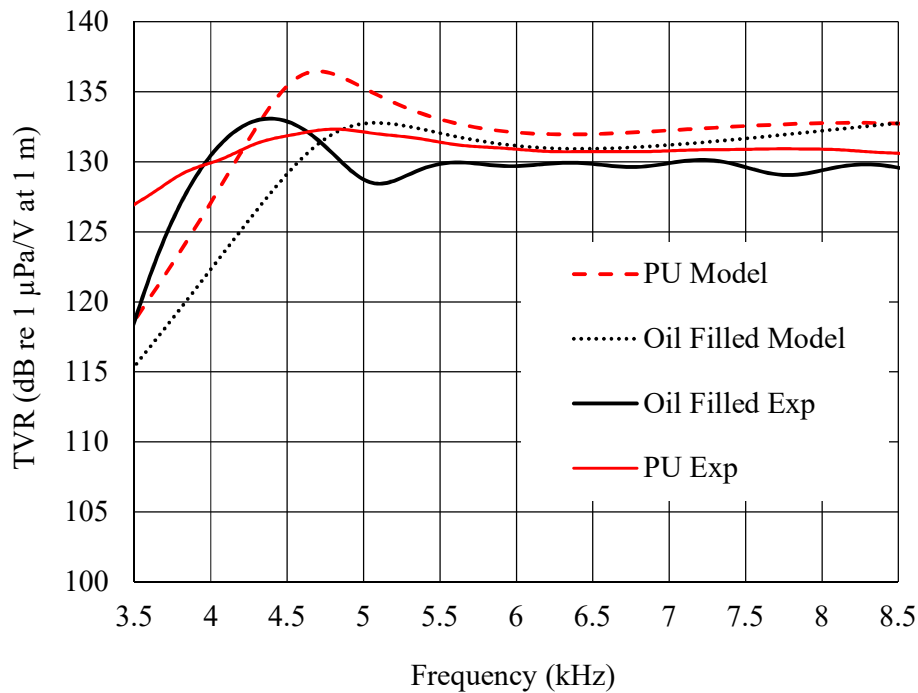
Fig. 4.27   Model and experimental TVR in open tank for PU and oil filled transducers.
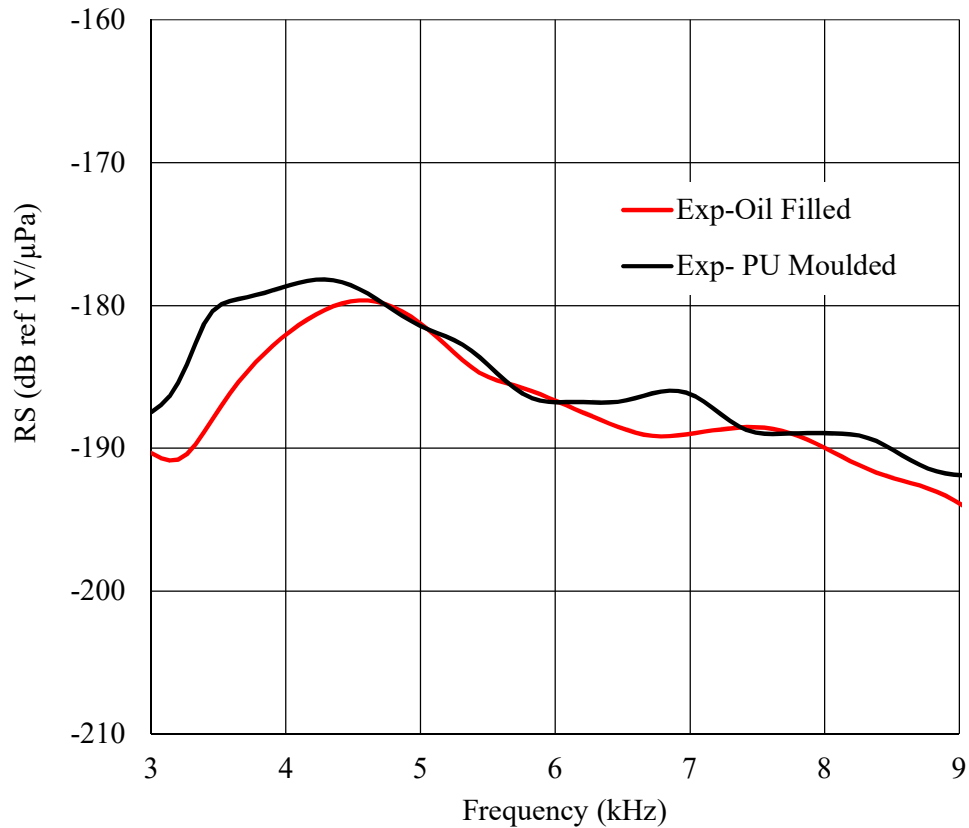
Fig. 4.28   Measured receiving sensitivity of PU moulded and oil filled transducers.

The horizontal and vertical directivities of the PU moulded, and oil filled RPC transducers measured at 4 and 6 kHz are shown in Figs. 4.29 and 4.30. The horizontal directivities of both the transducers at 4 and 6 kHz are Omni within 3 dB. The vertical directivities are toroidal in shape. However, the directivities of oil filled transducer are less directive compared to PU moulded transducer. Power and source level of the PU moulded, and oil filled transducers measured at 10 m depth are shown in Table 4.3. Both the transducers have source level more than 190 dB re 1 µPa at 1 m. The source level can be further enhanced by tuning the transducers.
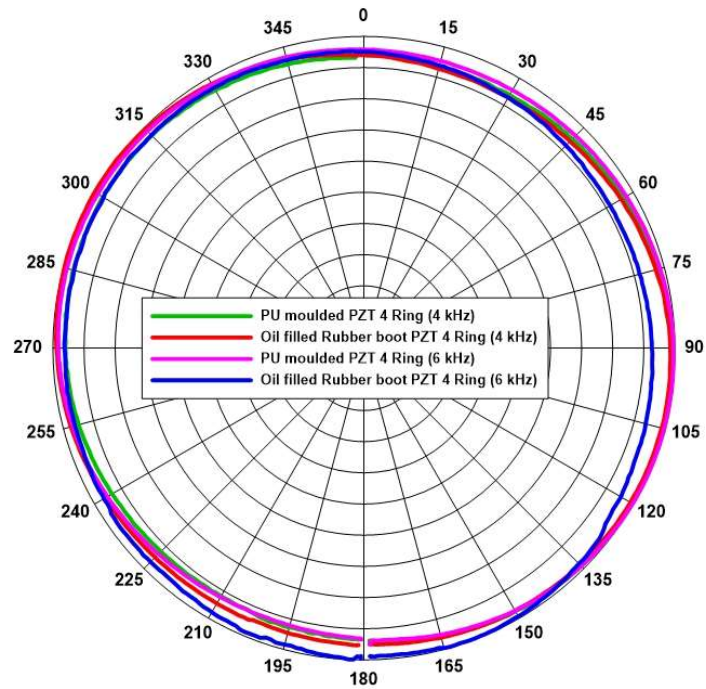
Fig. 4.29   Measured horizontal directivities of PU moulded and oil filled
transducers.
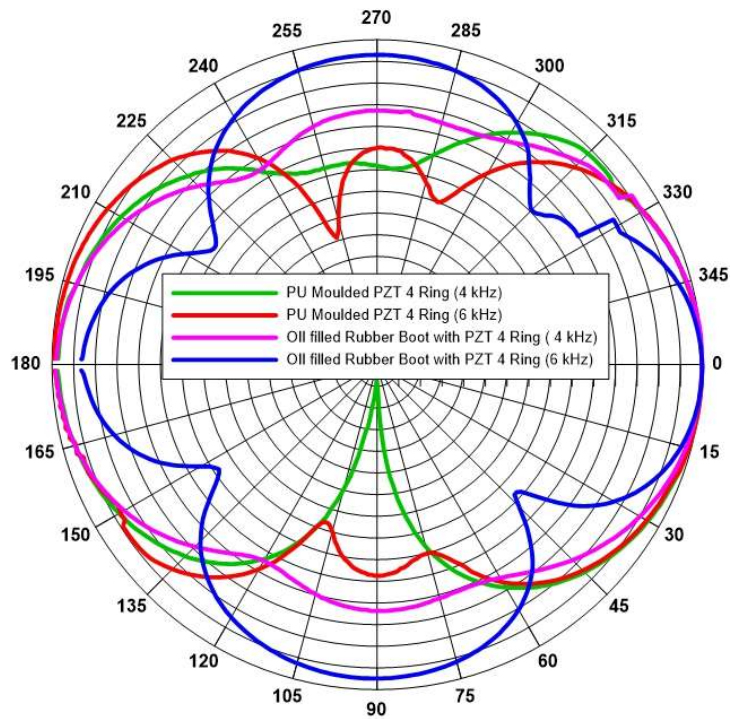
Fig. 4.30   Measured vertical directivities of PU moulded and oil filled transducers.

92

Table 4.3   Power and source level of RPC transducers.

Parameters	PU Moulded PZT4 Ring			Oil Filled rubber boot with PZT4 ring		
Frequency(kHz)	4	5	6	4	5	6
Voltage Vrms)	606.09	871.61	783.50	811.92	907.90	802.80
Current (I_{rms})	1.41	2.261	2.35	2.15	2.26	2.281
Phase (deg)	-57.37	-66.02	-69.06	-59.13	-64.63	-68.31
Impedance (Ω)	427.70	385.49	332.78	376.75	400.37	351.89
Power (W)	463.18	800.93	659.28	897.71	882.07	676.83
SL (dB)	190.13	191.49	190.38	190.98	191.97	190.01

After the open tank experiments, measurements in the pressurised chamber was carried out for the transducers. During pressurisation, PU moulded transducer resonance frequency is reduced to 3.8 kHz from 4.5 kHz (i.e., 18.4 % reduction) when the pressure is increased from 1 to 2 MPa but after that, it remained steady when the pressure is increased from 2 to 5 MPa as shown in Fig. 4.31. Reduction in resonance frequency is observed for oil filled transducer also when the pressure is increased from 0 to 1 MPa. The frequency changed to 3.6 kHz from 4.4 kHz, a reduction of about 22.2 % (Fig. 4.32). Beyond 2 MPa the change in resonance is not significant for oil filled transducer also.

The measured TVR under pressure for the PU moulded transducer is shown in Fig. 4.33. There is about 3 dB reduction in TVR in the band of 3-4 kHz with the increase in pressure from 1 to 5 MPa, but beyond 4 kHz TVR is stable and flat. The measured TVR under pressure for the oil filled transducer is shown in Fig. 4.34. With the increase in pressure from 0 to 7 MPa, the TVR is relatively stable, and the variation over the band is within ±1 dB, and it is similar to the measurement variation. The variation of

TVR from the open tank to the pressure chamber is also not very significant for both the transducers.
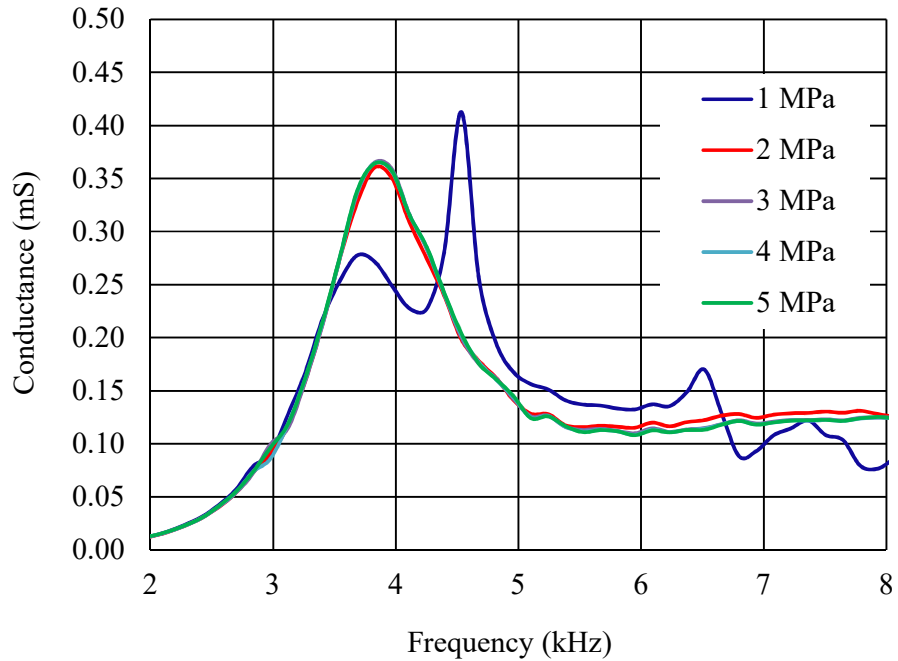
Fig. 4.31   Effect of pressure on resonance frequency of PU moulded transducer.
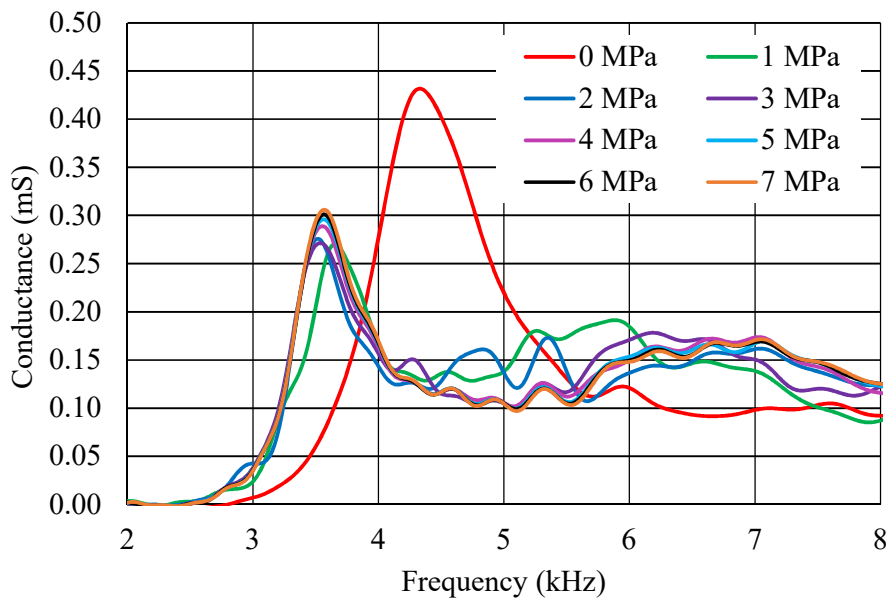
Fig. 4.32   Effect of pressure on the resonance frequency of oil filled transducer.
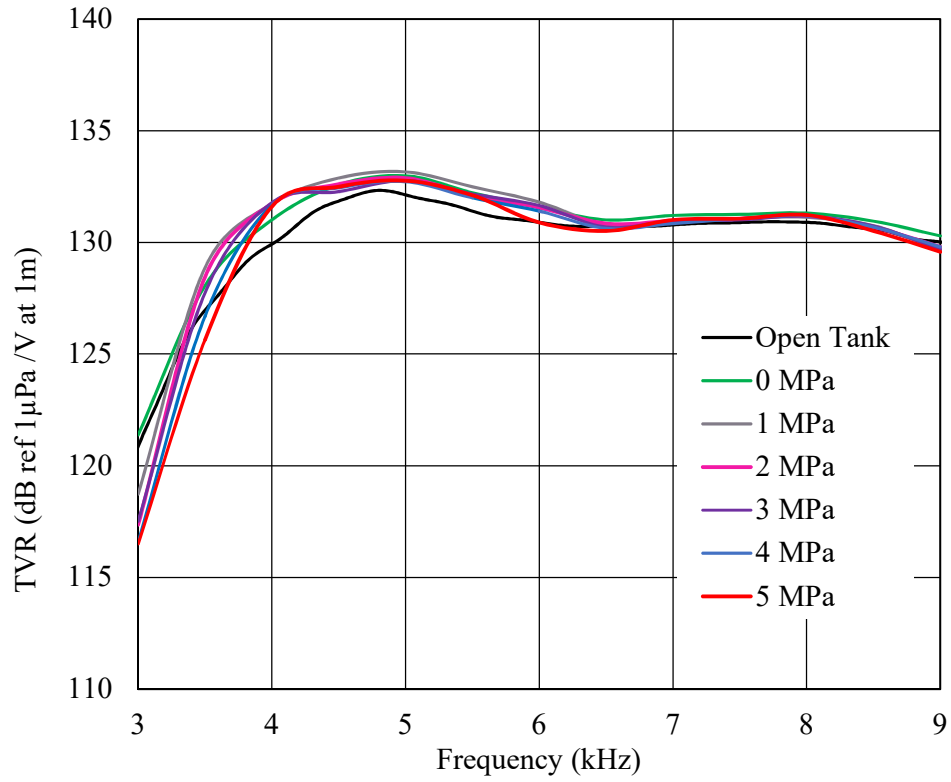
Fig. 4.33   Measured TVR of PU moulded transducer under pressure.
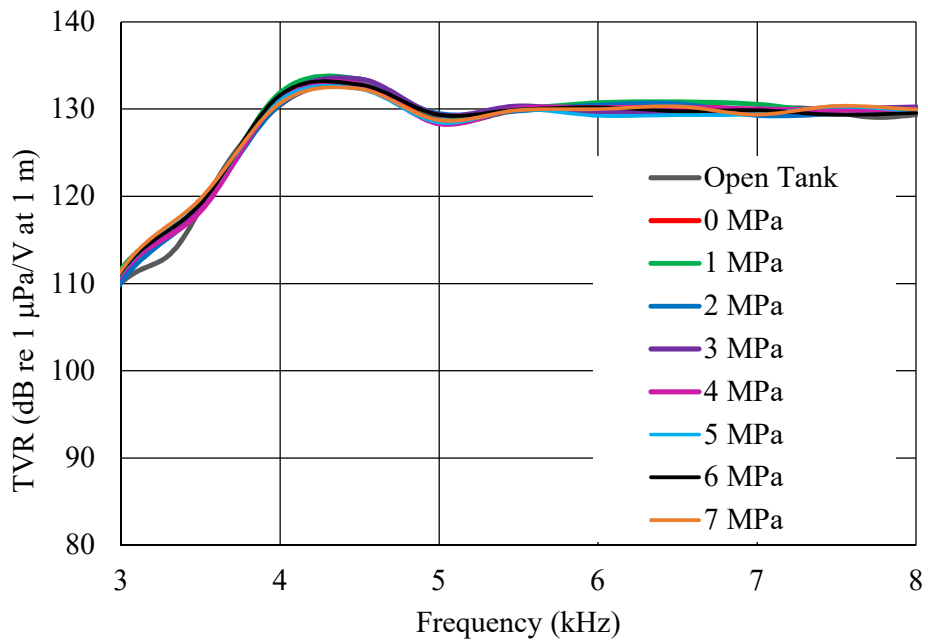
Fig. 4.34   Measured TVR of oil filled transducer under pressure.

After the acoustic measurements in open tank and under pressure, the transducers were subjected pressure test. Initially, the transducers were tested at 10 MPa in NPOL and later at NIOT at 60 MPa pressure for two hours to test the pressure withstanding capability (Fig. 4.35). The Continuity, capacitance and insulation resistance of the transducers were checked at regular intervals till the maximum pressure. There was no significant change in these values for both the transducers which indicate that the transducers can be safely operated upto 60 MPa.

Fig. 4.35   Pressure testing of transducers.

4.3   SEGMENTED RING TRANSDUCER

Free-flooded segmented ring transducers are ideal for deep sea applications and preferred over a one-piece radially expanding RPC because they have a higher electromechanical coupling, power output, and efficiency. The coupling coefficient of the segmented ring is 20% more than single piece ceramic ring because of the 33 mode operation of ceramic slabs of segmented ring compared to the 31 mode of ceramic ring (Hueter, 1971). Segmented ring transducers are manufactured by glueing together ceramic wedges or stacks of inexpensive ceramic slabs and metallic or non-metallic

wedges. Pre-stress is applied by fibre winding over the assembled segments. The resonance frequency of the segmented ring transducer can be lowered by using non-metallic wedges like Lucite or perforated metallic wedges. Renna (1972) in his US patent has reported oil-filled, fibreglass wound segmented ring transducer that enhances the bandwidth and efficiency by close coupling the cavity and hoop mode resonances. Lipper and Borden (2012, 2013) have reported output power reduction of 3 to 8.5 dB in the frequency band of 7-15 kHz for a polyurethane potted transducer compared to the oil-filled transducer, and such reduction will have grave consequences for deep submergence operations.

4.4 ALL-CERAMIC SEGMENTED RING

Radially Polarised Ceramic (RPC) rings are not suitable for low frequency transducers due to manufacturing limitations in making higher diameter rings. Higher diameter transducer can be made by glueing together ceramic wedges. However, the requirement of different sizes of ceramic wedges for different diameters is a disadvantage of all-ceramic segmented ring transducer. All-ceramic segmented ring transducer is pre-stressed by fibre winding over the assembled segments. PZT4 or PZT8 can be used as active material based on the power handling requirement of the transducer.

Encapsulation of the transducer can be carried out using direct moulding of rubber or polyurethane. It is also possible to assemble the transducer in a rubber boot filled with oil for encapsulation. The oil-filled transducer has an advantage over PU moulded transducer when operating in deep water (Lipper and Borden, 2012, 2013). Transducer modelling is carried out using the finite element package ATILA. All three methods of encapsulation described above are modelled. Based on the modelling studies,

transducers are manufactured and tested. Acoustic performances of the transducers manufactured are measured in an open tank and inside a pressurised chamber upto 7 MPa.

4.4.1   Transducer Description and Model

In the present study, an all-ceramic segmented ring transducer assembled with PZT4 wedges and fibre wrapped for pre-stressing is considered. The base model of the segmented ring selected for the study has a nominal outer diameter of 200 mm and is made out of 60 PZT4 wedges. Modelling studies are carried out to study the various parameters on its performance like diameter, thickness, height and type of PZT on TVR. Transducer encapsulation is carried out using direct polyurethane moulding, and oil filled boot. Silicone oil is used as the fill fluid. The transducer modelling is carried out using ATILA, a finite element package for sonar transducer design. $1/8^{th}$ of the transducer only need to be modelled because of the symmetry along X, Y and Z axes, as shown in Fig. 4.36 (a). An enlarged view of the model without water region is shown in Fig. 4.36 (b).

Parametric studies are carried out to investigate the effect of height, wall thickness, type of PZT, type of encapsulation and fill fluid on TVR. Effect of height on TVR is studied by varying the height from 50 to 150 mm, and the result is shown in Fig. 4.37. With the increase in height, the cavity mode resonance comes down because of larger volume entrapped in the cylinder. The hoop mode also becomes more predominant with an increase in height and added ceramic volume. Effect of wall thickness is studied by changing the wall thickness from 10 to 20 mm, and the results are shown in Fig. 4.38. As the wall thickness increases, the hoop mode becomes stronger and gives a higher

response. Since the inner diameter is kept constant, cavity resonance is not affected. Effect of ceramic material on TVR is studied by considering PZT4 and PZT8 as the active materials. The results shown in Fig. 4.39 indicate that PZT4 has about 2 dB higher TVR compared to PZT8 due to the higher d_{33} value of PZT4. However, in actual operation, PZT8 can handle about 400 V/mm compared to 200 V/mm for PZT4 that can compensate the difference in TVR.

(a)

(b)
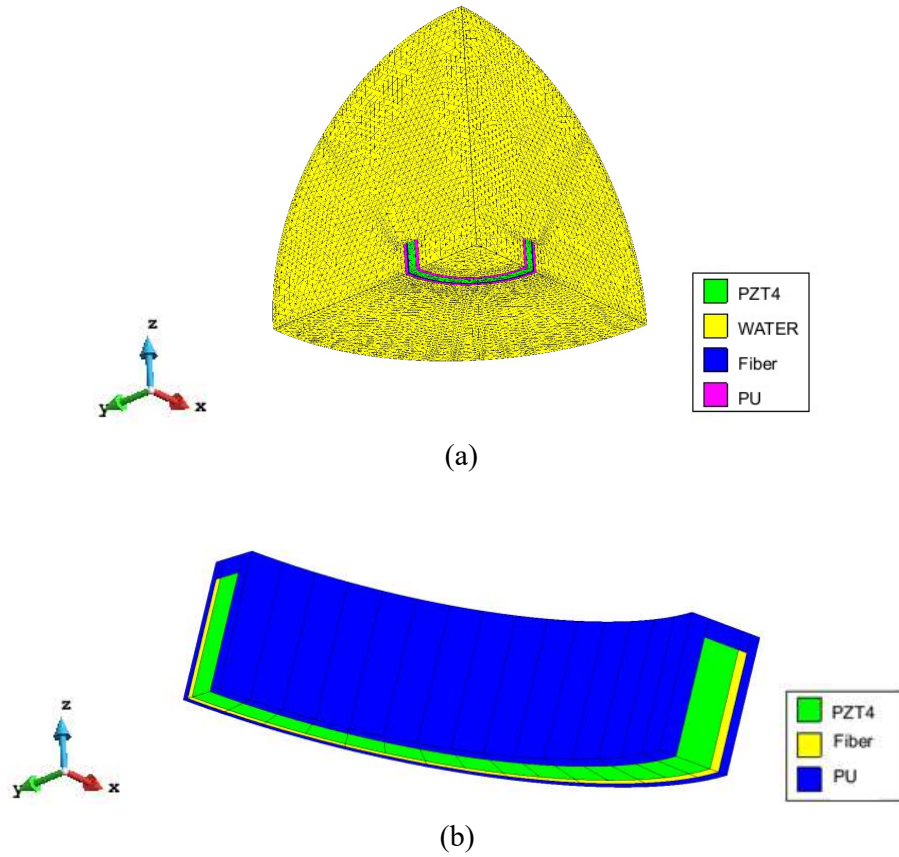
Fig. 4.36   Model of the transducer (a) with water (b) without water.
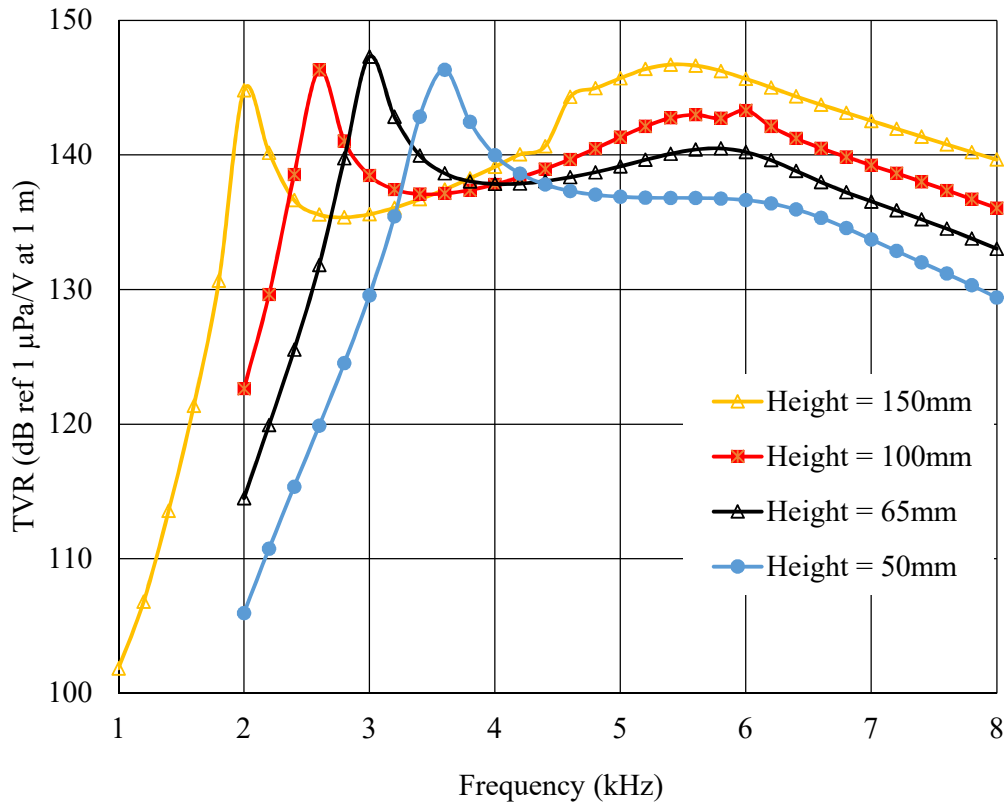
Fig. 4.37   Effect of height on TVR (Model).
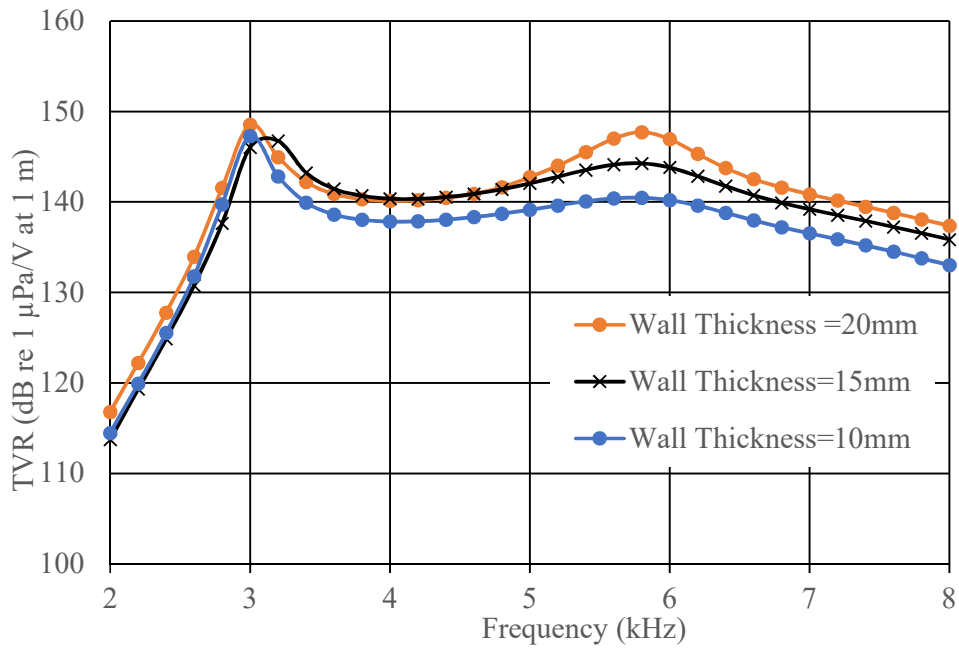
Fig. 4.38   Effect of ceramic wall thickness on TVR (Model).
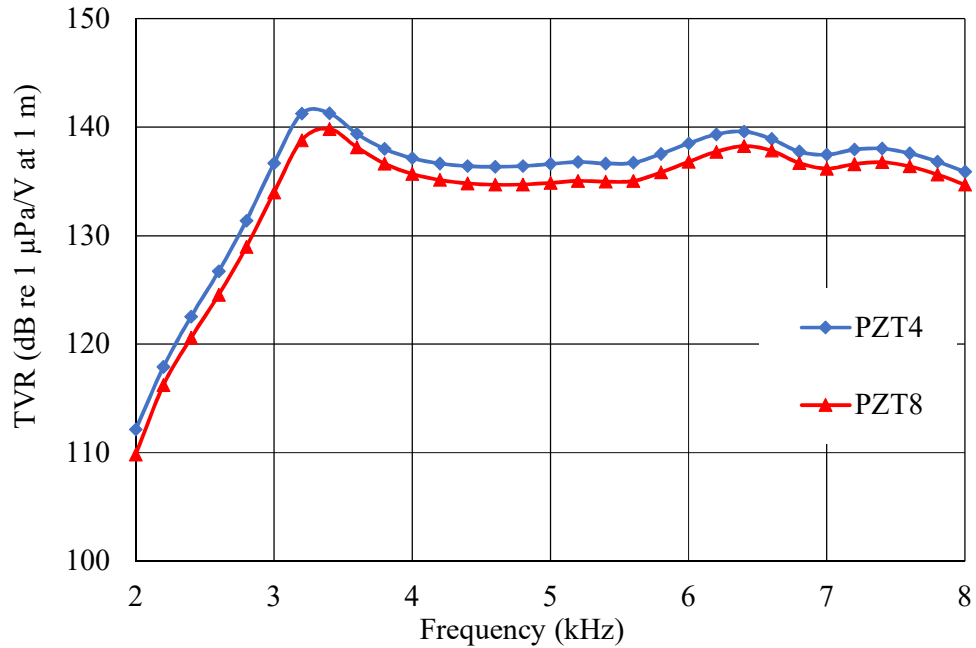
Fig. 4.39   Effect of ceramic material on TVR (Model).

Effect encapsulation on TVR is studied by modelling the transducer with PU and rubber moulding and oil filled rubber boot. The results are shown in Fig. 4.40. The results indicate that the response is similar except that for PU moulded transducer shows a lower resonance and higher response. Effect of fill fluids on Transmitting Voltage Response is studied by using different fill fluids like Silicone oil, Isopar-L, Transformer oil and Castor oil as shown in Fig. 4.41. The results indicate that fill fluids have no significant effect on TVR. Considering the manufacture and availability of ceramics, 194 mm OD segmented ring with 60 wedges in PZT4 material is considered for manufacture with PU moulding and oil filled rubber boot.

101
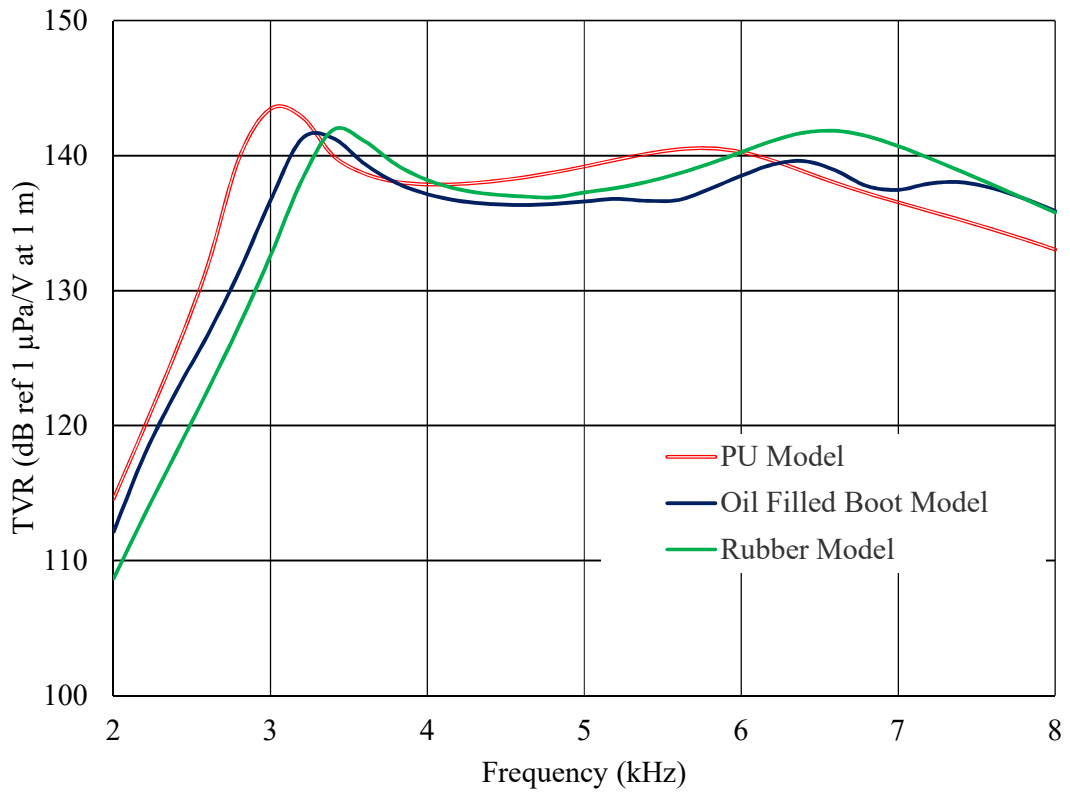
Fig. 4.40   Effect of encapsulation on TVR (Model)
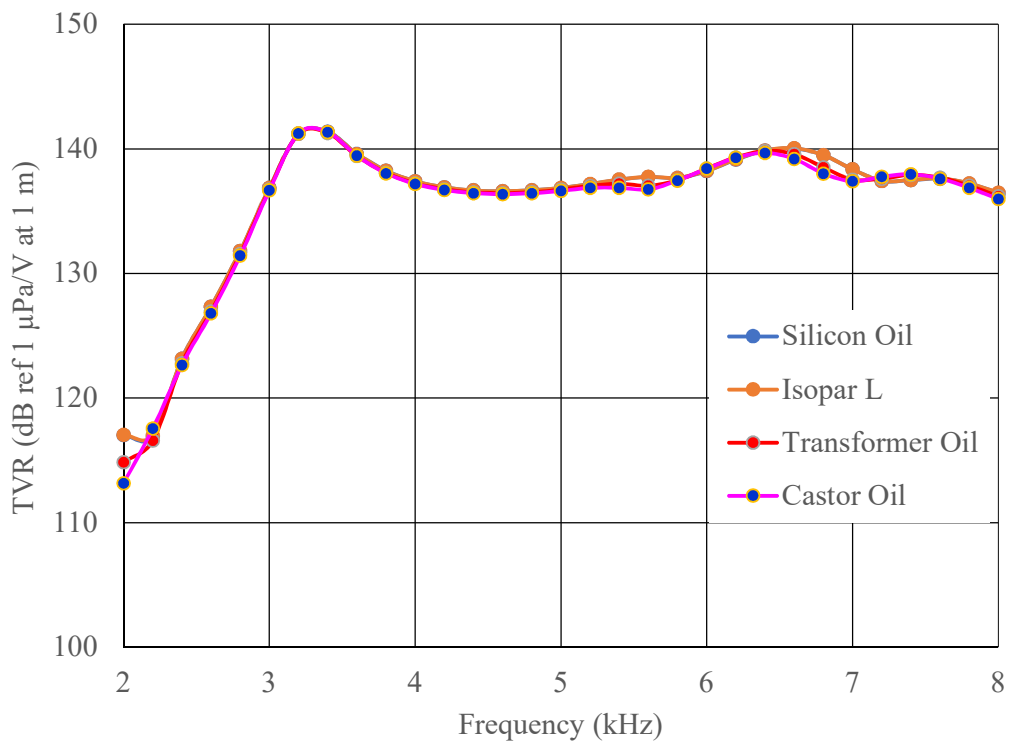
Fig. 4.41   Effect of Type of fill fluid on TVR (Model)

4.4.2 Pre-stressing of Segmented Ring Transducer

A major challenge in the design of segmented ring transducers is the pre-stressing of piezoceramic slabs. The transducers are excited by high voltage AC which causes high tensile and compressive stresses in the cylinder. The piezoceramic material is weak in tension. Hence the piezoceramic slabs in the transducers are to be given a compressive pre-stress bias to prevent failure under tension (Woollett, 1962). A commonly used method for pre-stressing the ring transducers is by fibre winding. Finding the value of tension at which the fibre is to be wound around the transducer to pre-stress the piezoceramic material is one of the critical design steps in the engineering development of a segmented ring transducer. The required pre-stress is found out by first calculating the static stress value corresponding to the DC voltage and then multiplying it by the mechanical quality factor and a factor of safety. The required tension in the fibre winding is estimated by solving the equations for a composite cylinder having an inner metal ceramic layer and an outer fibre winding layer. A custom-designed fixture and fibre winding machine are used for fibre winding the transducer. An epoxy resin is used for ensuring the mechanical integrity of the fibre winding layer. The transducer is then encapsulated using polyurethane material.

The dynamic strain ε_d of piezoelectric material due to an application of electric field E is given by Stansfield (1990),

$$\varepsilon_d = Q d_{33} E \tag{4.5}$$

where Q is the mechanical quality factor and d_{33} is the piezoelectric charge coefficient. The approximate expression for the tensile stress σ_t in the material is given by

$$\sigma_t = e_{33} \varepsilon_d \tag{4.6}$$

where e_{33} is the elastic coefficient. The pre-stress σ_p to be applied to prevent the tensile failure of the material is, $\sigma_p = K\sigma_t$ where K is the factor of safety. The quality factor is estimated using half power method from the conductance versus frequency curve of the piezoceramic slab in the transducer generated using the finite element method, using the following formula, $Q = f_R / (f_H - f_L)$ where f_R is resonance frequency, f_H and f_L are high and low-frequency points at which conductance is half the value at resonance.

The next step in the design is to estimate the fibre winding details such as the diameter of the yarn, thickness of the winding layer, number of layers and the fibre tension. The solution strategy to estimate the fibre tension closely follows the method presented by Zheng, Meng and Lei (2006) to estimate the pre-stress in fibre wound pressure vessels. Fig. 4.42 shows a sketch of the fibre wound piezoceramic cylinder. Let S be the minimum value of the pre-stress to be applied in the piezoceramic layer. The piezoceramic layer can be considered as a cylinder under external pressure, and the fibre layer can be assumed to be a cylinder under internal pressure as shown in Fig. 4.43.
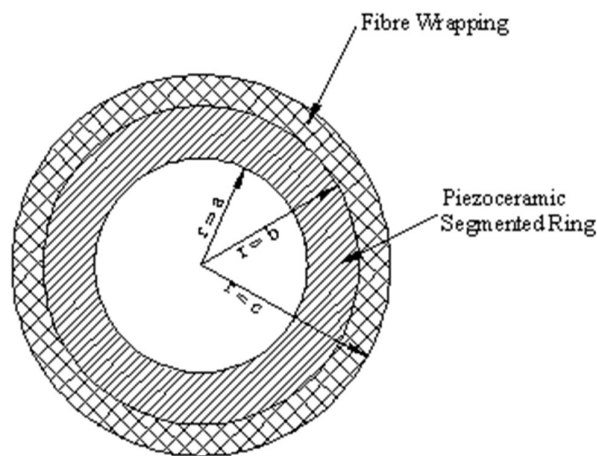
Fig. 4.42   Fibre wound segmented cylinder
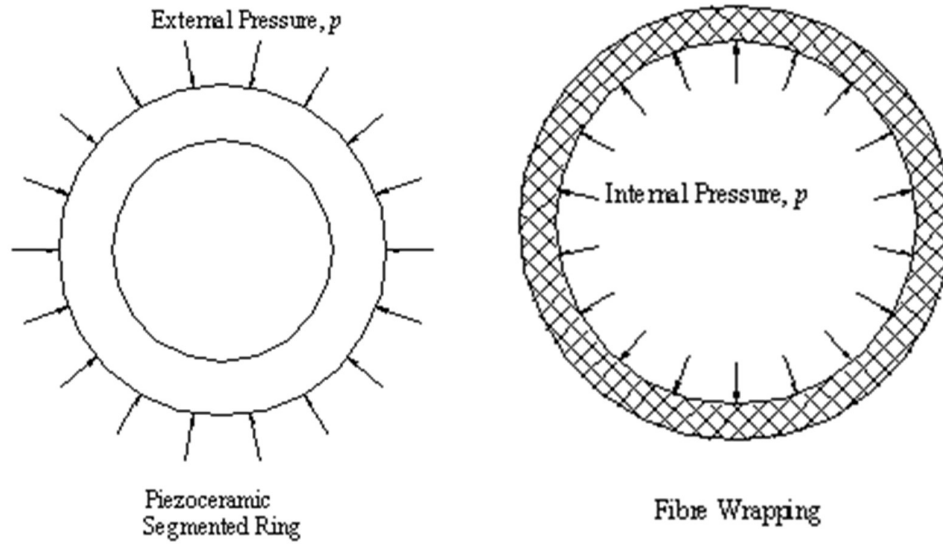
Fig. 4.43   Free body diagrams of piezoceramic and fibre layers

First, the external pressure on the piezoceramic ring to be applied to get a minimum pre-stress of S is found out. It is assumed that the segmented cylinder transducer has a perfect cylindrical geometry. It is also assumed that this layer is isotropic and linearly elastic. Also, since the cylinders under considerations are relatively short when compared to the radial dimensions and since the ends are not constrained to expand, plane stress conditions can be safely assumed. The hoop stress $\sigma_{\theta,e}$ in a thick elastic cylinder having an inner radius a and outer radius b under external pressure p under plane stress conditions is given by Srinath (2000).

$$\sigma_{\theta,e} = -\frac{pb^2}{b^2 - a^2}\left(1 + \frac{a^2}{r^2}\right) \tag{4.7}$$

It may be noted that the stress is minimum when $r = b$. Therefore, the hoop stress due to fibre wrapping at $r = b$ should be more than or equal to the required pre-stress.

The following assumptions are made in the analysis of the fibre winding layer (6).

✓ Fibre layer is transversely isotropic. Macroscopically, the mechanical property in the transverse direction is the same because the fibres are laid uniformly in transverse section.

✓ Fibre is linearly elastic.

✓ The load-bearing capacity of the resin is negligible when compared to that of the fibre.

✓ Fibre is continuous.

Based on the above assumptions, the hoop stress in the fibre winding layer having inner radius b and outer radius c under an internal pressure of p is given by Zheng, Meng and Lei (2006).

$$\sigma_{\theta,f} = \frac{p(1 + x_2)(c^{x_1} r^{x_2} + c^{x_2} r^{x_1})}{c^{x_1} b^{x_2} - c^{x_2} b^{x_1}}$$ (4.8)

where $x_1 = -1 + \sqrt{\dfrac{E_{11}}{E_{22}}}$, $x_2 = -1 - \sqrt{\dfrac{E_{11}}{E_{22}}}$ E_{11} and E_{22} are   longitudinal   and

transverse Young's modulus of the fibre layer respectively. This tensile stress is borne by the fibre. Since the fibre has a circular cross-section, the area of fibre cross section per unit area of the fibre winding layer cross section (defined as the packing efficiency, η) will be less than 100%. Let d be the diameter of the fibre. Therefore, the tension T in the fibre at a given radius r can be calculated as

$$T = \frac{\sigma_{\theta,f}(r)}{\eta} \frac{\pi d^2}{4}$$ (4.9)

Specified OD of the bare piezoceramic cylinder (excluding the thickness required for fibre winding and encapsulation) for this application is 194 mm, and wall thickness is 10 mm. The maximum electric field that can be applied to the PZT4 ceramic is 200

V/mm. The pre-stress needed for applying a field of 200 V/mm in the piezoceramic is 40 MPa. Considering a fibre yarn diameter of 0.6 mm, the fibre tension required for different fibre layer thickness values are shown in Table 4.4.

Table 4.4   Fibre tension for different fibre layer thicknesses

Fibre winding Thickness (mm)	Number of Fibre yarn Layers in the Lining	Fibre Yarn Tension (kg$_f$)	Minimum Required Strength of the Fibre yarn with factor of safety (kg$_f$)
2	3	10	30
3	5	6.1	18.3
4	6	5.1	15.3
5	8	3.8	11.4

Assuming that the stresses in the cylinder are limited to the compressive regime, the maximum possible tension in the fibre during operation will be double the initial tension. Applying a factor of safety of 1.5 over this, the minimum strength of the fibre required will be 3 times the fibre tension required. A fibre winding thickness of 4 mm is selected for full power application at an electric field of 200 V/mm.

4.4.3   Stress Analysis

The stresses acting on a transducer are due to pre-stress, hydrostatic operating conditions, and applied voltage. The static stress induced in the piezoceramic stack due to pre-stress is calculated in the previous section as 40 MPa. Effect of hydrostatic pressure on the transducer is studied by modelling the transducer with a thin layer of water around it and applying 1 Pa pressure on it through the water as shown in Fig. 4.44 and the maximum stress on the transducer is found (Fig. 4.45). The max von-Mises stress on the transducer with 1 Pa pressure is calculated using the equation 4.1, as 1.546 Pa. Assuming linear behaviour, the stress at 60 MPa pressure is found to be 92.76 MPa.

So the combined static stress is 132.76 MPa which is much below the maximum compressive strength of the PZT4 ceramics. Table 4.5 shows the maximum principal and shear stresses due to hydrostatic pressure and 1 V_{pp} excitation.
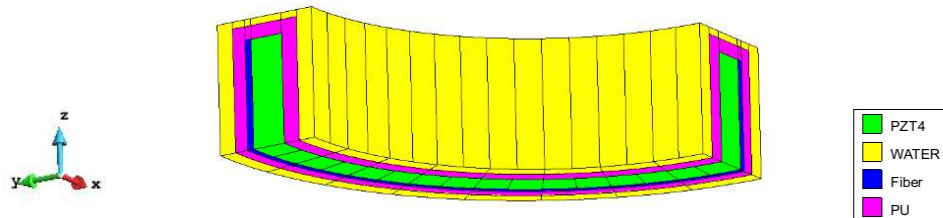
Fig. 4.44   Model for the study of hydrostatic pressure effect
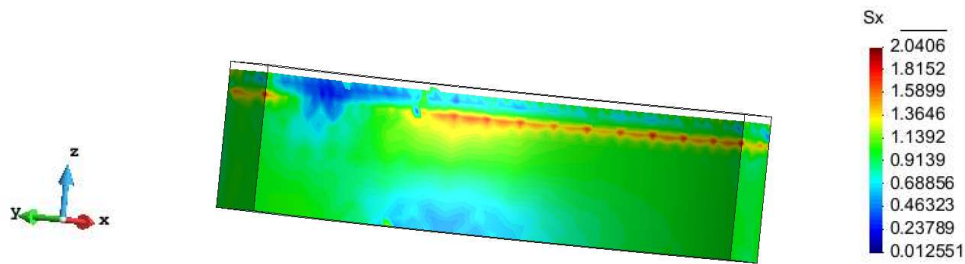
Fig. 4.45   Stress due to 1 Pa hydrostatic pressure

The dynamic stresses at 3 kHz are shown in Fig. 4.46 when 1 V_{pp} (peak-to-peak) is applied. The maximum von-Mises stress in the transducer is calculated as 21402 Pa at 3 kHz using the equation 4.1. The maximum voltage that can be applied to the ceramic wedge of 10 mm thickness during actual operation is 200 x 10 =2000 V_{pp}. Therefore, the maximum stress will be 42.8 MPa_{pp} at 3 kHz. The maximum rated dynamic or cyclic stress for PZT4 piezoceramics is 83 MPa and the actual stresses of 42.8 MPa is much less than the maximum rated stress.
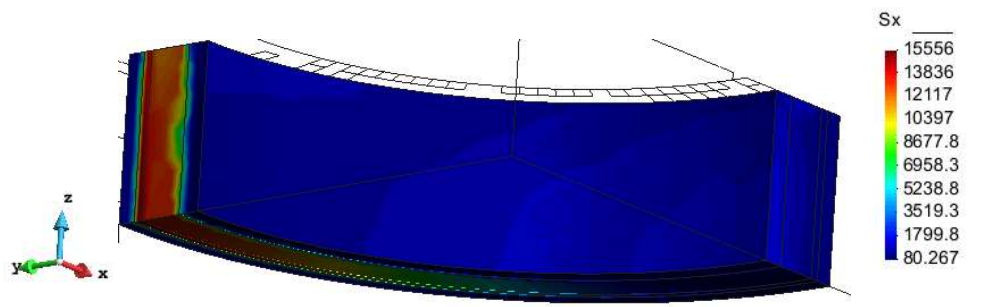
Fig. 4.46   Stress due to 1 Volt excitation

4.4.4   Transducer Manufacture

Segmented rings were assembled using thickness poled PZT4 wedges and metal electrodes in a special jig using an adhesive. The stack was kept under pressure for 24 hours for fully curing the adhesive. Once the cylinder was formed, it was subjected to pre-stress by fibre winding it in a winding machine. The winding machine has provision to adjust the speed of rotation, and tension in the fibre. The pre-stress required was calculated based on the maximum operating voltage. The adhesive was applied on each layer of the fibre for retaining the tension in it. The assembly was kept under tension in the winding machine until the adhesive on the fibre was fully cured. The positive and negative electrodes are wired and protected with an arc proof coating.

Table 4.5   Stress due to 1 Pa pressure and 1 V_{pp} excitation.

	Sx (Pa)	Sy (Pa)	Sz (Pa)	Sxy (Pa)	Syz (Pa)	Szx (Pa)	σ_v (Pa)
1 Pa Pressure	2.040	2.421	1.953	0.2779	0.3130	0.4895	1.546
1 V_{pp}	15556	15481	1396	3799	131	1793	21402.29

109

For direct PU moulding and oil filled rubber housing, special moulds are required. The rubber boot was made using a special rubber compound that can withstand oil and seawater environments. There are top and bottom rubber bushes with a groove for positioning the segmented ring inside the oil filled rubber housing. A top flange with provision for oil filling, air vent, and cable glands are placed above the top bush as shown in Fig. 4.47 (a). The rubber boot has an inner flange, and that is assembled to the top flange using another plate below the rubber flange using bolts. Outer diameter is sealed using a metallic belly band. Silicone oil is filled through the oil vent, and after filling, both oil and air vents are closed using O-rings and screws. Cable sealing is carried out by the assembly of rubber and metallic washers around the cable and tightening it with a gland nut. The top plate is connected to the bottom plate using bolts to prevent the boot from loading the weight of oil and segmented ring. The components used in the assembly of oil filled transducer are shown Fig. 4.48, and the fully assembled transducer is shown in Fig. 4.49(d).
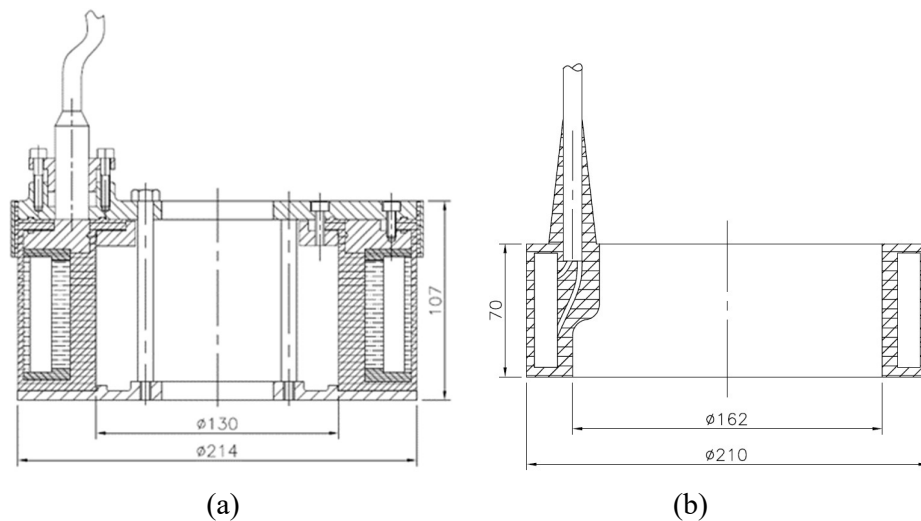
Fig. 4.47   Schematic diagram of (a) oil filled transducer (b) PU moulded.

Fig. 4.48   Components of oil filled segmented ring transducer

Polyurethane moulding was carried out in a special mould tool using a commercially available PU compound. Adhesion of PU with different materials like ceramic, fibre and cable materials need an adhesion promoting coating. Deaeration of the PU compound is important to prevent bubble formation. When there are bubbles in the moulded transducer, it can break down at high pressure in the deep water leading to the reduction in insulation resistance or shorting of the transducer, depends on the severity of damage. The schematic and fully assembled PU moulded transducer are shown in sin Figs. 4.47 (b) and 4.49(c).

4.4.5   Experiments Conducted

The transducers manufactured were initially tested in an open tank of 50 m length, 20 m width and 18 m depth. The transducer was positioned at a depth of 10 m and parameters like resonance frequency, Transmitting Voltage Response (TVR) and directivity were measured. The measurements were then repeated in the pressurised test chamber. The pressure inside the chamber can be fixed as per requirement, and the tests were carried out in steps of 1 MPa from 1 to 7 MPa. After that, transducers were tested in a pressure test facility at 10 MPa to check the pressure withstanding capability of transducers.

4.4.6 Results and Discussions

Modelled and measured Transmitting Voltage Responses in the open tank are shown in Fig. 4.50 for the PU and rubber moulded transducers. TVR values show reasonably good match between model and experiment except at resonance where the model values are higher since losses are not included in the model. The transducer has usable bandwidth 3 to 7 kHz where it has a TVR of above 130 dB. Measured receiving sensitivity of PU moulded and oil filled transducers are shown in Fig. 4.51. The results show that the PU moulded transducer has about 2 to 8 dB higher sensitivity than oil filled transducer in the band of 3-8 kHz.

(a)

(b)

(c)

(d)

Fig. 4.49   (a) Assembled segmented ring with ceramic wedges (b) fibre wrapped ring (c) PU moulded transducer (d) Transducer with oil filled boot
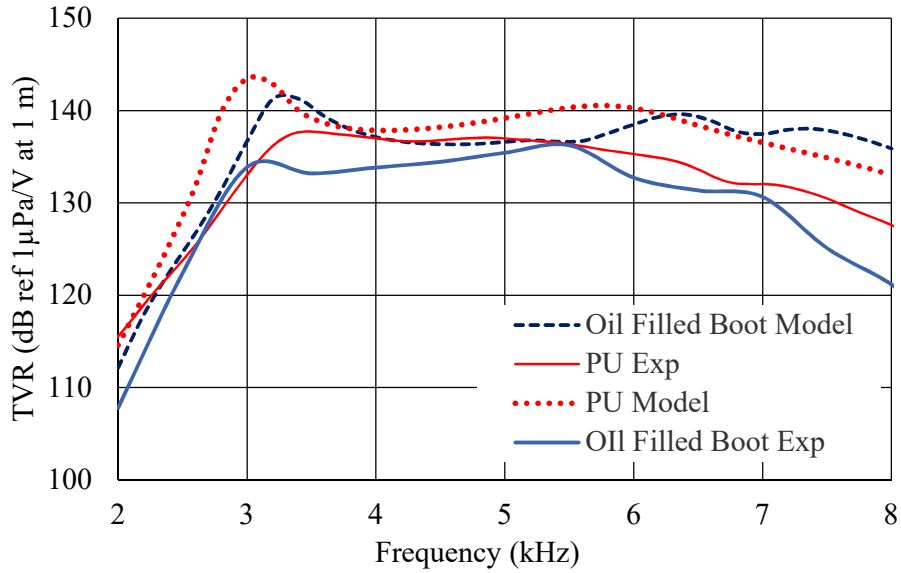
Fig. 4.50   Effect of encapsulation on TVR: model vs open tank experiment.
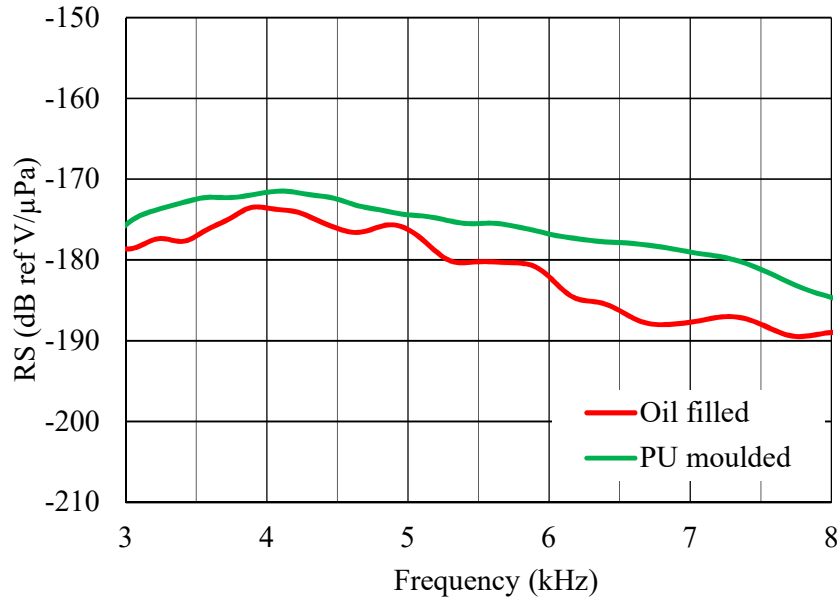
Fig. 4.51   Measured Receiving Sensitivity.

The horizontal and vertical directivities of the PU moulded, and oil filled all-ceramic segmented ring transducers measured at 4 and 6 kHz are shown in Figs. 4.52 and 4.53. The horizontal directivities of both the transducers at 4 and 6 kHz are Omni within 3 dB. The vertical directivities are toroidal in shape for PU moulded transducer and oil

filled transducer at 4 kHz, but for oil filled transducer it is almost Omni within 5dB at 6 kHz.

Power and source level of the PU moulded, and oil filled transducers are shown in Table 4.6. Both the transducers have source level of more than 194 dB re 1 µPa at 1 m. The source levels shown are for untuned transducers at 10 m depth so it can be enhanced by tuning the transducers and measuring in deeper depths since the transducer is capable of handling higher power.
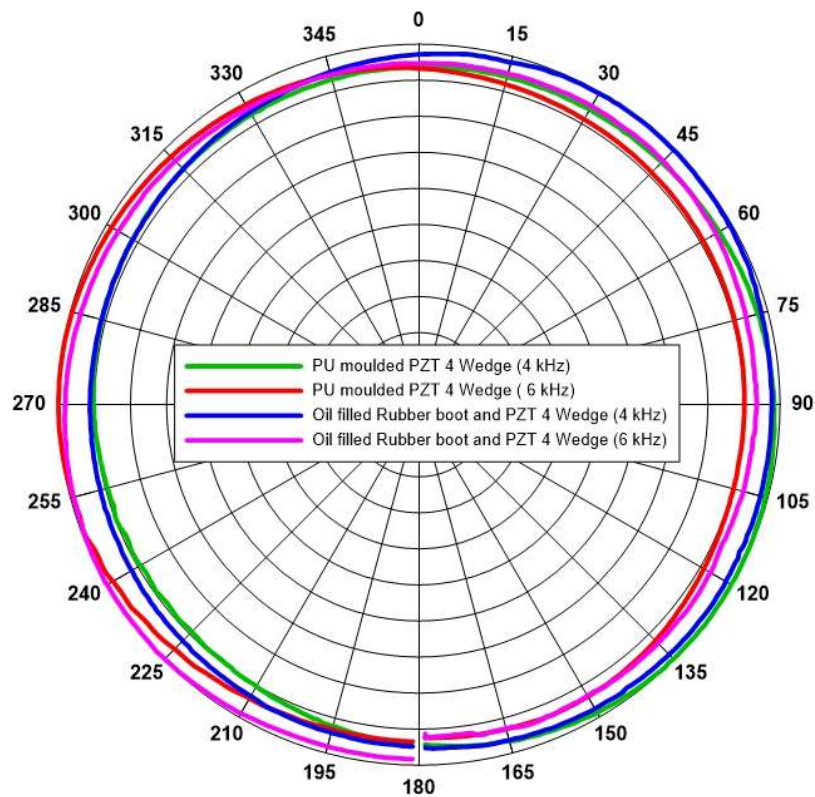
Fig. 4.52 Measured horizontal directivities of PU moulded and oil filled transducers.
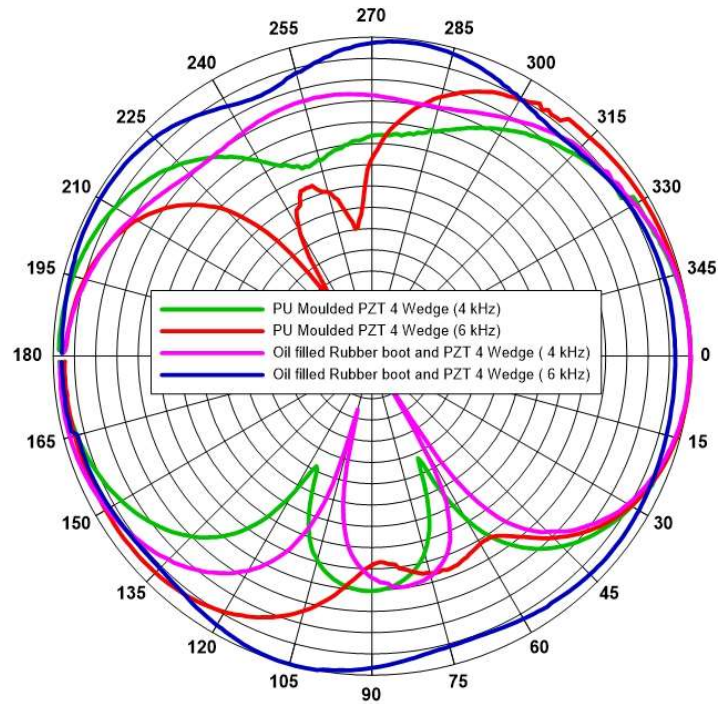
Fig. 4.53   Measured vertical directivities of PU moulded and oil filled
             transducers.

Table 4.6   Measured power and source level at 10 m depth.

Parameters	PU Moulded	Oil filled rubber boot
Frequency (kHz)	4	4
Voltage (V_{rms})	1165	1058.24
Current (I_{rms})	1.4	1.09
Phase (Degree)	-54.5	-64.68
Impedance (Ω)	830.2	970.26
Power (W)	947	493.67
SL (dB re 1 µPa at 1 m)	197.8	194.2

After the open tank experiments, the transducers were tested in a pressurised vessel for

its acoustic performance upto 7 MPa in steps of 1 MPa. The conductance and TVR of

the transducers were measured and shown in Figs. 4.54 to 4.57. The frequency vs

conductance plot indicates that the resonance frequency changed from 3.8 to 3.4 kHz

115

when pressure is increased to 1 MPa but beyond 1 MPa the there is no appreciable change in resonance frequency. For the oil filled transducer, the resonance frequency changed from 3.48 to 2.97 kHz when pressure is increased to 2 MPa but beyond 2 MPa the there is no appreciable change in resonance frequency.

The TVR plots show that TVR of the PU moulded and oil filled transducers are stable over the entire band and variation is within $\pm$ 1 dB, and it is similar to the measurement variation. The variation of TVR from open tank to the pressure chamber is also not very significant for both the transducers.
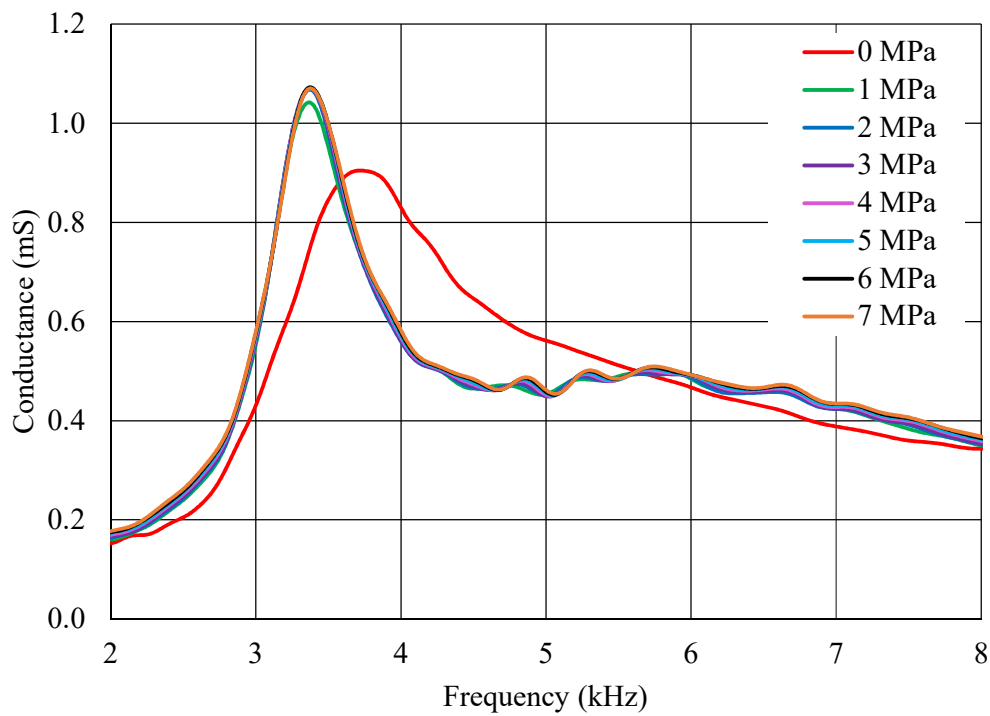
Fig. 4.54   Effect of pressure on the resonance frequency of PU moulded transducer.
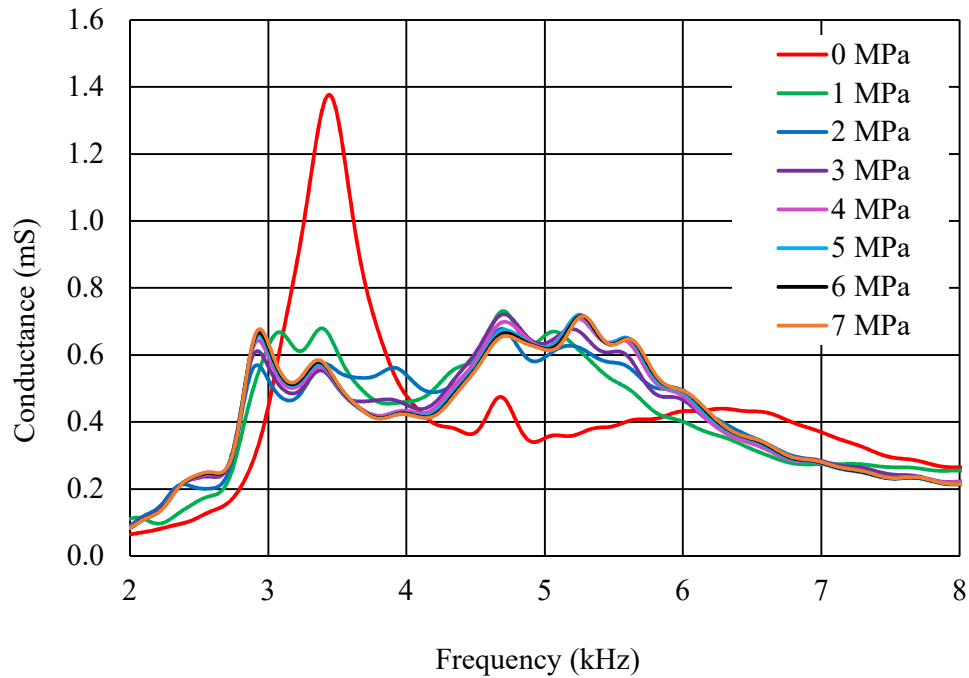
Fig. 4.55   Effect of pressure on the resonance frequency of oil filled transducer.
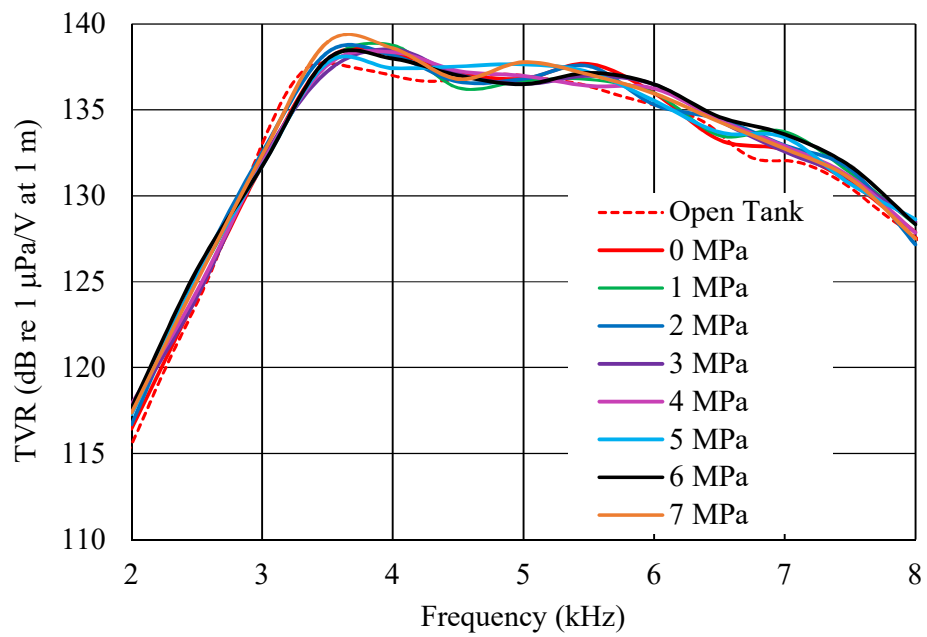
Fig. 4.56   Effect of pressure on TVR of PU moulded transducer.
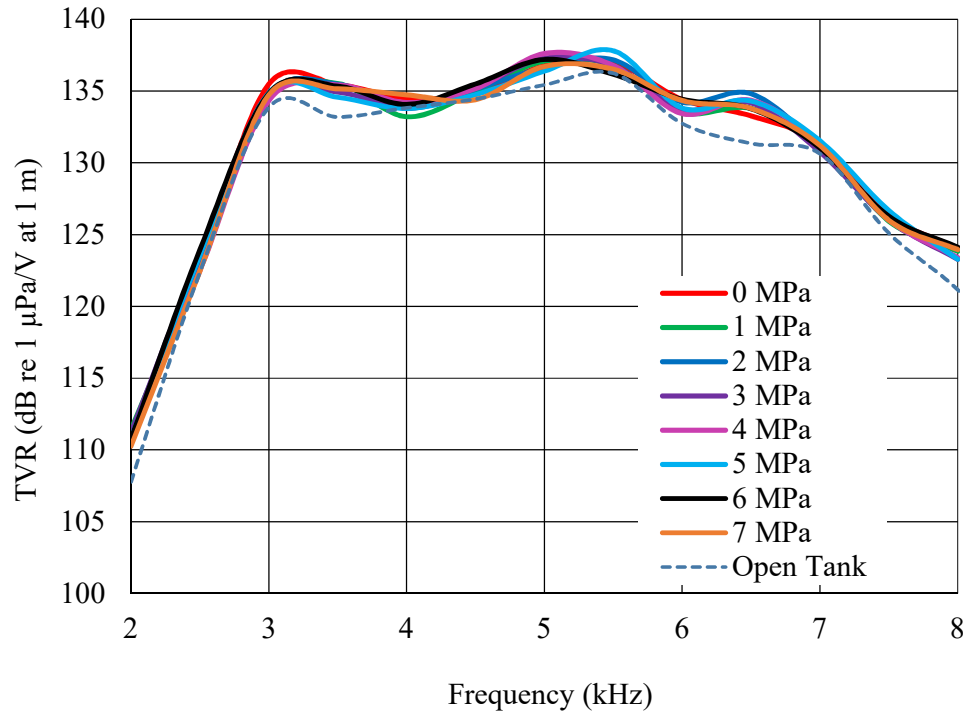
Fig. 4.57   Effect of pressure on TVR of an oil filled transducer.

After completing the acoustic test in the pressure vessel, the transducers were tested in a high-pressure test facility to check the pressure withstanding capability of the transducer from 0 to 10 MPa in steps of 1 MPa. At the maximum pressure, it was held for two hours. Capacitance and insulation resistance were measured to verify the health of the transducer during the test and found to be stable.

4.5   METAL CERAMIC SEGMENTED RING TRANSDUCER

Metal ceramic segmented ring transducers are made out of piezoceramic slabs and metallic wedges and preferred for low frequency, large diameter, free-flooded rings due to its ease of manufacture and low cost in comparison to all-ceramic segmented ring. Metal ceramic segmented ring transducers with different wedge and ceramic materials are modelled using ATILA. Transducers modelled are manufactured, assembled and

tested in an open tank and inside a pressurised vessel from 1 to 7 MPa. Performance parameters like resonance frequency, receiving sensitivity, transmitting voltage response and directivity are measured. Transducers are also tested to check its pressure withstanding capability.

Since piezoceramics are weak in tension, sufficient pre-stress is mandatory to apply high power to the ring transducer. Pre-stress to the segmented ring can be applied using fibre winding over the assembled segments. Wedges made out of non-metallic materials like Lucite, Nylon or perforated metallic wedges can be used to bring down the resonance frequency of the segmented ring transducer. However, the use of non-metallic wedges like Lucite with large elastic compliance reduces the overall response of the transducer (Butler, 1976). Brass and aluminium are commonly used as wedge material. Aluminium or titanium can be used as wedge material when weight is of prime importance, like dunking sonar application. PZT4 or PZT8 can be used as active material based on the power handling requirement of the transducer. Encapsulation can be carried out using direct polyurethane over-moulding or assembling the transducer in a rubber housing filled with oil. Direct rubber moulding is not recommended due to the high-temperature process, which can damage the piezoceramics and fibre wrapped around the transducer for pre-stressing.

4.5.1 Transducer Model

The active material of the transducer studied is piezoceramic slabs of PZT4 with 5 mm thickness. The transducer base model has an outside diameter of 214 mm and inside diameter of 130 mm. First, the transducer is studied for direct moulding over the ceramic ring with an encapsulation thickness of 5 mm all around. In the next case, the

119

transducer is positioned in a rubber casing in which the cavity around the ceramic is filled with a fill fluid. In order to study the effect of different type of fill fluids on the transducer, widely used fill fluids like Silicone oil, Castor oil and Isopar-L are considered. The effect of wedge material on transducer performance is studied by using materials like brass and aluminium. Effect of PZT is investigated with PZT4 and PZT8 ceramics. FEM software, ATILA is used to model the transducers. Because of the symmetry in X, Y and Z axis, only 1/8th of the transducer is modelled as shown in Fig. 4.58. Ten noded tetrahedral elements are used to model the piezoelectric, elastic, fill fluid, and water surrounding the transducer.

The basic model of the transducer considered is with Brass wedges and PZT4 ceramic slabs. The effect of height on TVR is modelled with different heights like 50, 75 and 100 mm. Like in the case of RPC and segmented ring transducers, with the increase in height cavity resonance comes down and the hoop mode response level increase as shown in Fig. 4.59.

Fig. 4.58   3D model of the transducer in water.
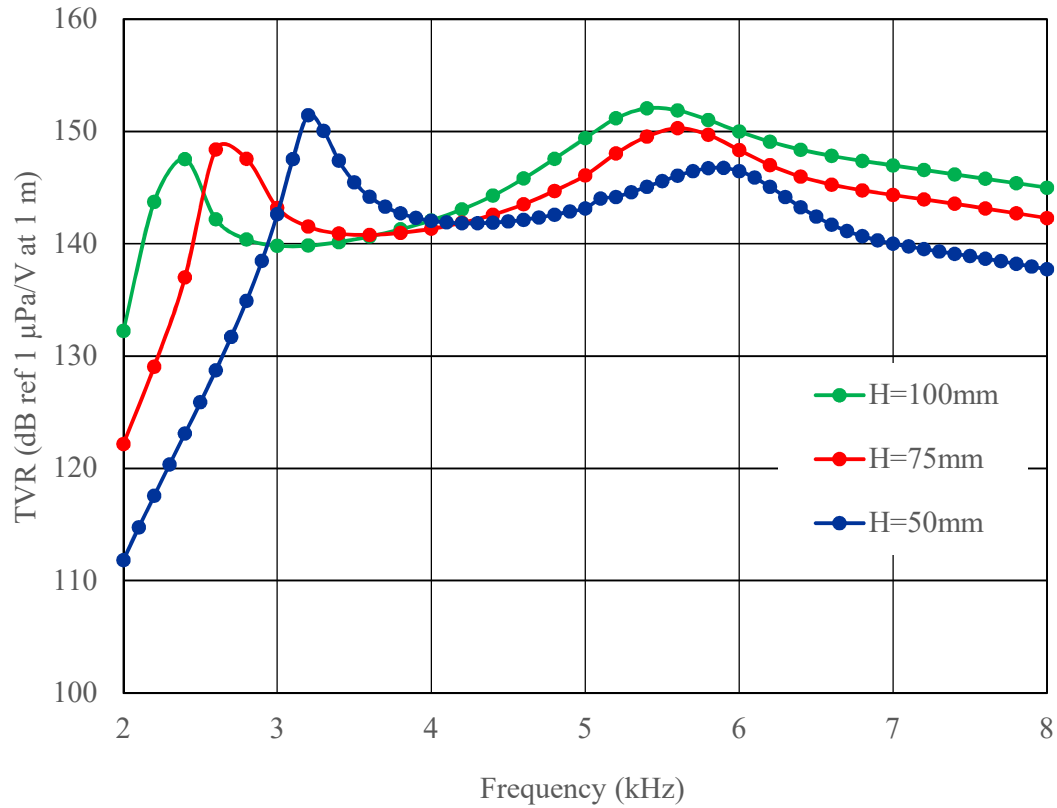
Fig. 4.59   Effect of height on TVR.

Effect of wedge material on TVR is shown in Fig. 4.60, and it indicates that at the first resonance, due to the cavity mode, TVR values are identical because of same physical dimensions. However, beyond the first resonance, transducer with brass wedges has about 2 dB higher TVR due to its higher effective coupling coefficient because of its less elastic compliance. The transducer with aluminium wedges weighs about one kilogram less compared to the transducer with brass wedges. Helicopter based dunking sonar where weight is a critical parameter and prefers to operate at a lower frequency, transducer with aluminium wedges can be an ideal choice.
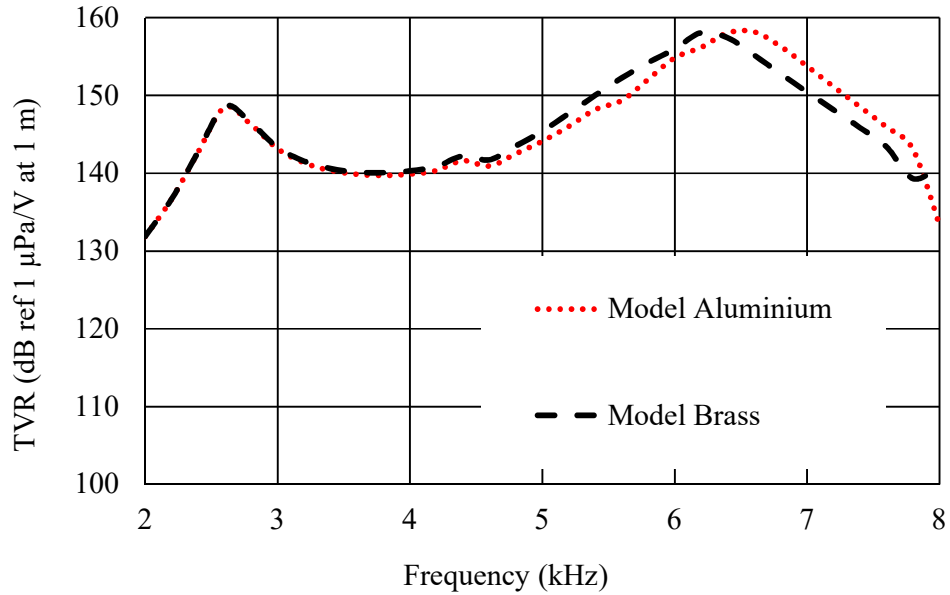
Fig. 4.60   Effect of wedge material on TVR.

Effect of PZT4 and PZT8 materials on the TVR is shown in Fig. 4.61. Both these transducers have aluminium wedges. PZT4 has higher d_{33} value compared to PZT8, and it is reflected in the TVR plots. However, PZT8 has higher voltage handling capability and can be subjected to higher electric power.

Effect of encapsulation is studied by comparing the direct polyurethane moulded transducers with the Silicone oil filled transducer. The transmitting voltage response (TVR) is shown in Fig. 4.62. The resonance frequency of the oil filled transducer is about 500 Hz lower than PU moulded transducer since PU has higher stiffness. The effect of different type of fill fluids on transducer performance is studied, and the results are shown in Fig. 4.63. The results indicate that there is no significant effect of fill fluid on TVR. So the selection of fill fluid should be based on other parameters like low toxicity, easily handled, chemically and thermally stable and cost.
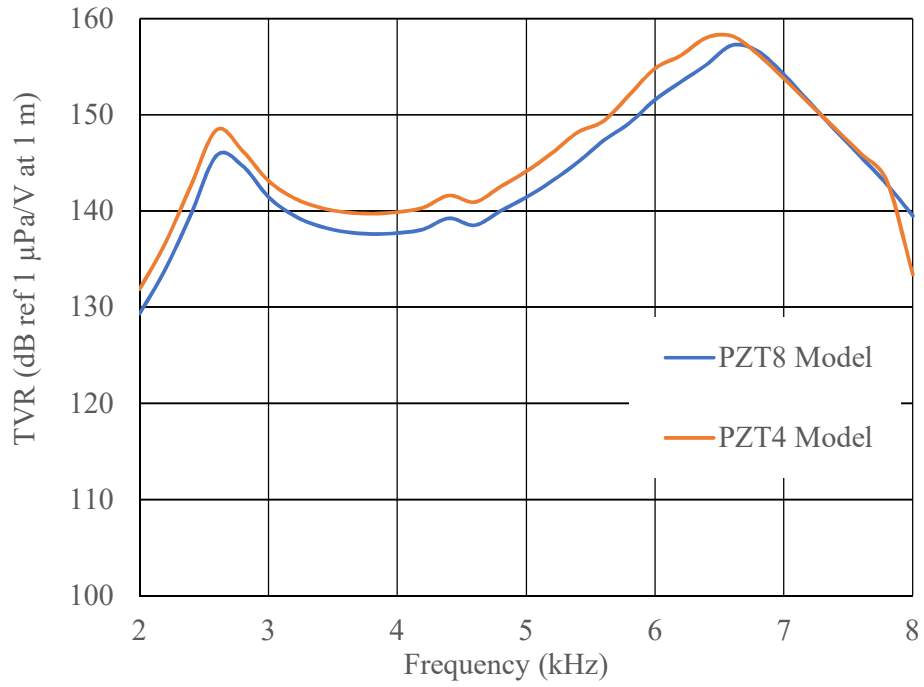
Fig. 4.61   Effect of ceramic material on TVR.
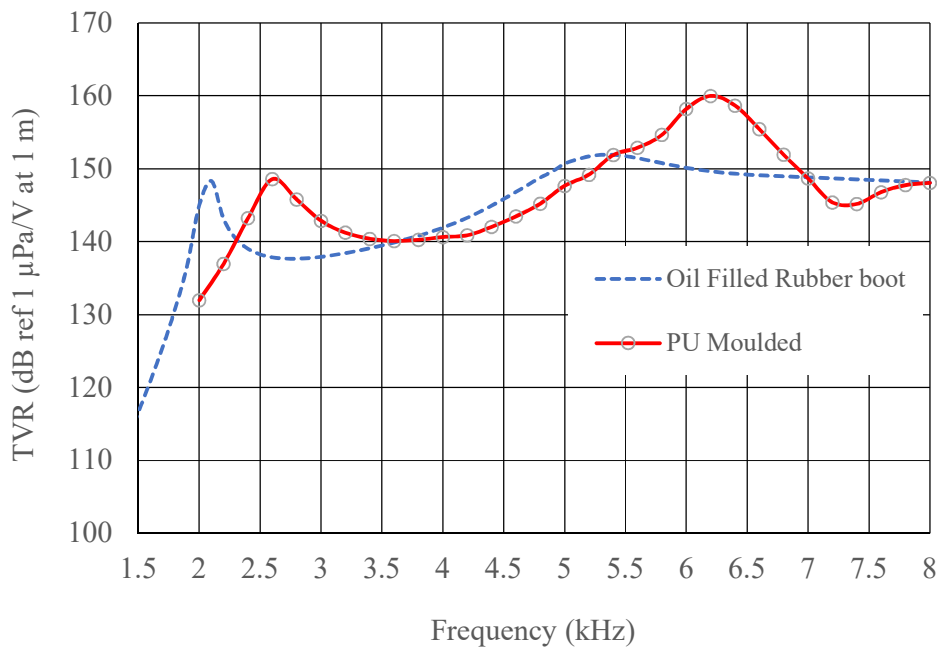
Fig. 4.62   Effect of encapsulation on TVR.
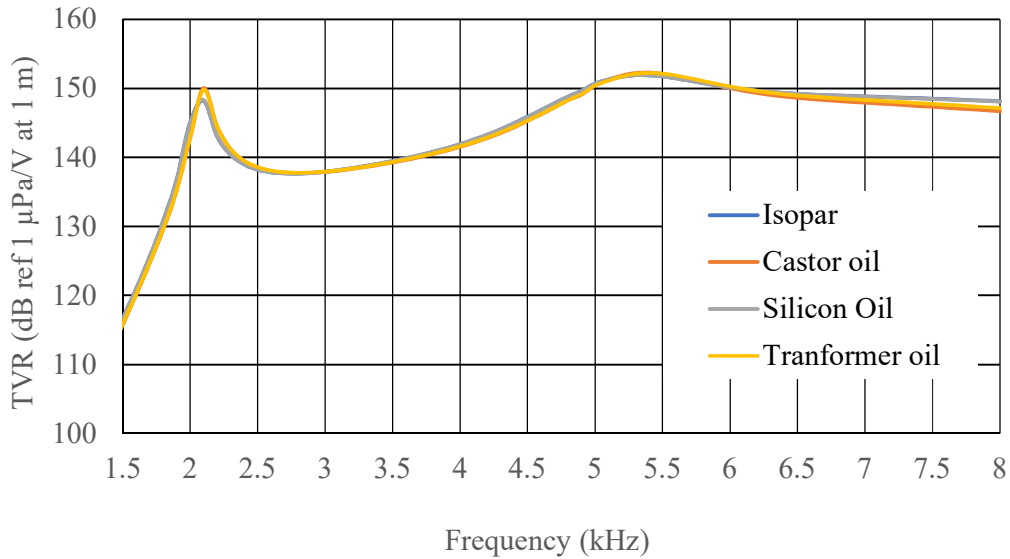
Fig. 4.63   Effect of type of fill fluid on TVR

4.5.2   Stress Analysis of Transducer

The stresses acting on a transducer are due to pre-stress, hydrostatic operating conditions, and applied voltage. The static stress induced in the piezoceramic stack due to pre-stress is calculated as 40 MPa based on the details given in section 4.4.2. Effect of hydrostatic pressure on the transducer is studied by modelling the transducer with a thin layer of water around it and applying 1 Pa pressure on it through the water as shown in Fig. 4.64. The maximum von-Mises stress on the transducer with 1 Pa pressure is 2.127 Pa and assuming linear behaviour, the stress at 60 MPa pressure is found to be 127.62 MPa. So the combined static stress is 167.62 MPa which is much below the maximum compressive strength of the PZT4 ceramics. Fig. 4.65 shows the stress distribution in the transducer.

The dynamic stress, Sx, at 6 kHz is shown in Fig. 4.66 when 1 V_{pp} is applied. The maximum von-Mises stress in the stack is calculated using the equation 4.1. The max von-Mises stress with 1 V_{pp} is 23998 Pa at 6 kHz. The maximum voltage that can be

applied to the ceramic slab of 5 mm wall thickness during actual operation is 1000 V_{pp}. Therefore, the maximum stress will be 23.99 MPa at 6 kHz. The maximum rated dynamic or cyclic stress for PZT4 piezoceramics is 83 MPa and the actual stress of 23.99 MPa is much less than the maximum rated stress. Table 4.7 shows the stresses due to hydrostatic pressure and 1 V_{pp} excitation.
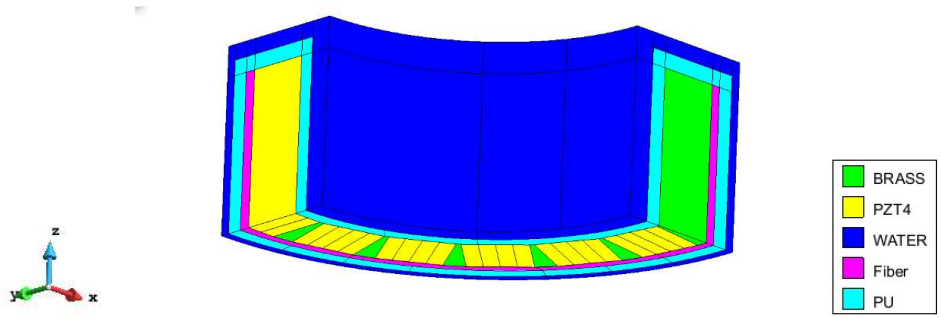
Fig. 4.64   Model for the study of hydrostatic pressure effect.
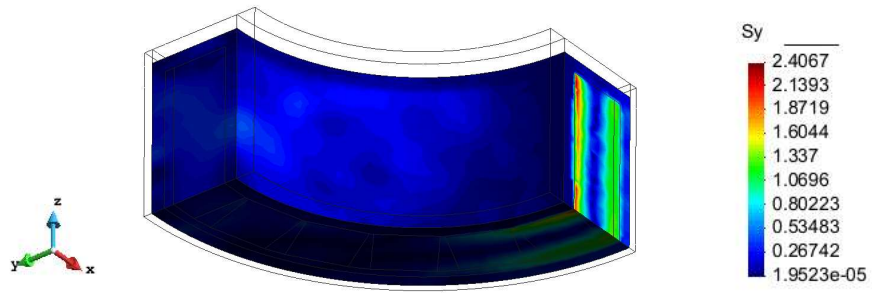
Fig. 4.65   Stress due to 1 Pa hydrostatic pressure.
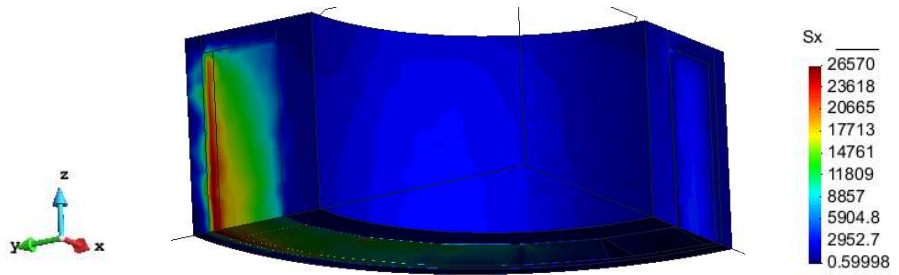
Fig. 4.66   Dynamic stress due to 1 $V_{pp.}$

Table 4.7   Stress due to 1 Pa pressure and 1 V_{pp} excitation.

	Sx (Pa)	Sy (Pa)	Sz (Pa)	Sxy (Pa)	Syz (Pa)	Szx (Pa)	σ_v (Pa)
1 Pa Pressure	2.07	2.40	0.681	0.293	0.081	0.071	2.127
1 V_{pp}	26570	23290	16923	8633	1648	1693	23998.59

4.5.3   Manufacture of Metal Ceramic Segmented Ring Transducer

The schematic assembly of the PU moulded, and oil filled transducers are shown in Figs. 4.67 and 4.68. The various stages involved in the transducer assembly are ceramic stacking, cylinder assembly, pre-stressing with fibre winding and encapsulation. The ceramics selected for the stack assembly were inspected to select ceramic slabs with high d_{33} (piezoelectric strain constant) values and nearly identical dimensions from the production lot. The wedges were machined to very tight tolerance to avoid major variations on the outer diameter of the transducers.
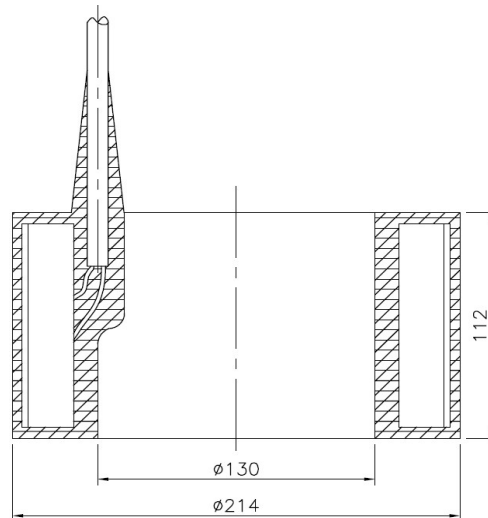
Fig. 4.67   Schematic diagram of PU moulded transducer.
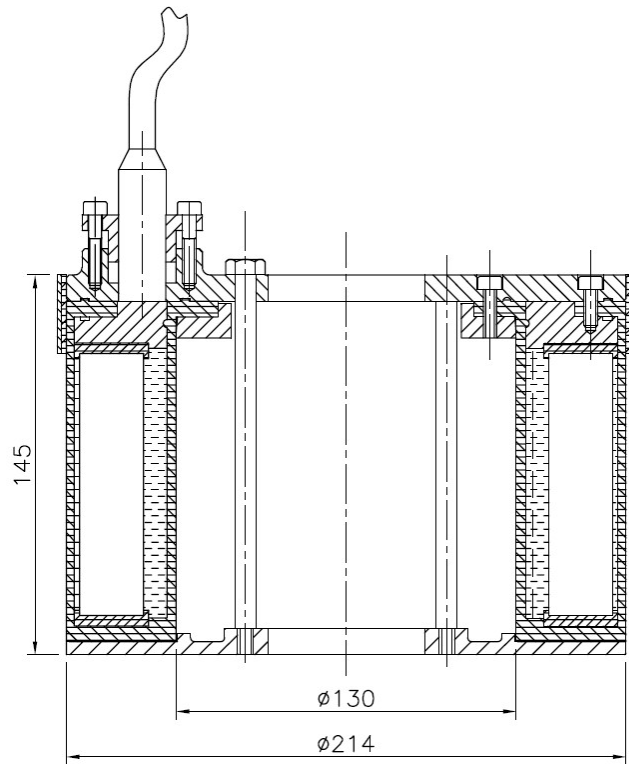
Fig. 4.68   Schematic diagram of the oil filled transducer.

A two-part adhesive with resin and hardener was used to glue the metal wedges and ceramic slabs. The ceramic stacking was carried out using a special jig in a hydraulic press as shown Figs. 4.69 (a) and (b). The stack was kept under pressure for 24 hours for fully curing the adhesive. Ceramic stacks with wedges were assembled in another specially designed assembly fixture to make the cylinder using adhesive as shown in Figs. 4.69 (c) and (d). Once the cylinder was made, it was subjected to pre-stress by fibre winding in a winding machine as shown Fig. 4.69 (e). The winding machine has provision to adjust the speed of rotation, and tension in the fibre. Glass fibre yarn with epoxy-based resin was used for pre-stressing the metal ceramic segment cylinder. Using the method discussed in the previous section 4.4.2, fibre tension and number of layers for these transducers were estimated as shown in Table 4.8. A fibre winding thickness of 5 mm with 8 layers is selected. An epoxy resin is continuously and

uniformly coated on the fibre to form a strong composite layer over the transducer. After the required layers are wound, the fibre is terminated onto the fibre winding fixture. The transducer is left on the winding machine and is operated at a predetermined speed. The centrifugal force thus generated prevents the epoxy resin from accumulating and is used to achieve a uniform composite layer over the transducer. After 24 hours, the transducer is removed from the fibre winding machine and stored in a dehumidified chamber for age curing. Polyurethane moulding was carried out in a special mould tool using a commercially available PU resin, Ezecast, a two-part rigid moulding compound. The mould tool and the PU moulded transducer are shown in Figs. 4.69 (f) and (g).

Table 4.8   Fibre tension for different fibre layer thicknesses

Fibre lining thickness (mm)	Number of fibre yarn layers in the lining	Fibre yarn tension in pre-stressed condition (kg_f)	Minimum required strength of the fibre yarn with factor of safety (kg_f)
2	3	20.9	62.7
3	5	12.7	38.1
4	6	10.6	31.8
5	8	8	24

Oil filled metal ceramic segmented ring transducer is similar in construction and assembly as the all-ceramic segmented ring transducer. The transducer is filled with silicone oil. Various components of the transducer and the fully assembled transducer are shown in Fig. 4.70.

(a)
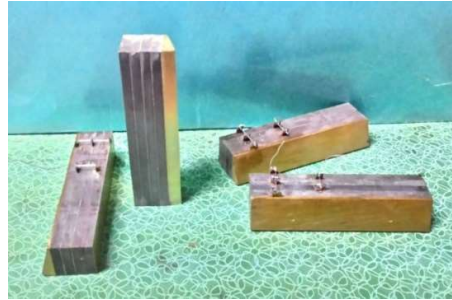
(b)
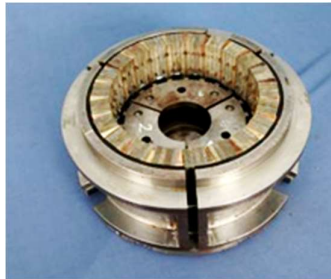
(c)

(d)
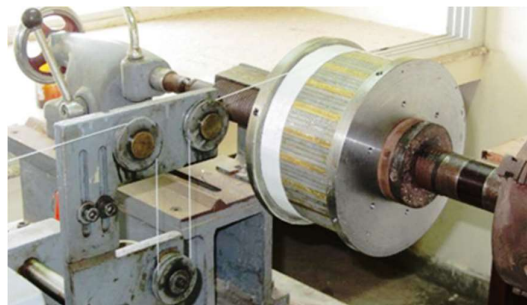
(e)

(f)

(g)

Fig. 4.69   Various stages of transducer manufacture. (a) Ceramics stacking, (b) Stacks with metallic wedges, (c) Cylinder assembly, (d) Assembled cylinder, (e) Fibre winding, (f) PU moulding tool, (g) PU moulded transducer.

Fig. 4.70   Parts and fully assembled oil filled metal ceramic transducer.

4.5.4   Experiments Conducted

The transducers manufactured were initially tested in an open tank at a depth of 10 m and parameters like resonance frequency, transmitting voltage response, receiving sensitivity, conductance, power, source level and directivity were measured. The measurements of TVR and conductance were then repeated in the pressurised test chamber from 1 to 7 MPa pressure. Pressure withstanding capability of all the transducers was tested at 10 MPa, and one of the transducers was also tested in a high pressure, hyperbaric test facility at 60 MPa.

4.5.5   Results and Discussions

Modelled and measured Transmitting Voltage Responses of the transducers in the open tank are shown in Fig. 4.71. TVR values indicate that both the transducer have a usable bandwidth of about two octaves where it has a TVR of about 130 dB or more. The measured results show that the PU moulded transducer has about 3dB higher TVR in the band of 2-8 kHz. Losses are not included in the model hence the values of TVR at resonances are more for the model than the measured values. Non-availability of actual material properties is also a reason for the variation.

130
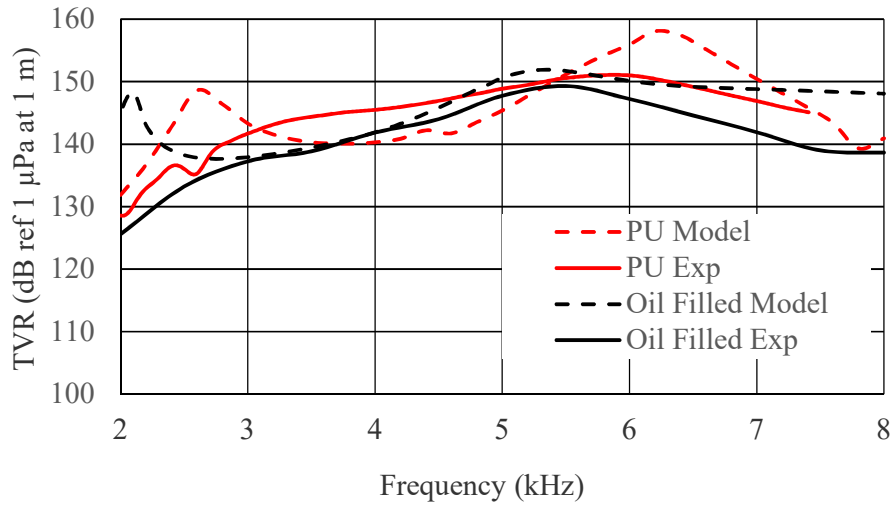
Fig. 4.71   Effect of encapsulation on TVR.

Effect of wedge materials on TVR is shown in Fig. 4.72, and it indicates that at the first resonance due to the cavity mode TVR values are identical because of same physical dimensions. However, beyond the first resonance, transducer with brass wedges has about 2 dB higher TVR due to its higher effective coupling coefficient because of its less elastic compliance.
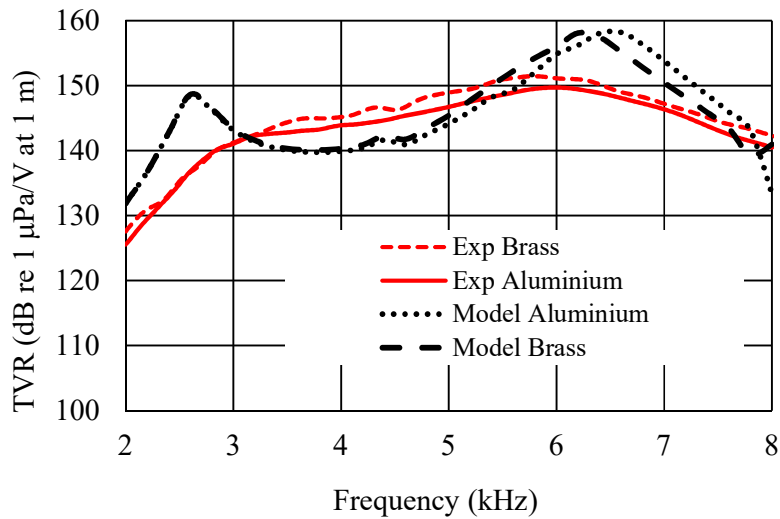
Fig. 4.72   Effect of wedge material on TVR of transducer.

Effect of PZT4 and PZT8 materials on the TVR is shown in Fig. 4.73. Both these transducers have aluminium wedges. PZT4 has higher d_{33} value compared to PZT8, and it is reflected in the TVR plots. However, PZT8 has higher voltage handling capability and can be subjected to higher electric power. The measured receiving sensitivity of the PU moulded and oil filled transducers are shown in Fig. 4.74 and the sensitivities are more than -190 dB over the band of 2 to 8 kHz. The horizontal and vertical directivities of both the transducers at 4 and 6 kHz frequencies are shown in Figs. 4.75 and 4.76. The horizontal directivities of the transducers are Omni within 3 dB for the frequencies. Vertical directivity is toroidal for the PU moulded transducer, but for the oil filled transducer, it is less directive compared to PU moulded transducer. Power and source level measured for the transducers are shown in Table 4.9. The source levels of both the transducers are more than 200 dB at 5 kHz.
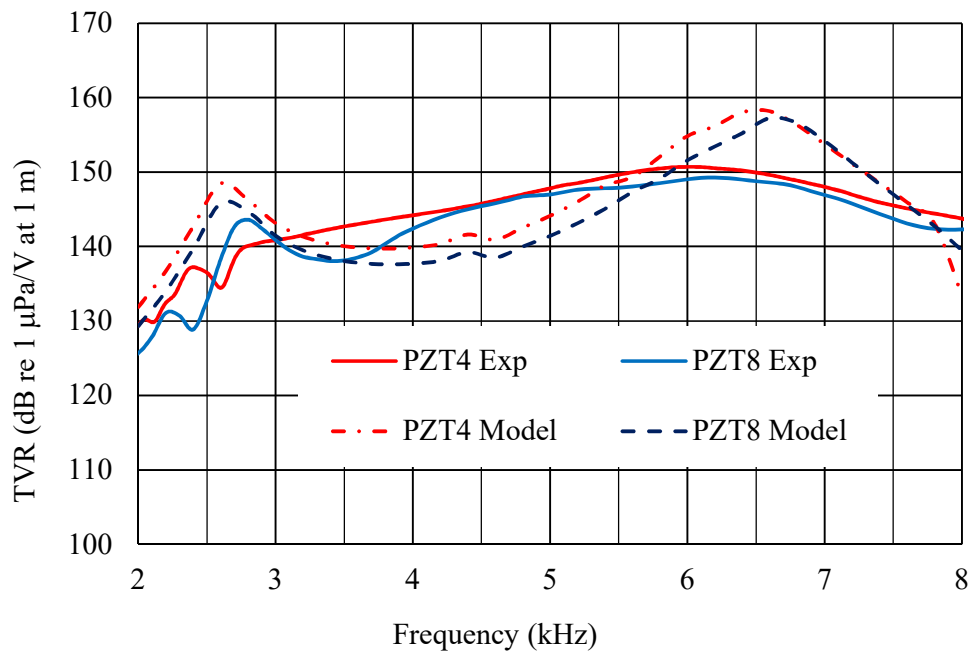
Fig. 4.73   Effect of PZT material on TVR of the transducer.

132
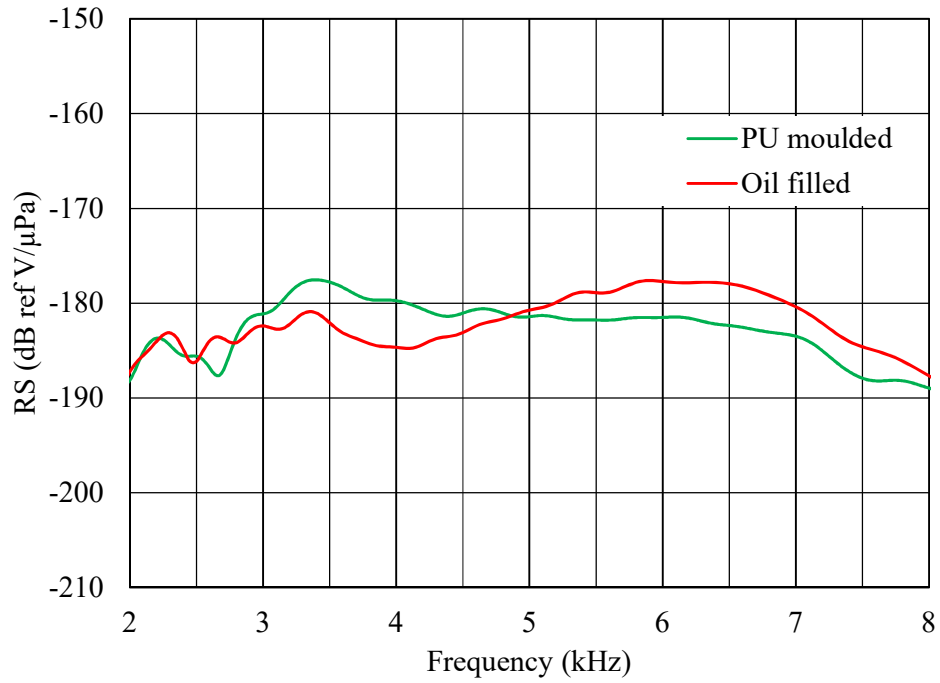
Fig. 4.74   Measured RS of the PU moulded and oil filled transducer.
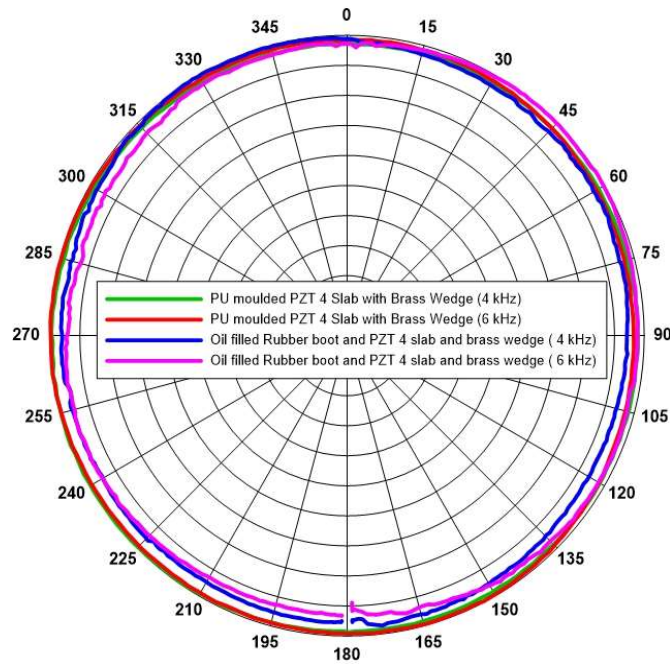
Fig. 4.75   Measured horizontal directivities of PU moulded and oil filled transducers.

133
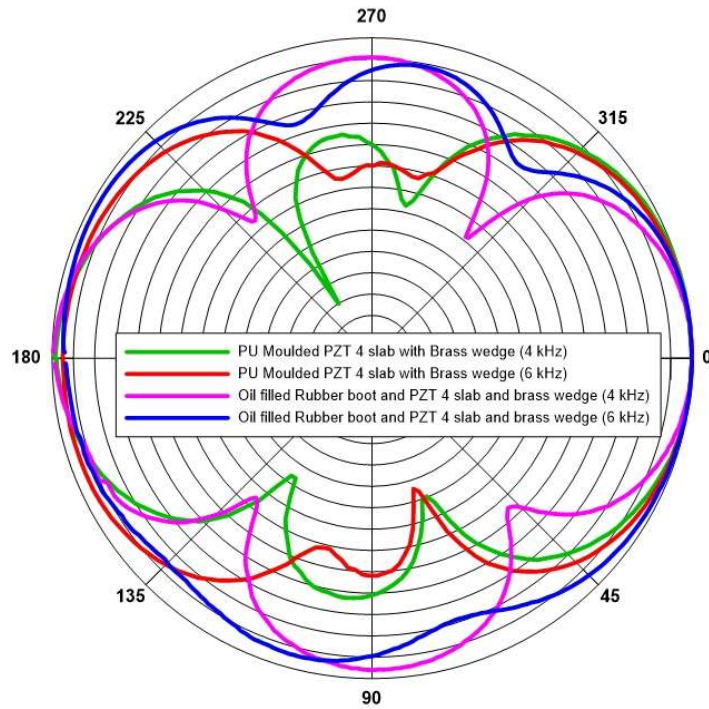
Fig. 4.76   Measured vertical directivities of PU moulded and oil filled transducers.

Table 4.9   Power and source level of the metal ceramic transducers.

	Untuned	Tuned	Untuned	Tuned
Parameters	PU Moulded	PU Moulded	Oil filled	Oil filled
Frequency (kHz)	5	5	5	5
Voltage (V_{rms})	208.48	512.7	229.52	442.37
Current (I_{rms})	3.16	2.9	4.01	3.94
Phase (deg)	-62.3	7	-64.52	0.36
Impedance (Ω)	66.0	180	57.22	112.28
Power (W)	303.6	1460	396	1742.91
SL (dB re 1 µPa at 1 m)	196.3	200.8	195.0	200.3

After the open tank experiments, transducers were tested in a pressurised vessel for their acoustic performance from 1 to 7 MPa in steps of 1 MPa. Measured conductance and TVR of transducers under different pressures are shown in Figs. 4.77 to 4.80. The frequency vs conductance plot for the PU moulded transducer indicates that there is no appreciable change in resonance frequency with change in pressure. However, for the

oil filled transducer the resonance frequency changed from 5.96 kHz to 5.61 kHz as the pressure is increased to 2 MPa but beyond 2 MPa it is stable. The TVR plots show that during the low-frequency region of 2-3 kHz there is about 2-5 dB reduction with an increase in pressure from 1 to 7 MPa for the PU moulded transducer. However, beyond the first resonance, in the frequency band of interest, the variation in TVR is not considerable and stable. For oil filled transducer, the change in TVR over the band is observed to be within ± 1 dB, and it is similar to measurement variations. After the high-pressure acoustic tests transducers were subjected to pressure withstanding test at 10 MPa in NPOL. One PU moulded transducer was tested in a hyperbaric test facility at 60 MPa for two hours along with RPC based transducers as shown in Fig. 4.81 and cleared the pressure test.
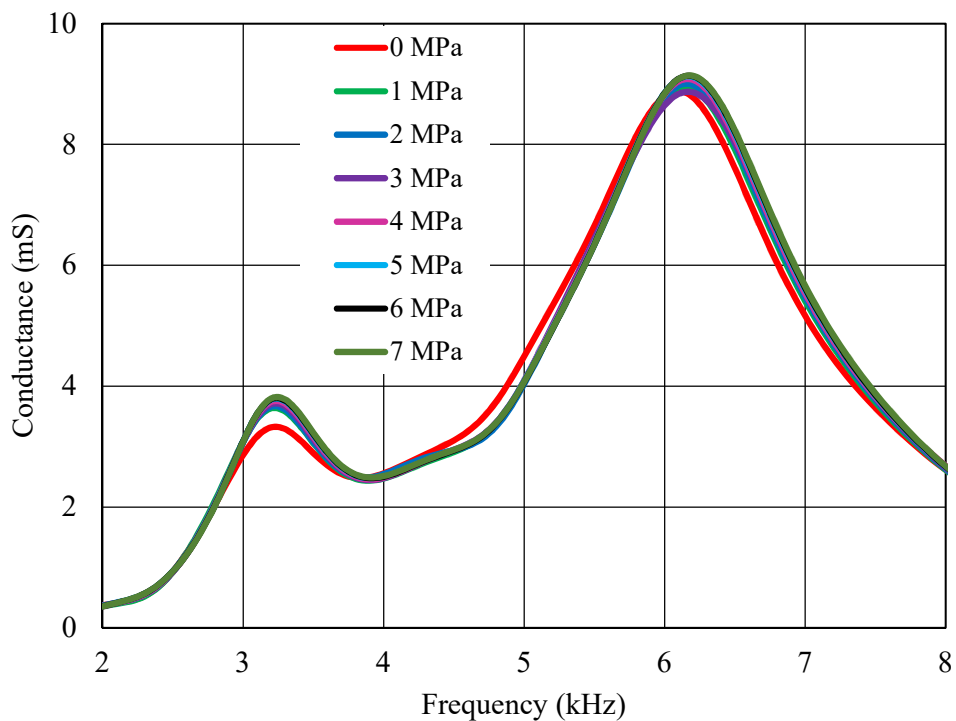
Fig. 4.77   Effect of depth on the resonance frequency of PU moulded transducer.
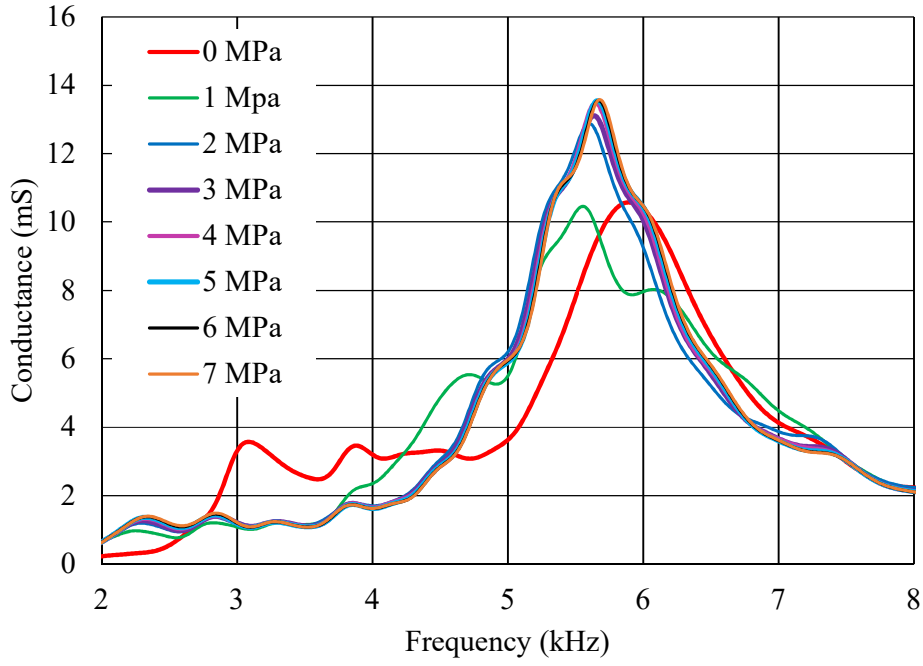
Fig. 4.78   Effect of depth on the resonance frequency of oil filled transducer.
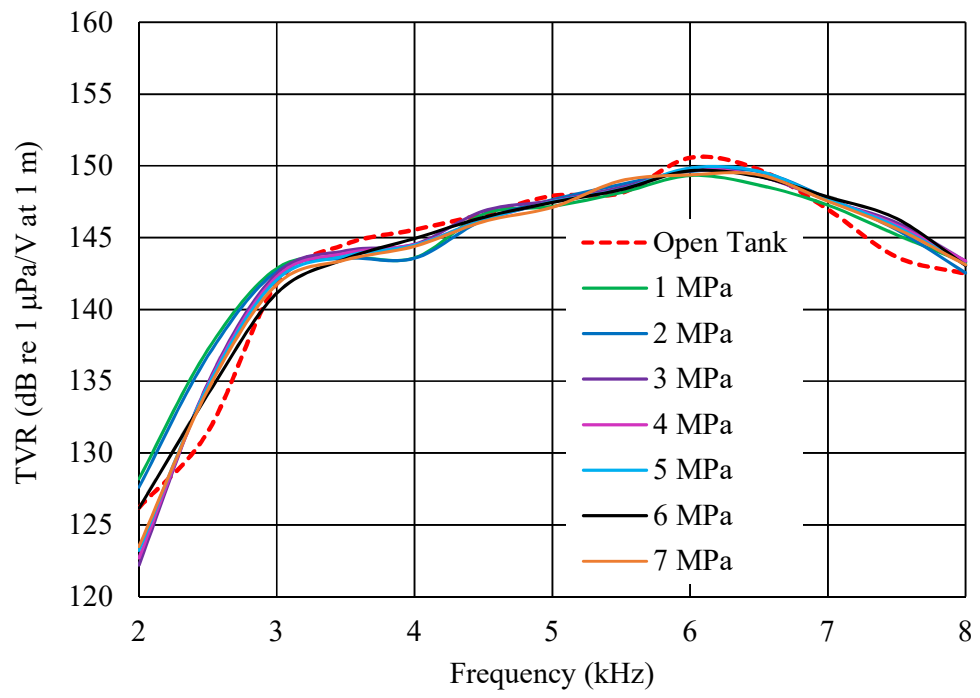
Fig. 4.79   TVR under different pressures for PU moulded transducer.
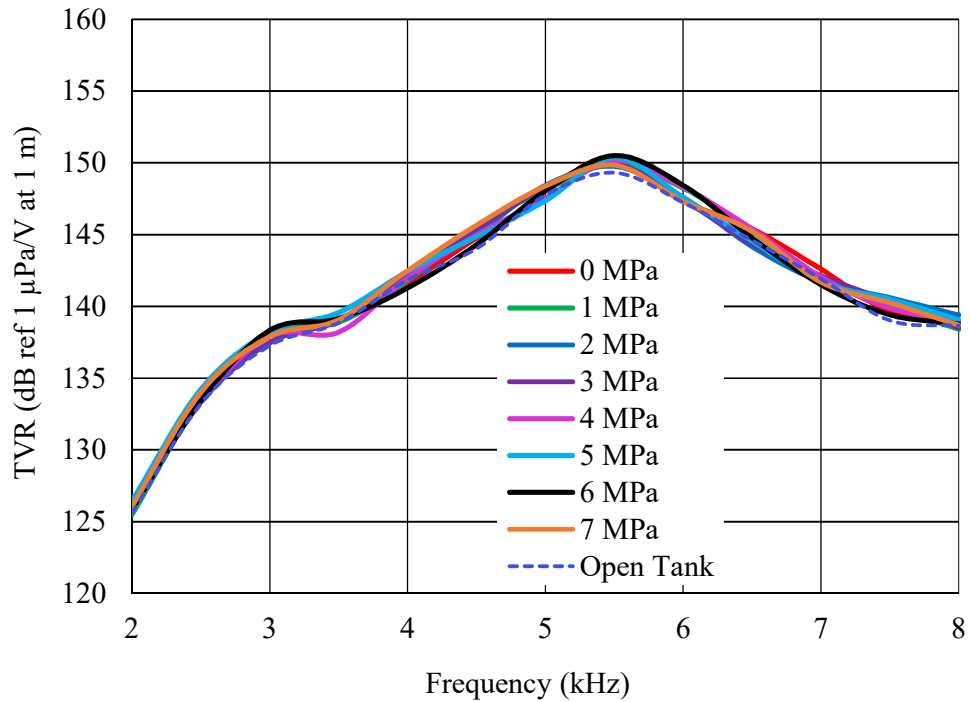
Fig. 4.80   TVR under different pressures for oil filled transducer

Fig. 4.81   Pressure test in the hyperbaric test facility.

4.5.6   Summary

Free-flooded PU moulded, and oil filled transducers with RPC were modelled using ATILA and manufactured. Transducers manufactured were tested in an open acoustic tank and under pressure upto 7 MPa to study the effect of depth on their acoustic

performance. The studies indicate that the resonance frequency of oil filled transducer with rubber boot has lower resonance, compared to PU moulded transducer and at resonance, it has slightly higher TVR. There is a reduction in resonance frequency with pressure for both the transducers. Beyond 2 MPa, resonance frequency remained stable for both types of transducers. Both transducers handled more than 800 W at 5 kHz and source level is more than 190 dB in the untuned condition which can be enhanced by tuning. The measured receiving sensitivity shows that PU moulded transducer has higher sensitivity compared to oil filled transducer. The transducers are also subjected to 60 MPa to test its pressure withstanding capability.

All-ceramic segmented ring transducers moulded with PU, rubber and assembled in an oil filled boot were modelled using ATILA, and the modelled results were compared with open tank experiments. Acoustic performance of the transducers manufactured was measured in an open tank and inside a pressurised vessel upto 7 MPa pressure. Results indicate that the transducers have a stable response in the band of interest and more than 194 dB source level. The receiving sensitivity of transducers is more than -190 dB, but RS of the PU moulded transducer is about 2 to 8 dB higher compared to the oil filled transducer in the band of 3-8 kHz. Transducers were tested at 10 MPa for their pressure withstanding capability.

Segmented ring transducers made with stacks of ceramic slabs and metal wedges were assembled and tested. A specially designed holding fixture was used for the fibre winding of the transducers. Transducer variants were assembled and tested with different, wedge and ceramic materials. Acoustic performance of the transducers manufactured was tested in an open tank and inside a pressurised vessel from 1 to 7

MPa. Results indicate that the transducers have stable response above 2 MPa and a usable bandwidth of about two octaves. The variation in TVR in the band of interest is within ± 1 dB. The brass wedged transducer has about 2 dB higher TVR beyond the first resonance, compared to aluminium wedged transducer. The measured RS of PU moulded and oil filled transducers are more than -190 dB in the band of 3-8 kHz. All the transducers manufactured were tested at 10 MPa for their pressure withstanding capability and one of the transducers was also tested at 60 MPa.

CHAPTER 5

DIRECTIONAL TRANSDUCERS

5.1 INTRODUCTION

Free-flooded ring transducers are Omnidirectional in the horizontal plane, but there are many applications like underwater communication systems and modems that need to operate in the directional mode to focus the acoustic energy in the direction of interest. Making the transducer directional increases the Directivity Index and source level. Steering the beam to the desired direction in a communication system makes it more secure. Free-flooded ring transducers with RPC and metal ceramic segmented ring are made directional by exciting fundamental extensional vibration modes of the cylindrical transducer and combining them. The fundamental extensional vibration modes of the ring are Omni, dipole and quadrupole as shown in Fig. 5.1.

<div align="center">

1st mode

Omni

2nd mode

Dipole

3rd mode

Quadrupole

</div>
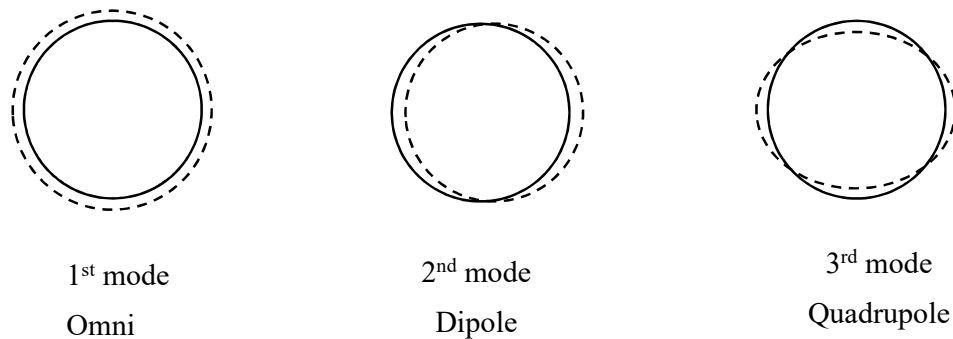
Fig. 5.1   The first three extensional modes of vibration of a cylindrical transducer.

Butler *et al*. (2001, 2003, and 2004) have demonstrated that directional transmission in the cylindrical transducer is possible by simultaneously exciting the Omni, dipole and quadrupole modes. When a cylindrical transducer is excited with the harmonic signal, it undergoes symmetric vibrations along the horizontal plane. The even component of excitation, i.e., $\cos(n\varphi)$ is symmetric about the circumference, where n is the mode

number. The fundamental mode $n = 0$, generates an Omnidirectional response, the second mode $n = 1$ produces a dipole pattern corresponding to $\cos(\varphi)$ with two lobes separated by 180°; and the third mode $n = 2$ generates quadrupole pattern corresponding to $\cos(2\varphi)$ with four lobes separated by 90° apart. The far-field pressure distribution, P, for the transducer is given by Butler *et al.* (2004),

$$P_n(r) = \frac{2}{\pi} \int_0^\pi P(r, \varphi) \cos(n\varphi) \, d\varphi \qquad (5.1)$$

where r is the distance of the field point from the transducer and φ is the azimuthal angle. The required cardioid or super-cardioid directivity function can be generated by considering only the first, two and three terms in the equation 5.1, respectively. Therefore, considering the first three extensional modes, n=0, 1 and 2, the normalised directivity function becomes,

$$\frac{P(\varphi)}{P(0)} = \frac{(1 + A \cos\varphi + B \cos 2)}{(1 + A + B)} \qquad (5.2)$$

The first, second and third terms in the equation 5.2 correspond to Omni, dipole and quadrupole modes, respectively. For A = B = 0, the pattern is Omnidirectional; for A = 1 and B = 0, it is a cardioid; and for A = 1 and B $\neq$ 0, it is a super-cardioid. The normalised pressure distribution functions of these three combinations are shown schematically in Fig. 5.2. The value of the weighting factor B varies from 0 to 1, accordingly the level of the rear lobe on the super-cardioid increases and the width of the main beam decreases. The normalised pressure distribution function of the transducer can be simulated using equation 5.2 for different values of B.

n =0
A = B = 0
Omnidirectional

n =1
cos(φ)
Dipole

A =1, B = 0
Cardioid

n = 0
Omni

n =1
cos(φ)
Dipole

n = 2
cos(2φ)
Quadrupole

A = 1, B ≠ 0
Super-cardioid
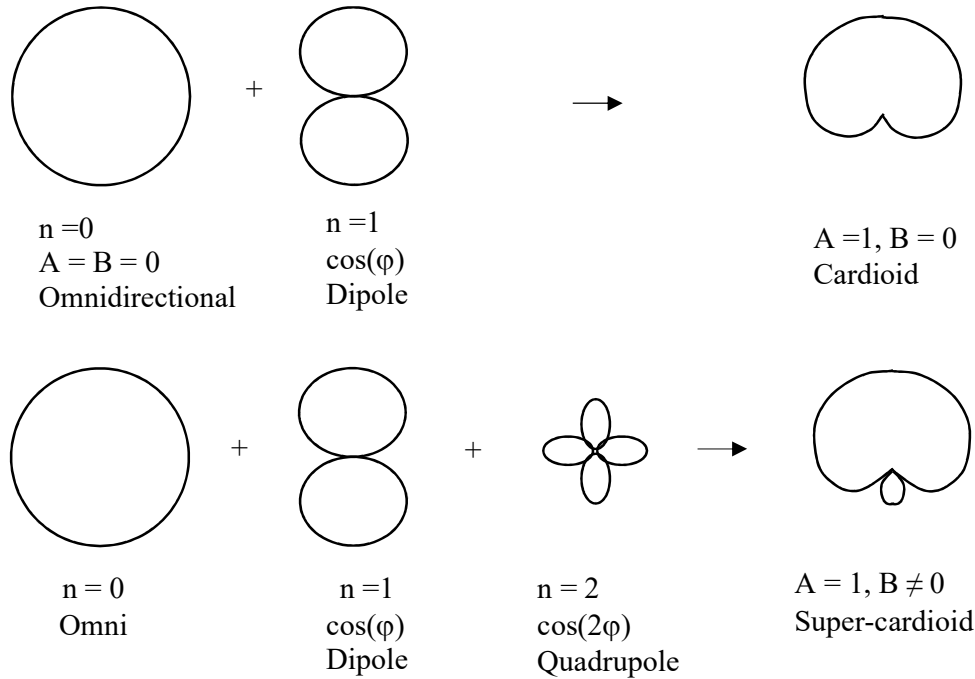
Fig. 5.2   Extensional modes of vibration and their combination to generate cardioid
and super-cardioid directivity patterns.

5.2   DIRECTIONAL RPC TRANSDUCER

In practice, a PZT cylinder can be made to vibrate in different modes by dividing the

electrode into multiple sectors and driving with appropriate voltage functions on each

sector. The cylindrical transducer can be made out of radially polarised piezoceramic

cylinder (RPC) or a segmented cylinder. However, it is convenient to use an RPC. Fig.

5.3 shows an RPC in which the electrode on the curved inner surface is divided into

eight equal sectors and the common electrode on the outer curved surface. The

electrodes are paired according to the details given in Table 5.1. The voltage applied to

each electrode pair determines the excitation mode and the corresponding directivity

pattern. For example, if all the electrode pairs are driven with equal voltage, i.e., V_1 =

$V_2 = V_3 = V_4 = 1$ V, then all the sectors are driven in phase, and the directivity pattern

is Omnidirectional. For the voltage distribution, $V_1 = V_2 = 1$ V and $V_3 = V_4 = -1$ V, the

upper and lower halves of the cylinder are driven 180° out of phase, and the resulting

142

directivity pattern is a dipole. For the voltage distribution, $V_1 = V_4 = 1$ V and $V_2 = V_3$ = -1 V, each adjacent quadrant of the cylinder is driven 90° out of phase, and the resulting directivity pattern is a quadrupole. The voltage distribution applied to four pairs of electrode segments for exciting the cylinder to different modes of vibration are given in Table. 5.2.
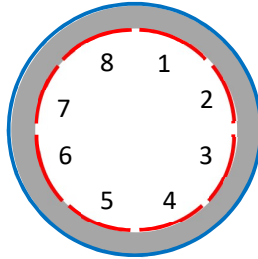
Fig. 5.3   Arrangement of electrodes of a cylindrical transducer.

Table 5.1   Inter-connection of electrode pairs and the voltage applied to them.

Electrode pairs	Voltage
1 & 8	V1
2 & 7	V2
3 & 6	V3
4 & 5	V4

Table 5.2   Voltage distribution for exciting different modes of vibration.

Mode	V1	V2	V3	V4
Omni	1	1	1	1
Dipole	1	1	-1	-1
Quadrupole	1	-1	-1	1

The required directional response can be generated using the cylindrical transducer by the appropriate superpositioning of far-field pressure corresponding to the three modes of vibration using the procedure given by Butler *et al.* (2001, 2003, 2004). In the first step, the transducer is driven in Omni mode by applying a voltage V_0 equally to all the

segments as given in Table 5.2 and the complex Transmitting Voltage Response, TVR_0 is measured at a fixed point in the far field. Therefore, $V_0 = P_0/TVR_0$ where P_0 is pressure corresponding to the Omni mode. In the second and third steps, the transducer is driven in dipole and quadrupole modes, respectively, according to the voltage distribution given in Table 5.2 and the corresponding complex TVR values are measured along the respective maximum response axis. Therefore, $V_d = P_d/TVR_d$ and $V_q = P_q/TVR_q$ where the subscripts 'd' and 'q' refer to the dipole and quadrupole modes, respectively. The pressure values are normalised in each mode of excitation as given in equation 5.2 with respect to P_0 and the corresponding weighting factors, A and B are used for determining the voltage distribution required to superimpose the Omni, dipole and quadrupole modes of vibrations. Therefore,

$$V_o = \frac{1}{TVR_o} \qquad V_d = \frac{A}{TVR_d} \qquad \text{and} \qquad V_q = \frac{B}{TVR_q} \qquad\qquad (5.3)$$

The parameters P, V and TVR, are all complex quantities. Using these three values of voltages, namely; V_0, V_d and V_q, the complex voltages to be applied to the four segments, namely, V_1, V_2, V_3 and V_4 are calculated using the information given in Table 5.2 and the relations,

$$V_1 = V_o + V_d + V_q \qquad\qquad (5.4a)$$

$$V_2 = V_o + V_d - V_q \qquad\qquad (5.4b)$$

$$V_3 = V_o - V_d - V_q \qquad\qquad (5.4c)$$

$$V_4 = V_o - V_d + V_q \qquad\qquad (5.4d)$$

By applying these voltage functions to the four pairs of electrode segments of a cylindrical transducer, the directional response can be generated in the far field.

5.2.1 Transducer Manufacture

It is easier to use RPCs for directional transmission because of the easiness in manufacture. However, manufacturing limitations in making higher diameter rings restrict its use for low frequencies. As in the Omnidirectional transducer, RPC of 150 mm OD, 140 mm ID and 50 mm height is used for the directional transducer also. The inner electrode is divided into eight equal sectors by removing the electrode in the lengthwise direction as shown in Fig 5.4. Individual sectors inside the RPC and the common outer electrode are connected using multi-core cable. Encapsulation of the transducer is carried out using polyurethane in a metallic mould as shown Fig 5.5. The moulded transducer is shown in Fig 5.6.
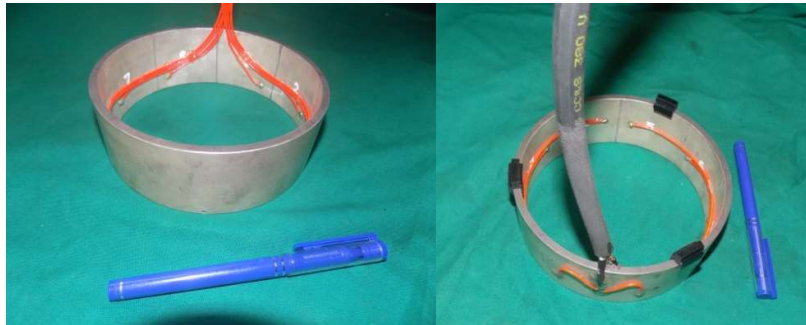
Fig. 5.4   RPC with eight inner electrodes and common outer electrode.

Fig. 5.5   RPC transducer moulding.

Fig. 5.6   PU moulded directional RPC transducer.

5.2.2   Experiments and Results

A multichannel power amplifier is used to excite different sectors of the transducer with the calculated voltages as per equation 5.4 (a), (b), (c) and (d) discussed in the previous section and details given in Table 5.1 and 5.2. Measured directivities for Omni, cardioid and super-cardioid modes are shown in Figs. 5.7 and 5.8 at 5 kHz. The front to back ratio for cardioid and super-cardioid modes are more than 15 dB, and for the super-cardioid case, the beam is more directional.

(a)   (b)
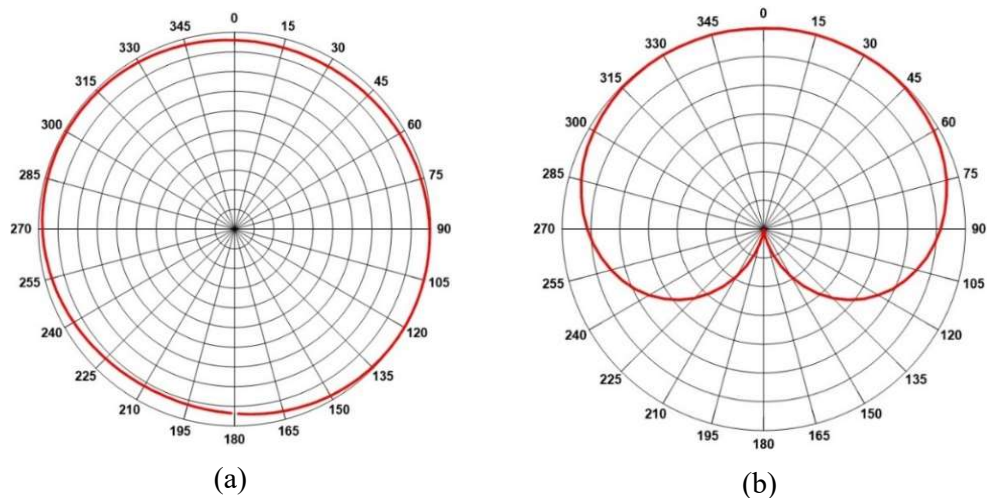
Fig. 5.7   Measured horizontal directivity (a) Omni mode (b) Cardioid mode at 5 kHz.
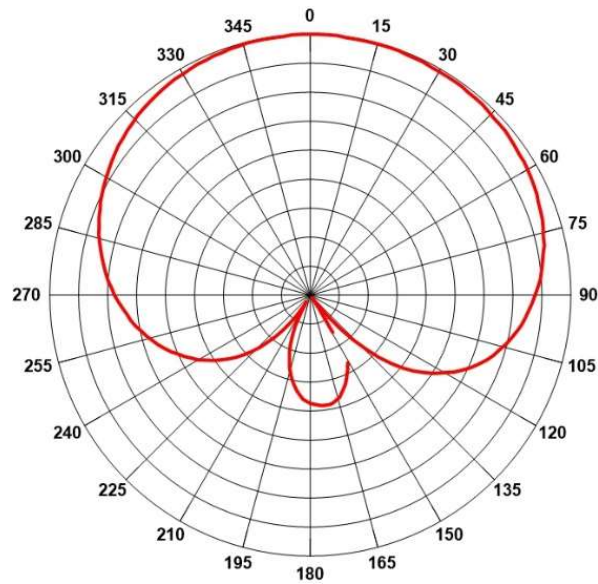
Fig. 5.8   Measured horizontal directivity in super-cardioid mode at 5 kHz.

Measured TVR of the transducer in different modes are shown in Fig. 5.9. Compared to Omni mode the super-cardioid mode has 7.5 dB higher TVR at 5 kHz. The power and source level measured are shown in Table 5.3. The directional source level obtained is 191.2 dB at 5 kHz.
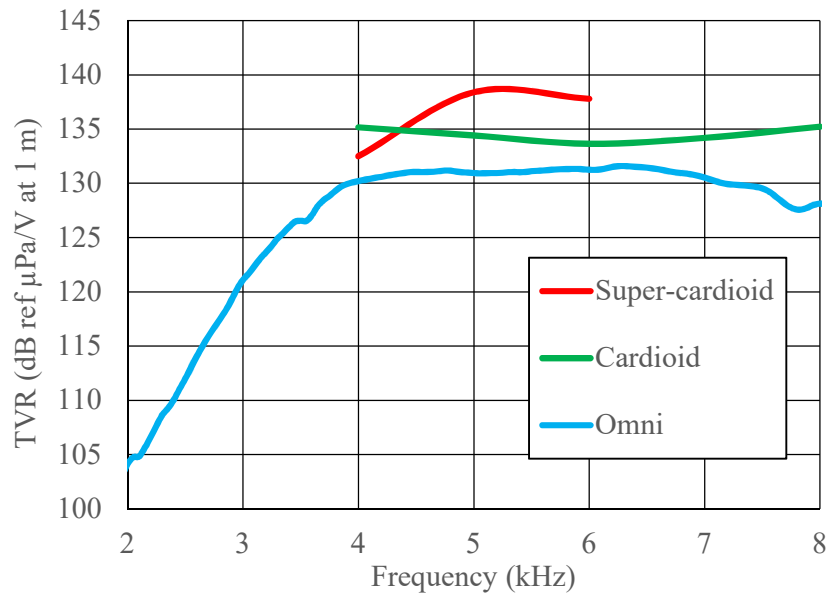
Fig. 5.9   Measured TVR of Omni and cardioid modes of RPC transducer.

Table 5.3   Power and source level of directional RPC transducer.

Parameters	Directional RPC transducer		
Frequency (kHz)	4	5	6
Power (W)	423	535	642
Hydrophone output (mV$_{rms}$)	43.95	79.37	82.01
SL (dB re μPa at 1 m) Super-cardioid mode	185.2	191.2	190.8
TVR (dB re μPa/V) Super-cardioid mode	132.5	138.4	137.8
TVR (dB re μPa/V) Cardioid	135.2	134.4	133.7
TVR (dB re μPa/V) in Omni	133.2	130.9	131.25

5.3   DIRECTIONAL SEGMENTED RING TRANSDUCER

When low frequency, directional transducers are required, metal ceramic segmented ring transducer is an ideal choice because metal wedges and ceramic stacks made out of regular PZT slabs can be used to make large diameter transducers. Metal ceramic transducer is also capable of delivering much higher power and source level compared to RPC based transducers. Similar to the Omnidirectional transducer, metal ceramic segmented ring of 214 mm diameter is used for directional transducer also. Only PU moulded transducer is developed for the directional case.

5.3.1   Transducer Manufacture

Considering similar approach as in the case of RPC based directional transducer, metal ceramic segmented ring transducer is also made directional. The segmented ring is made out of 88 slabs and 22 wedges. The ring is divided into eight equal sectors with 11 ceramic slabs in each sector. Thin FRP sheets are used in between each sector to isolate the sectors electrically. Negative terminals of all sectors are connected to a common terminal, and positive terminals are connected to separate electrical leads of a multi-core cable as shown in Fig. 5.10. The assembly is encapsulated in polyurethane

using a special mould. The mould tool and PU moulded directional segmented ring transducer are shown in Fig. 5.11.
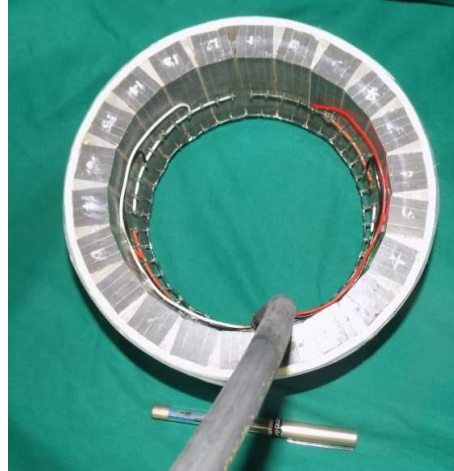
Fig. 5.10   Sector wise wiring details of segmented ring transducer.

Fig. 5.11   Mould tool and PU moulded directional segmented ring transducer.

5.3.2   Results and Discussions

Different sectors of the transducer are excited using a multichannel power amplifier as per the details are given in Table 5.1 and 5.2   with the calculated voltages as per

equation 5.4 (a), (b), (c) and (d). Voltages are calculated for different frequencies and applied to the transducer to get the directional response. Measured directivities at 4 kHz for Omni, cardioid and super-cardioid modes are shown in Figs. 5.12 and 5.13. In Omni mode, the beam pattern is Omni within 1 dB. Super-cardioid mode is more directional than cardioid mode but has less front to back ratio. The front to back ratio for cardioid and super-cardioid modes are more than 15 dB. The measured TVR of the transducer in Omni, cardioid and super-cardioid modes are shown in Fig. 5.14 and the measured power and source level are shown in Table 5.4. The source level measured at 4 kHz for the super-cardioid mode is 197 dB re 1 µPa at 1 m. TVR measured at 4 kHz for super-cardioid modes is 1.2 dB more than the Omni mode. The measurements were carried out at 10 m depth, and the transducer is capable of handling much more power in deeper waters.
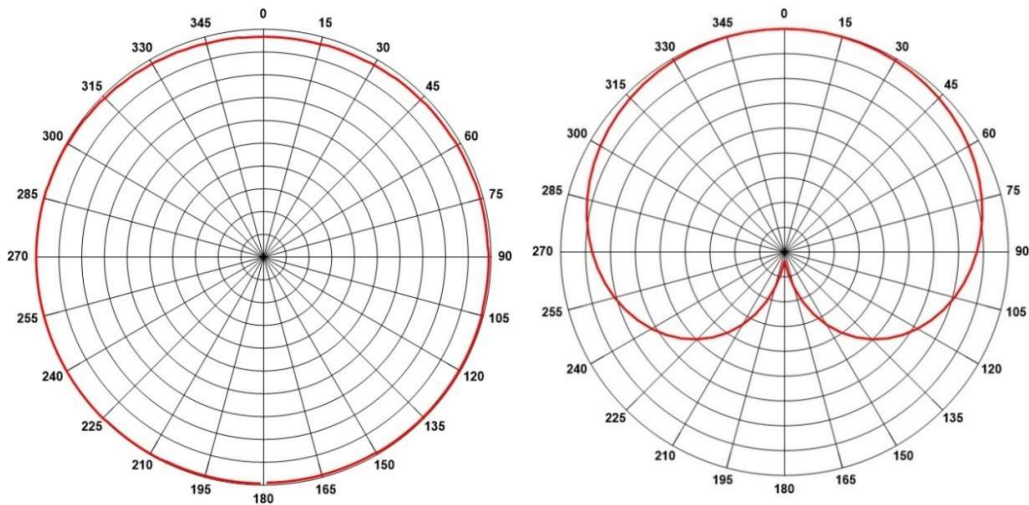
Fig. 5.12   Measured Omni and cardioid directivity at 4 kHz.
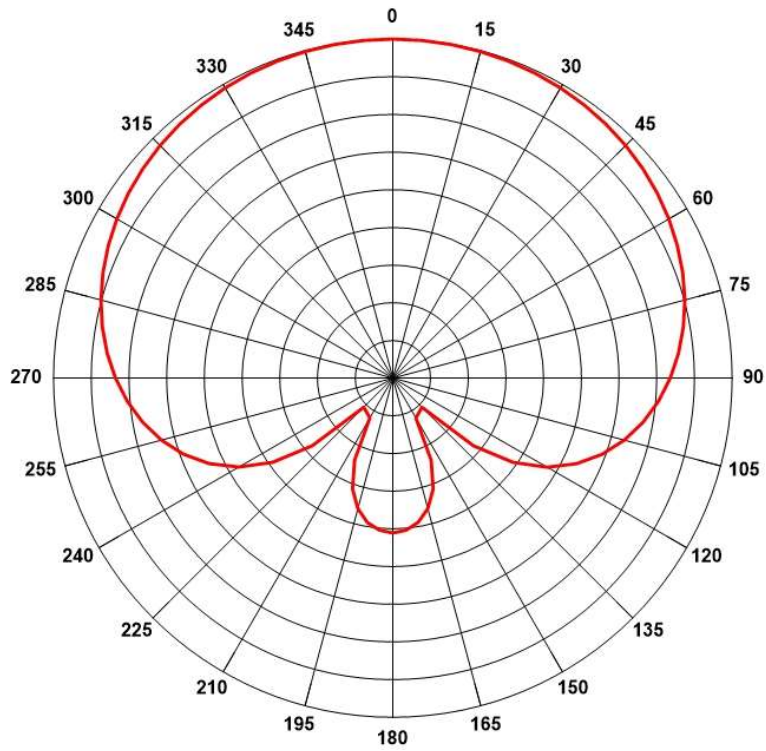
Fig. 5.13   Measured horizontal directivity in super-cardioid mode at 4 kHz.
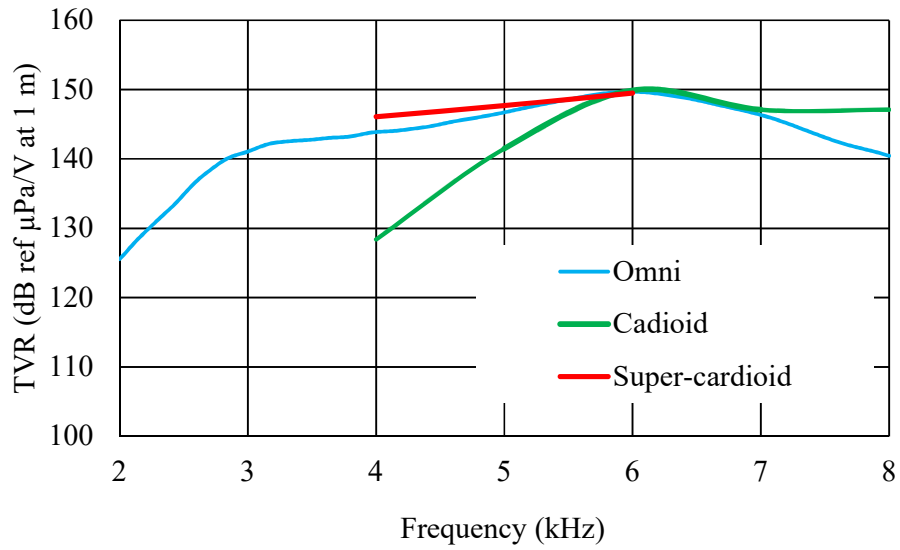
Fig. 5.14   Measured TVR of Omni and cardioid modes.

151

Table 5.4   Power and source level of directional segmented ring transducer.

Parameters	Metal Ceramic Segmented Ring Transducer		
Frequency (kHz)	4	5	6
Power (W)	788.5	854	635
Hydrophone output (mV$_{rms}$)	281.6	273.7	300
SL (dB re µPa at 1 m) Super-Cardioid mode	197	196.9	198.3
TVR (dB re µPa/V) Super-Cardioid mode	146.1	147.7	149.5
TVR (dB re µPa/V) Cardioid	128.4	141.5	149.9
TVR (dB re µPa/V) in Omni	144.9	147	149.7

5.3.3   Summary of Directional Transducer Development

Directional transducers with RPC and metal ceramic segmented ring are realised by exciting multiple modes with different voltages and phases. Cardioid and super-cardioid modes are generated using both transducers. Excellent front to back ratio of more than 15 dB is achieved for both transducers, but the beam width is higher for cardioid mode than the super-cardioid mode. In super-cardioid, the beam width is narrower but front to back ratio is less. Based on the actual requirement the modes can be decided. Power and source level in directional mode is measured in an open tank and presented. Depth capability is also tested upto 1000 m of water.

CHAPTER 6

CONCLUSIONS

This chapter brings out the highlights of the work undertaken to realise the research objective of design and development of deep submergence transducers. Literature review, parametric studies, manufacture, acoustic test in an open tank, and under pressure in a pressure chamber and pressure withstanding tests were carried out for three types of Omni and two types of directional free-flooded ring transducers. This chapter also brings out the scope for future research in this area.

6.1 HIGHLIGHTS OF THE THESIS

Based on the detailed literature review, free-flooded ring transducer was identified as the deep submergence transducer for development. Three types of Omnidirectional transducers based on RPC, ceramic wedges and metal wedges and stacks of ceramic slabs were modelled using a commercially available finite element software, ATILA. Effect of various parameters like outer diameter, height, ceramic and wedge material, ceramic wall thickness, type of encapsulation and fill fluids on transmitting voltage response of these transducers were studied. Directional transducers based on RPC and metal ceramic were also developed. Transducer variants were manufactured and tested in an open tank at 10 m depth and in a pressurised vessel upto 7 MPa pressure. All the transducers developed have source level of more than 190 dB re 1 µPa at 1 m. The pressure withstanding capability of all transducers was tested at 10 MPa, and three transducers were also tested at 60 MPa. Successful testing of the transducers indicates that they can be deployed in more than 98% area of ocean where the depth of water is less than 6000 m. This chapter also brings out the scope and direction for future research

in this area. The details of transducers manufactured for the study are shown in Table 6.1, and their photographs are shown in Fig. 6.1.

Table 6.1   Free-flooded ring transducer variants developed.

| Sl. No. | Type of Transducer | | | Omni / Directional |
	RPC transducer	Segmented ring transducer with metal wedges and stacks of ceramic slabs.	Segmented ring transducer with ceramic wedges.	
1	PU moulded PZT4 ring.	PU moulded PZT4 slabs with brass wedges.	PU moulded PZT4 wedges.	Omni
2	Oil filled rubber boot with PZT4 ring.	Oil filled rubber boot with PZT4 slab and brass wedge.	Oil filled rubber boot and PZT4 wedges.	Omni
3	--	PU moulded PZT8 slabs with Aluminium wedges.	--	Omni
4	--	PU moulded PZT4 slab with Aluminium wedge.	--	Omni
5	PU moulded directional transducer with PZT4 ring.	PU moulded transducer with PZT4 slabs and Aluminium wedges.	--	Directional
Number of transducers made.	3	5	2	

Fig. 6.1   Free-flooded ring transducer variants developed.

Following are the salient highlights of the design and development of Omni and directional, deep submergence, free-flooded ring transducers.

The studies revealed that the free-flooded ring transducer made with RPC, housed in a fluid-filled rubber boot has a higher response at resonance compared to direct PU moulded transducer. RPC based transducers studied can be effectively used for frequencies above 3.5 kHz with an operating band upto 9 kHz. Simple PU moulding is sufficient if source level requirements are not very stringent at resonance. Except around resonance, PU moulded RPC transducer has higher response compared to the oil filled transducer. PU moulded RPC based transducer has flatter band compared to oil filled RPC transducer. The transducer has stable response under pressure over the frequency band above 2 MPa pressure.

The brass wedged, metal ceramic segmented ring transducer has about 2 dB higher TVR beyond the first resonance, compared to aluminium wedged transducer of the same dimensions. The results show that there is no significant influence of pressure in the frequency band of interest on TVR of the transducers studied indicating stable operation under pressure. In all three cases of transducers studied, the type of fill fluid does not influence TVR. All-ceramic, segmented ring transducer is not cost effective compared to metal wedge transducer with stacks of ceramic slabs since for each diameter specific ceramic wedges are to be manufactured.

Directional capability for RPC and metal ceramic segmented ring transducers are demonstrated by varying the input voltage to different sectors and exciting, different modes. More than 15 dB front to back ratio is achieved for cardioid and super-cardioid

beam patterns. The same transducer can operate in Omni and directional mode based on operational requirement using this technique.

The depth capability of three transducers was demonstrated by testing upto 60 MPa. Increasing the depth further was limited due to the connector and cable used. Direct rubber over-moulding is not recommended for a transducer with fibre winding due to the high process temperature. The transducers developed are simple in construction and without any depth compensation devices. The seals used are simple cable glands that withstood 60 MPa, making it very cost effective.

6.2   FUTURE SCOPE FOR RESEARCH

The work presented in this thesis has a significant role to play given its practical applications. This work also has a significant prospect for further research for improving the overall performance. Some of the possible proposals for future work in this area are listed below.

The resonance frequency of transducer can be changed to the desired frequency by increasing or decreasing the diameter, height or a combination of them. Advanced ceramic technology like single crystal PMN-PT can be tried to improve the source level. Ageing studies can be carried out to estimate the life of the transducers. Transducers can be tested at higher depths with suitable cables and connectors, capable of withstanding higher depths. Multiple numbers of transducers can be stacked to form an array to increase the source level and making it more directional in the vertical plane.

6.3   SUMMARY

In this chapter, the significant highlights of the work done and the general conclusions arrived at along with the scope and direction for future research in this area are presented. Omni and directional free-flooded ring transducer variants operating below 10 kHz were modelled, manufactured, and tested for the acoustic performance in an open tank at 10 m depth and in a pressure vessel up to 7 MPa. Omni and directional transducers are developed with source level of more than 190 dB re 1 µPa at 1 m. Transducers developed were successfully tested for pressure withstanding capability upto 10 MPa, and few transducer variants were tested upto 60 MPa.

REFERENCES

1. **Adam, J. A.** (1985) Probing beneath the sea, *IEEE Spectrum*, 22(4), 55-64.

2. **Ahmad, J., D. T. I. Francis** and **R. F. W. Coates** (1995) A fluid-filled flextensional device for ocean acoustic tomography, *Proceedings of OCEANS '95,* 3, 2021-2026.

3. **Ahmad, J., D. T .I. Francis** and **R. F. W. Coates** (1996) Modelling, development and calibration of a wideband depth capable flextensional transducer, *European conference on underwater acoustics*, Heraklion, Crete, Greece, 1097-1102.

4. **Anifrani, K**. (1990) A new design of a class V flextensional transducers using ATILA code, *Proc. Institute of Acoustics,* 12(4), 21-30.

5. **Armstrong, B. A.** and **G. W. McMahon** (1984) Discussion of the finite element modelling and performance of ring shell projectors, *IEEE Proceedings*, 131(F), 275- 279.

6. **Arnold, D. B.** and **G. Bromfield** (1996) Flextensional transducers, US Patent No.5345428.

7. **Aronov, B., T. Oishi, L. Reinhart,** and **D. Brown** (2001) Broadband, multimode, free-flooded, baffled circular ring projectors, *Journal of Acoustical Society of America*, 109(5), 2364.

8. **ATILA user's manual (**1997) Version 5.1.1, Institute Superieur d'Eletronique du Nord, Acoustic Laboratory, LILLE CEDEX, France.

9. **Barkey, M. E., M. C. Turgeon** and **T. Varun Nare** (2008) Buckling of stiffened thin walled truncated cones subjected to external pressure, *Experimental Mechanics*, 48, 281-291.

10. **Behrendt, J. W.** (1971) Free-flooded deep submergence transducer, US Patent No.3624429.

11. **Behrendt, J. W., L. Jolla** and **G. L. Hunsker** (1970) Deep submergence transducer, US Patent No.3541502.

12. **Benson, B., Y. Li, R. Kastner, B. Faunce, K. Domond, D. Kimball** and **C. Schurgers** (2010) Design of a low-cost, underwater acoustic modem for short range sensor networks, *Proceedings of Oceans 2010 conference*, 4-27 May, Sydney, Australia.

13. **Berlincourt, D. A., D. R. Curran,** and **H. Jaffe** (1964) Piezoelectric and piezomagnetic materials and their function in transducers, *Physical Acoustics*, 1(a), Academic Press, 170-270.

14. **Berlincourt, D.** and **H. H. A**. **Krueger** and **C. Near** (2010) Properties of piezoelectricity ceramics, Technical Publication TP-226, Morgan Electroceramics.

15. **Blottman, J. B.** (1990) ATILA Finite element modelling of the Spartan ring shell transducer, *Proceedings of ATILA users workshop*, 65-74.

16. **Bonin, Y. R** and **J. S. Hutton** (1996) Increasing the depth capability of barrel stave projectors, *Canadian Acoustics*, 24(3), 50.

17. **Bose, M. R. S. C.** and **D. D. Ebenezer** (2001a) Design curves for the sonar class IV piezo ceramic flextensional transducer, Journal *of Acoustical Society India,* 29(1), 211-219.

18. **Bose, M. R. S. C.** and **D. D. Ebenezer** (2001b) Pre-stress in class IV flextensional sonar transducers, *Proceedings of the Symposium on Ocean Electronics, SYMPOL* 2001, 22-29.

19. **Bossut, R.** and **J. N. Decarpigny** (1989) Finite element modelling of a radiating structure using dipolar damping elements, *Journal of Acoustical Society of America,* 86, 4, 1234-1244.

20. **Boucher, D**. (1990) Low frequency tonpilz transducer optimisation with the ATILA code, *Proceedings of ATILA users workshop,* 16-20.

21. **Boucher, D.** (1996) Electroacoustic transducer compressing a flexible and sealed transmitting shell, US Patent No.5515343.

22. **Brigham, G.** and **B. Glass** (1980) Present status in flextensional transducer technology, *Journal of Acoustical Society of America,* 68, 1046-1052.

23. **Brigham**, **G. A.** (1974) Analysis of class-IV flextensional transducer by the use of wave mechanics*, Journal of Acoustical Society of America,* 56, 31-39.

24. **Brind, R. J**. (1988) Finite element modelling of the ARE low frequency flextensional transducers, *Proceedings of Institute of Acoustics,* 10(9), 105-129.

25. **Bromfield, G.** (1990) *Class IV flextensional transducers*, Power Transducers for Sonics and Ultrasonics, Springer-Verlag, New York, 48-59.

26. **Brown, D.** (2004) Baffled ring directional transducers and arrays, US Patent No.6768702.

27. **Busher, M. K.** (2008) Notes on the development over the last 35 years of methods for the manufacture of piezoelectric transducers. In book *History of Russian Underwater Acoustics*, edited by **O. A. Godin**, 961- 973.

28. **Butler, A. L., J. L. Butler, and J.A. Rice** (2001) A Trimodal directional transducer, *Journal of Acoustical Society of America,* 109(5), 2363.

29. **Butler, A. L., J. L. Butler, W. Dalton, J. Baker** and **P. Pietryk** (2003) A tri-modal directional modem transducer, *Proceedings of OCEANS2003*, San Diego, September 22-26, 1554-1559.

30. **Butler, A .L., J. L. Butler, W. L. Dalton,** and **J. A. Rice** (2000) Multimode directional telesonar transducer, *Proc. IEEE OCEANS'2000*, 1289-1292.

31. **Butler, A. L** and **J. L. Butler** (2002) A deep submergence, very low frequency, broadband, multiport transducer, *OCEANS'2002 MTS/IEEE*, 4, 2350- 2353.

32. **Butler, J. L.** (1976) Model for a ring transducer, *Journal of Acoustical Society of America*, 59(2), 480-481.

33. **Butler, J. L.** and **A. L. Butler** (2011) The modal projector, *Journal of Acoustical Society of America*, 129 (4), 1881-1889.

34. **Butler, J. L., A. L. Butler** and **J. A. Rice** (2004) A tri-modal directional transducer, *Journal of Acoustical Society of America*, 115 (2), 658-665.

35. **Butler, J. L., K. D. Rolt** and **F. A. Tito** (1994) Piezoelectric ceramic mechanical and stress study, *Journal of Acoustical Society of America*, 96, No.3, 1914-1917.

36. **Butler, S. C.** (1997) Triply resonant broadband Transducers, *MTS/IEEE OCEANS'02*, 29-31 Oct. 2334-2341.

37. **Butler, S. C., J. L. Butler, A. L. Butler,** and **G. H. Cavanagh** (1997) A low frequency directional flextensional transducer and line array, *Journal of Acoustical Society of America,* 102(1), 308-314.

38. **Capps, R. N., C. M. Thomson** and **F. J. Weber** (1981) *Handbook of sonar passive materials*, NRL memorandum report No. 4311.

39. **Chhith, S.** and **Y. Roh** (2009) Wideband tonpilz transducer with a cavity inside a head mass, *Ultrasonics Symposium (IUS) IEEE International*. 20-23 Sept. 2734-2737.

40. **Clayton, L.** (2009) Fishing with multiphysics, Direct coupled-field simulation including piezoelectric, acoustic and mechanical analysis enables engineers to tune transducer performance for monitoring huge trawler nets, Accessed 3rd June 2017, http://www.ansys.com/-/media/Ansys/corporate/resourcelibrary/article/AA-V4-I1-Fishing-with-Multiphysics.pdf

41. **Clearwaters, W. L** (1962) Electrostrictive transducer, US Patent No.3043967.

42. **Dahlstrom, D. K**. (1988) Flextensional underwater transducer, U.S. Patent No.4,764,907. (Reviewed in *Journal of Acoustical Society of America,* 85, 1389).

43. **DeAngelis, D. A.** and **G .W. Schulze** (2016) Performance of PZT8 versus PZT4 piezoceramic materials in ultrasonic transducers, *Physics Procedia*, 87, 85-92.

44. **Debus, J. C., B. Hamonic,** and **D. Boucher**, (1996) Development of a ring transducer for acoustic tomography, 3rd *European Conference, on Underwater Acoustics*, Heraklion, Crete, Greece, 24-28 June, 791-796.

45. **Decarpigny, J. N., B. Hamonic,** and **O. B. Wilson Jr.** (1991) The design of low frequency underwater acoustic projectors: Present status and future trends, *IEEE Journal of Oceanic Engineering*, 16(1), 107-122.

46. **Desilets, C., G. Wojcik, L. Nikodym and   K. Mesterton** (1999) Analyses and measurements of acoustically matched, air-coupled tonpilz transducers, *Proceedings of IEEE Ultrasonics Symposium,* 2, 1045 - 1048.

47. **Dogan, A.** (2006) Optimizing mechanical quality factor of cymbal transducer, *Ferroelectrics*, 331, 65-71.

48. **Dubus, B., P. Bigotte, F. Claeyssen, N. Lhermet, G. Grosso,** and **D. Boucher** (1996) Low frequency magnetostrictive projectors for Oceanography and sonar, *European Conference on Underwater Acoustics*, Heraklion, Crete, Greece, 1019-1124.

49. **Dubus, D., J. C. Debus, J. N. Decarpigny** and **D. Boucher** (1991) Analysis of mechanical limitations of high power piezoelectric transducers using finite element modelling, *Ultrasonics*, 29 (3), 201-207.

50. **Dufourcq, P., J. Adda, M. Lethiche** and **E. Sernit** (1991) Transducers for great depths, Power Transducers for Sonics and Ultrasonics, Proceedings of the

International Workshop, Held in Toulon, France, June 12 and 13, Editors **B. F. Hamonic, J. N Decarpigny, O. B. Wilson,** Chap.7, 75-85.

51. **Edouard, M, G. Lubranco, V. Suppa, J. Brun** and **J. Guido** (2002) Collapsible annular acoustic transmission antenna, US Patent No. 6345014.

52. **Edouard, M., B. Loubiers, P**. **Bocquillon** and **O. Lacour** (2000) Pre-stressed annular acoustic transducer. US Patent No.6065349.

53. **Ehrlich, S.** (1992) Deep submergence transducer, US Patent No.5172344.

54. **Erman, A. U**. and **A. E. Suvaci** (2003) Computational analysis on cymbal transducer, *Chem. Eng. Comm*. 190, 853-860.

55. **Eyries, M.** (2004) Naval hull mounted sonar for naval ship, US Patent No. 2004/0052160 A1, 18 Mar.

56. **Falcus, S. J.** (1994) Loading flextensional transducer shells, US Patent No.5,337461, 16 Aug.

57. **Falcus, S. J.** (1998) Segmented ring transducers, US Patent No.5,739,625.

58. **Fife, M. E., J. E. Martin,** and **W. D. Wilder (**1979) Flexural disk transducers for low frequency applications, *Journal of Acoustical Society of America*, 65, S1, S126-S126.

59. **Francis, D. T. I**., **J. R. Oswin** and **P. C. Macey** (1996) Comparing FE/BE Models with measurement: Flextensional Transducers, *Proceedings of Institute of Acoustics,* 18(10), 31-40.

60. **Gall, Y. L.** (1999) Low frequency Janus Helmholtz transducer for great depth, acoustical oceanography, *Proceedings of the Institute of Acoustics, Sonar Transducers '99*, Birmingham, 21.

61. **Gall, Y. L., D. Boucher** and **X. Lurton** (1993a) Depth unlimited versions of the Janus Helmholtz: a new interpretation of working principles-Some experimental results, *Proceedings of U. D. T*., Cannes, France, 241-245.

62. **Gall, Y. L., D. Boucher, X. Lurton** and **A. M. Bruneau** (1994) Great depth, high efficiency, broadband, reliable low frequency transducer for acoustical oceanography, *Proceedings of OCEANS94*, 2, II-284-288.

63. **Gall, Y. L., D. Boucher, X. Lurton,** and **A. M. Bruneau** (1993b) A 300 Hz Janus Helmholtz transducer for ocean acoustic tomography, *Proceedings of OCEANS '93*, Engineering in Harmony with Ocean, I 278 - I 281.

64. **Gallaher, A. B**. (1997) Numerical predictions of the performance of a compact volumetric sonar array of free-flooded ring projectors*, Proceedings of UDT'97*, 41-44.

65. **Gallaher, A. B.** (1995) Performance prediction of an array of free flooding ring transducers, *Proceedings of Institute of Acoustics,* 17(3), 34-43.

66. **George, J.** and **K. P. B. Moosad** (2013) Multiport projector for low frequency applications, *Sea Tech*, NPOL Technical Journal, 10(1), 33-37.

67. **Green, C. E**. (1965) Mosaic construction for electroacoustical cylindrical transducers, US Patent No.3177382.

68. **Groves, Jr. I. D**. (1971) *The design of deep submergence hydrophones*, NRL Report No. 7339.

69. **Haijun, P., Z. Kai** and **Du Yiqun** (2010) Design method of cymbal transducer structure parameters based on finite element analysis, *IEEE International Conference on Computer Design and Applications (ICCDA 2010),* V4-269-273.

70. **Hamonic, B., J. C. Debus** and **J. N. Decarpigny** (1989) Analysis of a radiating thin-shell sonar transducer using the finite-element method *Journal of Acoustical Society of America*, 86(4), 1245-1253.

71. **Hardie, D. J. W**. (1990) The effect of depth pressure on a flextensional transducer, *Proceedings of Institute of Acoustics,* 12(4), 40-48.

72. **Harris, W. T.** (1964) Ring-shaped transducers. US Patent No.3142035.

73. **Hayes, H. C.** (1936) Sound generating and directing apparatus, US Patent No.2064911.

74. **Henriquez, T. A.** and **A.M. Young** (1980) The Helmholtz resonator as a high power deep submergence source for frequencies below 500 Hz, *Journal of Acoustical Society of America*, 67(5), 1555-1558.

75. **Holloway, J. W.** (1974) Alternate lead ceramic stave free-flooded cylindrical transducer, US Patent No.3845333.

76. **Howarth, T. R.** and **R. Y. Ting** (1997) Development of a broadband underwater sound projector, *Proceedings of MTS/IEEE OCEANS'97 conference,* 1195-1201.

77. **Hueter, T. F** (1971) Twenty years of underwater acoustics: Generation and reception, *Journal of Acoustical Society of America,* 51, 3(2), 1025-1039.

78. **Hughes, W. J.** (1998) Transducers, underwater acoustic, encyclopaedia, *Applied Physics*, 22, 67- 84.

79. **Hugus III, G. D.** (1969) *Pressure compensating for gas-filled transducer,* NRL Report, No. 6981.

80. **IEC 60565** (2006) Underwater acoustics hydrophones calibration in the frequency range 0.01 Hz to 1 MHz, International Electrotechnical Commission, International standard.

81. **Ifayefunmi, O.** and **J. Błachut** (2012) Combined stability of unstiffened cones - Theory, experiments and design codes, *International Journal of Pressure Vessels and Piping,* S93-94, 57-68.

82. **Iula, A., F. Vazquez, M. Pappalardo,** and **J. A. Gallego** (2002) Finite element three-dimensional analysis of the vibrational behaviour of the Langevin type transducer, *Ultrasonics*, 40, 513-517.

83. **Jarng, S.S.** (2003) Comparison of barrel stave sonar transducer simulations between a coupled FE BEM and ATILA, *IEEE Sensors*: 3(4), 439-446.

84. **Jiwu, L.** (2016) The design of a kind of free-flooded ring transducer used in underwater communication, *IEEE/OES China Ocean Acoustics (COA),* 1-3.

85. **Jones, D. F.** (1996) Performance analysis of a low frequency barrel stave flextensional projector, *ONR workshop on Transducer materials and transducers*, Marc, Penn Stater Conference Centre, State College, PA.

86. **Jones, D. F.** and **D. A. Christopher** (1999) A broadband Omnidirectional barrel stave flextensional transducer, Acoustics Research letters online, *Journal of Acoustical Society of America*, 106(2), L13-L17.

87. **Jones, D. F.** and **J. F. Lindberg** (1995) Recent transduction development in Canada and United States, *Proceedings of Institute of Acoustics,* 17(3), 15- 29.

88. **Jones, D. F.** and **M. B. Moffett** (1993) *Water depth and drive voltage dependence of the acoustic parameters of a barrel stave flextensional projector*, Report Number: DREA-ORAL-1993-JONES-D-1.

89. **Junger, M .C.** (1969) *Design parameters of free-flooded ring transducers*, Technical Report U-308-210, Prepared for Office of Naval Research, Acoustics Programs.

90. **Kai, Z.** and **W. De Shi** (2011) Study on optimisation of structure parameters to tonpilz transducer, Proceedings of IEEE 2nd International Conference on Computing, Control and Industrial Engineering*, 414-416.

91. **Kendig, P. M.** and **H. J. Clarke** (1965) Experimental liquid filled transducer array for deep ocean operations, *Journal of Acoustical Society of America,* 37(1), 99- 103.

92. **Kendig, P. M.** and **H. J. Clarke** (1967) Underwater transducer array for deep submergence. US Patent No.3337843, 22 August.

93. **Kinsler, L. E., A. R. Frey, A. B. Coppens** and **J .V. Sanders** (2000) *Fundamentals of Acoustics*, John Willey & Sons Inc., New York.

94. **Kumar, S.S., K. V. J. Vincent, A. Ushakumari, P. C. Francis, T. P. Sameer Babu, M. V. Vibin, P. Muralikrishna, T. M. Jayamma, M. R. Subash Chandrabose**, and **M. Suresh** (2013) TRITON: A compact UWACS for Indian naval platforms, *Sea Tech*, 10(2), 15-20.

95. **Kuntsal, E.** (2003) Free-flooded ring transducers: Design methods and their interaction in vertical arrays, *Proceedings of OCEANS2003*, 4, 2074- 2078.

96. **Kuntsal, E.** and **W. A. Bunke** (1992) Guidelines for specifying underwater electroacoustic transducers, *Proceedings of UDT'92 Conference*, 229-236.

97. **Langner, C. G.** (1999)   Buckle arrestors for deepwater pipelines, Offshore Technology Conference, OTC-10711-MS, Houston, TX, U.S.A.

98. **Letiche, M.** and **P. L. Scala** (1990) *Great depth class V flextensional transducer for sonics and ultrasonics*, Edited by **M. D McCollum, B. F. Hamonic** and **O. B. Wilson**, Springer Verlag, Berlin, 1990 142-149.

99. **Li, H, H. Chan** and **C. Choy** (2001) Vibration characteristics of piezoceramic rings, *Ferroelectric,* 263, 211-216.

100. **Lipper, A.** and **J. Borden** (2012) Urethane transducer encapsulation versus oil filled boot encapsulation of transducers. In Proceedings of IEEE OCEANS2012, 1-4.

101. **Lipper, A.**   and **J. Borden** (2013) Comparing encapsulation methods of piezoelectric transducers, Oil Filled Boot Transducers Demonstrate Deepwater Performance, *Sea Technology*, 31-34.

102. **Macey, P. C**. (2001) Applications of PAFEC vibroacoustic to the audio industry, RS17: Measuring, modelling or muddling. Held at Stratford Hotel, Stratford.

103. **Marine diversity wiki** (2017) Deep-sea, Accessed 3rd June 2017. http://www.marbef.org/wiki/Deep_sea

104. **Martin, J. E.** (1964) Increased Bandwidth for deep submergence transducers, *Journal of Acoustical Society of America*, 36(5), 1026-1026.

105. **Massa, D. P.** (2017) An Overview of Electroacoustic Transducers, Massa Products, 1-18, Accessed 18 June 2017, https://www.massa.com/wp-content/uploads/DPM_Overview_of_Electroacoustic_Transducers.pdf

106. **Massa, F.** (1985) Some Personal Recollections of Early Experiences on the New Frontier of Electroacoustic During the Late 1920's and Early 1930's, *J. Acoustic Soc. Am.* 77(4), 1298-1302.

107. **McMahon, G. W.** (1964) Performance of open ferroelectric ceramic cylinders in underwater transducers, *Journal of Acoustical Society of America*, 36, 528-533.

108. **McMahon, G. W.** (1990) The ring shell flextensional transducer (Class V), *Proc. Power transducers for sonics and ultrasonics*, Ed. **B. F. Hamonic, O. B. Wilson** and **J. N. Decarpigny**, Springer Verlag, Berlin, 60-74.

109. **McMahon, G .W.** and **B.A. Armstrong** (1985) Underwater transducer with depth compensation, US Patent No.4524693, June.

110. **McMahon, G. W.** and **E. L**. **Skiba** (1991) *Examples manual for program MAVART,* User's Manual for Program MAVART, Defence Research Establishment Atlantic, Canada.

111. **Meglio, A. Di, D. T. I. Francis** and **R. F. W. Coates** (1996) PHOEBE: A 3D transducer modelling environment, *3rd European Conference, on Underwater Acoustics*, Heraklion, Crete, Greece 24-28 June 1996, 1007-1012.

112. **Mehnert, T. H.** (1972) *Handbook of fluid-filled depth/pressure compensated systems for deep ocean applications.* Naval Ship Research and Development Centre, Annapolis Laboratory, Maryland, USA.

113. **Merchant, H. C.** (1966) Underwater transducer apparatus, US Patent No.3258738.

114. **Mero, J. L**. (1965) *The Mineral Resources of the Sea,* Elsevier Publishing Company, Amsterdam, 1, 106.

115. **Miller, H. B.** (1960) Composite electromechanical transducer, U.S. Patent No.2,930,912; Reviewed in *Journal of Acoustical Society of America*, 33(11), 1648.

116. **Miller, H. B.** (1963) Origin of mechanical bias for transducers, *Journal of Acoustical Society of America*, 35(9), 1455.

117. **Miller, H. B.** (1989) Origin of the 33-driven ceramic ring stack transducer, *Journal of Acoustical Society of America*, 86(4), 1602-1603.

118. **Moffet, M. B.** (1993) On the power limitations of sonic transducers, *Journal of Acoustical Society of America,* 84(6), 3503-3505.

119. **Moffet, M. B .** and **W. L. Clay, Jr.** (1991) High power test of a barrel stave transducer, *Journal of Acoustical Society of America,* 89(4), Pt2., 1858.

120. **Moosad, K. P. B.** (2003) Fluid-filled class IV flextensional transducer, *Proceedings of SYMPOL-2003*, 171-176.

121. **Moosad, K. P. B.** (2011) Class IV flextensional transducer with a reflector, *Journal of Applied Acoustics* 72, 2-3, 127-131.

122. **Morris, R.** (1984) Some practical considerations in the design of sandwich transducers and their arrays, *IEEE Proceedings*, 131(3), 280-284.

123. **Moscaa, F., G. Matte** and **T. Shimura** (2013) Low frequency source for very long range underwater communication, *Journal of Acoustical Society of America*, 133 (1), EL61-67.

124. **Naidu, B. P., A. B. Rao, N. S. Prasad** and **Trinath** (2010) Low frequency acoustic projectors for underwater applications, *Integrated Ferroelectrics*, 118, 86-94.

125. **Nakamura, T., I. Nakano, T. Tsuchiya** and **I. Kaihou** (1996) Development of 200 Hz transceiver system for ocean acoustic tomography, *3rd European Conference on Underwater Acoustics*, Heraklion, Crete, 797-802.

126. **NIOT, Chennai** (2017) Hyperbaric Test Facility, Accessed 3rd June 2017. https://www.niot.res.in/index.php/node/index/136/

127. **NPOL, DRDO** (2017) Facilities available, Accessed 9th June 2017. https://www.drdo.gov.in/drdo/labs1/NPOL/English/indexnew.jsp?pg=facility.jsp

128. **Oishi, T., B. Aronov,** and **D.A. Brown** (2007) Broadband multimode baffled piezoelectric cylindrical shell transducers, *Journal of Acoustical Society of America*, 121(6), 3465-3471.

129. **Oswin, J**. and **G .A. Steel**, (1990) Flextensional transducers with unlimited depth capability, *Proceedings of Institute of Acoustics,* 12(4), 1990, 13-20.

130. **Oswin, J. R.** and **A. Turner** (1984) Design limitations of aluminium shell, class IV flextensional transducers, *Proc. I. O. A*., 6(3), 94-101.

131. **Oswin, J. R.** (1995) Titanium flextensional transducers, *Proceedings of Institute of Acoustics.,* 17(3), 210-219.

132. **Pak, A.** and **A. Abdullah** (2008) Correct prediction of the vibration behaviour of a high power ultrasonic transducer by FEM simulation, *The International Journal of Advanced Manufacturing Technology, 39 (1) 21-28.*

133. **Parker, D. E**. (1966) Reinforced ceramic cylinder transducer, US Patent No.3230505.

134. **Ponchaud, K. J**. (1988) Sonar Transducers, US Patent No.4731764.

135. **Prabu, B., N. Rathinam, R. Srinivasan** and **K. A. S. Naarayen** (2009) Finite element analysis of buckling of thin cylindrical shell, subjected to uniform external pressure, *Journal of Solid Mechanics,* 1, No. 2, 148-158.

136. **PZFlex** (2017) Software Features & Specifications, Accessed 3rd June 2017. https://pzflex.com/software/

137. **Ramesh, R.** and **D. D. Ebenezer** (2005) Analysis of axially polarised piezoelectric ceramic rings, *Ferroelectrics*, 323, 17-23.

138. **Ramesh, R.**, **C. Durga Prasad, T. K. VinodKumar** and **L. A. Gavane** (2006) Experimental and finite element modelling studies on a single layer and multilayer 1-3 piezocomposite transducers, *Ultrasonics* 44, 341-349.

139. **Renna, Jr. N.** (1972) Underwater acoustic projector, US Patent No.3706967.

140. **Roberts, P.**, **N. Andronis** and **A. Ghiotto** (2012) Voices from the deep acoustic communication with a submarine at the bottom of the Mariana Trench, *Proceedings of Acoustics 2012*, Fremantle, Australia.

141. **Rolt, K. D**. (1990) History of flextensional electroacoustic transducer*, Journal of Acoustical Society of America*, 87 (3), 1, 1340-1349.

142. **Roux, G., G. Lubrano** and **V. Suppa** (2005) Acoustic transducer with pre-stressed ring, US Patent No.6,879,090.

143. **Royster, L. H.** (1970) The Flextenstional concept: A new approach to the design of underwater acoustic transducer, *Journal of Applied Acoustics*, 3, 117-125.

144. **Sanchez, A., S. Blanc, P. Yester** and **J. J. Serrano** (2011) A low cost and high efficient acoustic modem for underwater sensor networks, *IEEE, Oceans2011.*

145. **Sandwith, C. J., A. Sieger,** and **G. Hugus** (1987) Failure analysis through autopsy of undersea acoustic transducers, *OCEANS'87,* 49-454.

146. **Scarpitta, A. A., D. Boucher** and **T. Wintz** (1996) Method and apparatus for emitting high power acoustic waves using transducers, US Patent No.5483502, 9, Jan.

147. **Schmid, S. R., B. J. Hamrock** and **B. O. Jacobson** (2013) *Fundamentals of Machine Elements,* Third Edition, CRC Press, 181.

148. **Semenov, A. G., Y. N. Kupenko,** and **I. P. Goliamina** (1994) Ocean tomographic systems low frequency depth independent sound transducer source, *Proceedings of OCEANS '94. Oceans Engineering for Today's Technology and Tomorrow's Preservation,* 1, I/377 - I/379.

149. **Sernit, E., B. Fromont** and **J. Adda** (1998) Underwater acoustic transmitter for large submersion, US Patent No.5784341, 21, Jul.

150. **Sherman, C. H. and J. L. Butler** (2016) *Transducers and Arrays for Underwater Sound,* Monograph series in underwater acoustics, 2nd Edition, Springer, New York, USA, 9, 360-374.

151. **Singh, S., S. E. Webster, L. Freytag**, **L. L. Whitcomb, K. Ball, J. Bailey,** and **C. Taylor** (2009) Acoustic communication performance of the WHOA micro modem in sea trials of the Nereus Vehicle to 11,000 m Depth, *Oceans2009.*

152. **Sreejith, S. P.** and **D. D. Ebenezer**, (2009) Free-flooded, piezoelectric ceramic, broadband transducers, SYMOPL2009.

153. **Srinath, L. S.** (2000) *Advanced mechanics of solids*, Tata McGraw Hill Publishing Co., New Delhi, India.

154. **Stansfield, D**. (1990) *Underwater electroacoustic transducers*, (Bath University Press and Institute of Acoustics, 1990) 33-36, 183-184.

155. **Thompson, S. C., M. P. Johnson, E. A . McLaughin** and **J. F. Lindberg** (1993) Performance and recent developments with doubly resonant wideband transducers,

in *Transducers for Sonics and Ultrasonics*, edited by M. D. McCollum *et al.*, (TECHNOMIC, U.S.A., Lancaster, Pennsylvania, 1993), pp. 239-249.

156. **Tianfang, Z., L. Yu, L. Wei** (2016) A study of deep water bender disk transducer, *IEEE-OES,* China Ocean Acoustics Symposium.

157. **Tocquet, B. (**1979) Piezoelectric transducers and acoustic antennas which can be immersed to a great depth, US Patent No.4151437.

158. **Toulis, W. J.** (1966a) Flexural Extensional Electro Mechanical Transducer, US Patent No.3277433.

159. **Toulis, W. J.** (1966b) Flexural Extensional Electro Mechanical Transducer, US Patent No.3274537.

160. **Tressler, J. F. (**2006) A comparison of the underwater acoustic performance of single crystal versus piezoelectric ceramic based cymbal projectors, *Journal of Acoustical Society of America*, 119 (2), 879-890.

161. **ULTRA Electronics** (2014), Free-flooded ring for low frequency active sonar, Brochure.

162. **ULTRA Electronics** (2017) Ring shell projector, brochure. Accessed 23rd Sept 2017. http://www.ultra-ms.com/uploads/ms/pdfs/Ringshell%20Projector.pdf

163. **Urick, R. J.** (1983) *Principles of Underwater Sound*, 3rd Edition, McGraw-Hill Book Company, 72-80.

164. **Vernitron Limited** (1976) Bulletin 66017/B.

165. **Waite, A. D.** (2002) *SONAR for Practicing Engineers*, 3rd Edition, John Wiley & Sons Ltd., West Sussex, U.K.

166. **Widener, M. W.** (1986) The Development of a deep submergence air-backed transducer, *Journal of Acoustical Society of America*, 80(6), 1852-53.

167. **Williams 3rd, A. J.** and **F. T. Thwaites** (2013) Urethane potting of acoustic transducers for acoustic travel time current meters*, Proceedings of the International Symposium on Ocean Electronics, SYMPOL2013*, Kochi 23-25 Oct, Kochi, and published in IEEE Xplore.

168. **Wills, J., W. Ye** and **J. Heidemann** (2006) Low power acoustic modem for dense underwater sensor networks, *WUWNet'06*, Los Angeles, California, USA.

169. **Woollett, R. S.** (1962) Theoretical power limits of sonar transducers, *IRE International Conventional Proceedings,* 6, 90-94.

170. **Woollett, R. S.** (1963) Trends and Problems in sonar transducer design, *IEEE Trans. Ultrason.*, Engg., 116-124.

171. **Woollett, R. S.** (1968) Power limitations of sonic transducers, *IEEE Trans. Sonics and Ultrasonics*, SU-15(4), 218-228.

172. **Woollett, R. S.** (1976) *VLF Flexural Disk Transducers Using Disks of 1 m in Diameter*, NURC report, TR 5509.

173. **Woollett, R. S.** (1980) Basic problems caused by depth and size constraints in low frequency underwater transducers, *Journal of Acoustical Society of America*, 68, 1031-1037.

174. **Woollett, R. S.** (1975) Underwater Helmholtz resonator transducers, *Journal of Acoustical Society of America*, 58(S1), S80.

175. **Xin-ran, X**. (2012) Theoretical and experimental study on a new structure free-flooded ring transducer, *Proceedings of the IEEE Symposium on Piezoelectricity, Acoustic Waves and Device Applications (SPAWDA),* 81-84.

176. **Yao, Q.** and **L. Bjørnø** (1996) Depth restrictions and solutions for barrel stave flextensional transducers, *European Conference, on Underwater Acoustics*, Heraklion, Crete, Greece, 1037-1042.

177. **Zhang, J., W .J. Hughes, P. Bouchilloux, R.J . Meyer Jr., K. Uchino** and **R. E. Newnham** (1999) A class V flextensional transducer: The cymbal, *Ultrasonics,* 37, 387-393.

178. **Zhang, J. D.** (1995) Finite element modelling of the performance of a high-frequency hydrophone, *Proceedings of Institute of Acoustics*, 17, 154-163.

179. **Zheng, C. X., J. Meng** and **S. H. Lei** (2006) Mechanical analysis of carbon fibre wound high-pressure hydrogen storage vessel and pre-stress control in the manufacturing process, *Proceedings of International Technology and Innovation Conference*, University of Florida, United States, 1188-1193.

180. **Zhengyao, H.** and **M. Yuan-Ling** (2011) Advantage analysis of PMN-PT material for free-flooded ring transducers, *Chinese Physics B*, 20(8),084301-1-084301-7.

181. **Zhou Q., D.Wu, J. Jin, C. Hu, X. Xu, J.Williams, J. Cannata,   L. Lim,** and **K.Shung** (2008) Design and fabrication of PZN-7%PT single crystal high frequency angled needle ultrasound transducers, *IEEE Transactions on Ultrasonics, Ferroelectrics and Frequency Control,* 55(6), 1394–1399.

LIST OF PAPERS BASED ON THE THESIS

1. **Subash Chandrabose M. R.** and D. D. Ebenezer (2014) Oil filled free-flooded segmented ring transducers for deep sea applications, *Journal of Acoustical Society of India,* 41 (3), 119-124.

2. **Subash Chandrabose M. R**., V. P. Shan, N. Praveenkumar and D.D. Ebenezer, (2016) Free-flooded ring transducers for deep sea applications, *Journal of Acoustical Society of India,* Vol 43 (4), 2016, 177-185.

3. **Subash Chandrabose M. R.,** V. P. Shan, B. Jayakumar, R. M. Abraham and D. D. Ebenezer (2017) Metal ceramic segmented ring transducers under deep submergence conditions, *Defence Science Journal*, Vol. 67(6), 2017, 612-616.

4. **Subash Chandrabose M. R.** and D. D. Ebenezer (2012) Design curves for free-flooded deep submergence ring transducers in annular fill fluids, *Proceedings of the National Symposium on Acoustics, NSA 2012*. 5-7 December 2012, Thiruchengode, 234-240.

5. **Subash Chandrabose M. R.** and D. D. Ebenezer (2013a) Oil filled free-flooded ring transducer for deep submergence applications, *Proceedings of the International Symposium on Ocean Electronics SYMPOL2013*, 23-25 Oct 2013, Kochi, 331-335 and published in IEEE Xplore.

6. **Subash Chandrabose M. R.** and D. D. Ebenezer (2013b) Oil filled free-flooded segmented ring transducer for deep submergence applications, Proceedings of the *International Symposium on Acoustics, Acoustics2013,* New Delhi, 10-15 November, paper 179, 1083-1088.

7. George, J., R. M. Abraham, P. P. Sathyanarayana and **M. R. Subash Chandrabose** (2015) Pre-stressing of a metal ceramic segmented ring acoustic transducer through fibre winding, *Proceedings of the National Symposium on Acoustics, NSA2015*, 7-9 October, NIO, Goa.

8. **Subash Chandrabose M. R.,** V. P. Shan, R. Ramesh and D. D. Ebenezer (2018) Directional free-flooded segmented ring transducer, Proceedings of the *International Conference on Sonar Systems & Sensors, ICONS2018,* 22-24 February, Kochi, India, 339-342.

OTHER PUBLICATIONS

1. Abraham, R.M., T. K. Vinod, E. R. Ratheesh, Shan V.P., **M. R. Subash Chandrabose** (2018), Design and Development of Low Frequency High-Power Free Flooded Ring Transducers, Proceedings of the *International Conference on Sonar Systems & Sensors, ICONS2018,* 22-24 February, Kochi, India, 343-346.

2. Joseph, L., P. P. Satyanarayan, R. Krishnakumar, P. Annadurai, K. P. B. Moosad, **Subash Chandrabose M. R.**, and D. D. Ebenezer (2012) Optimization of a Class IV Flextensional Transducer, *Proceedings of the National Symposium on Acoustics*, *NSA2012*.

3. **Subash Chandrabose M. R.**, D. D. Ebenezer, V. Mohanan and L. Joseph (2008) Design curves for class IV flextensional transducers, Proceedings of TASSET 2008, *National Symposium on Towed Array Sonar Systems: Engineering & Technology*, Oct., NPOL, Kochi, India.

4. Moosad, K. P. B., D. D. Ebenezer, **M. R. Subash Chandrabose,** G. Chandrasekhar, P. Abraham, P. Krishnakumar and P. Annadurai (2008). Design and Development of a Flextensional Transducer for Active Towed Arrays, Proceedings of TASSET 2008, *National Symposium on Towed Array Sonar Systems: Engineering & Technology*, Oct., NPOL, Kochi, India.

5. **Subash Chandrabose M .R.**, K. P. B. Moosad, P. P. Satyanarayan, Pushpa Abraham, K. M. Prakash, M. Rajendran, R. Krishnakumar and R. Rajesh (2008). Design and Development of a Towed Acoustic Source for Active Towed Array Sonar, *National Symposium on Towed Array Sonar Systems: Engineering & Technology*, Oct., NPOL, Kochi, India.

6. Joby, P. M., J. Peter, M. R. Sooraj, R. Augustine, R. Ramesh and **M. R. Subash Chandrabose** (2005) Impedance matching circuit for wideband transducers, *Proceedings of the National Symposium on Ocean Electronics, SYMPOL2005*, Cochin University of Science & Technology, Cochin, Dec. 239-250.

7. **Subash Chandrabose M. R.**, V. Mohanan, K. G. Jacob and R. Nirmala (2003). Development of a wideband transducer, *Proceedings of the National Symposium on Ocean Electronics*, *SYMPOL2003*, Cochin University of Science & Technology, Cochin, Dec. 202-206.

8. Ebenezer, D. D. and **M. R. Subash Chandrabose** (2002) Wideband Tonpilz transducers, *Proceedings of International Conference on Sonar Systems and Sensors, ICONS2002*, Kochi, Dec. 2002.

9. **Subash Chandrabose M. R.** (2001) 3-D FEM Modeling of a Class - I Barrel Stave Projector, *Proceedings of the National Symposium on Ocean Electronics,* (SYMPOL2001), Cochin University of Science & Technology, Cochin, Dec 2001, 40-47.

10. **Subash Chandrabose M. R.** and D. D. Ebenezer (2001) Pre-stress in Class IV Flextensional Sonar Transducers, *Proceedings of the National Symposium on Ocean Electronics, SYMPOL2001*, Cochin University of Science & Technology, Cochin, Dec. 22-29.

11. **Subash Chandrabose M. R.** and D.D. Ebenezer (2001) Design Curves for Sonar Class IV Piezoceramic Flextensional Transducers, *Proceedings of the National Symposium on Acoustics*, *NSA2001*, Vellore Engineering College, Vellore, October 2001, 211-219.

12. Palaninathan, R., G. Thomas, **M. R. Subash Chandrabose**, S.P. Damodaran and P. Chellapandi (2001) Experimental studies on LMFBR inner vessel Models *Transactions of international conference on Structural Mechanics in Reactor Technology, SmiRT16*, Washington DC, August, Paper 1109.

13. **Subash Chandrabose M. R.,** G. Thomas, R. Palaninathan, S.P. Damodaran and P. Chellapandi (2001) Buckling investigations on nuclear reactor inner vessel Model *Journal of Experimental Mechanics*, 41, No.2, June 2001, 144-151.

Monograph

1. **Subash Chandrabose M. R.** and R. Ramesh (2013) *Underwater Transducers: An Overview*, Published by NPOL, Kochi.

Patent

1. Reji, J., Shivkumar, P.P. Sathyanarayan and **M. R. Subash Chandrabose** (2012) Acoustic gel for non-cavitating underwater transducers, Application No: 3822/DEL/2012.

2. Sunilkumar S., K. V. J. Vincent, A. Ushakumari, V. Mohanan, M. V. Vibin, T. P. Sameer Babu, P. Muralikrishna, **M. R. Subash Chandrabose** and M. Suresh (2014) A compact underwater acoustic wireless communication system incorporating multiband voice and digital telemetry with integrated front-end electronics, processing, display and remote operation. Application No: 3745/DEL/2014.

CURRICULUM VITAE

1. Name in full (in capital letters)   : **SUBASH CHANDRABOSE M. R.**

2. Date of birth   : 25.07.1963

3. Ph.D Registration No. & Date   : 3897, 1st Nov. 2010

4. Educational Qualifications   :

Degree	Year	College / University	Specialisation
B. Tech	1985	College of Engineering, Trivandrum, Kerala University	Mechanical Engineering.
M. Tech	2000	IIT, Madras	Engineering Mechanics.
M.B.A.	2007	School of Management Studies, Cochin University of Science & Technology	Human Resource Management

5. Details of Employment

Grade/Post	From	To	Lab/Establishment
Scientist-B	22-07-1986	30-06-1991	GTRE, Bangalore
Scientist-C	01-07-1991	21-07-1995	GTRE, Bangalore
Scientist-C	22-07-1995	30-06-1996	NPOL, Kochi
Scientist-D	01-07-1996	30-06-2002	NPOL, Kochi
Scientist-E	01-07-2002	30-06-2007	NPOL, Kochi
Scientist-F	01-07-2007	30-06-2014	NPOL, Kochi
Scientist-G	01-07-2014	Till Date	NPOL, Kochi